Heriot-Watt University

Drivers of population cycles in ecological systems

Jennifer Joan Heather Reynolds

April 1, 2012

Submitted for the degree of
Doctor of Philosophy in Mathematics
on completion of research in the
Department of Mathematics,
School of Mathematical and Computer Sciences.

Abstract

In this thesis, mathematical models are used to investigate potential drivers of population cycles. Population cycles are a common ecological phenomenon, yet the mechanisms underpinning these oscillations are not always known. We focus on two distinct systems, and evaluate potential causes of cyclic dynamics.

In the first part of the thesis, we develop and analyse a host–pathogen model, incorporating density-dependent prophylaxis (DDP). DDP describes when individuals invest more in immunity at high population densities, due to the increased risk of becoming infected by a pathogen. The implications of this for the population dynamics of both host and pathogen are examined. We find that the delay in the onset of DDP is critical in determining whether DDP increases or decreases the likelihood of population cycles.

Secondly, we focus on a particular cyclic vole population, that of Kielder Forest, Northern UK. We construct a model to test the hypothesis that the population oscillations observed in this location are caused by the interaction between the voles and the silica in the grass they consume. We extend our model by including seasonal forcing, and study the effects of this on the population dynamics.

Acknowledgements

First, and foremost, I thank my supervisors, Jonathan Sherratt and Andy White, for all their invaluable help and advice; thank you for always finding the time for our chats. I would also like to thank my family and Craig for their support and for showing so much interest in my work (or at least convincingly feigning interest!). Many thanks to the Mathematics department at Heriot-Watt, and to my fellow PhD students, who have helped to make my years here so enjoyable. With thanks too to my collaborators. Finally, I acknowledge the Engineering and Physical Sciences Research Council for providing funding for this work.

Contents

Chapter 1

Introduction

This thesis explores the population dynamics of ecological systems. In natural systems, any one species is subject to many different influences and this can lead to a variety of often complex population dynamical behaviours. A broad aim of population dynamical studies is to document the empirical patterns of population change and attempt to uncover the mechanisms driving the observed patterns (Turchin, 2003). Practically no animal population remains the same for any great length of time, and the numbers of most species are subject to fluctuations (Elton, 1927). In some cases the fluctuations in numbers are extraordinarily regular; periodic fluctuations in numbers, or population cycles, are well-documented.

1.1 Population cycles

Population cycles are regular and repeated oscillations in population density. Cycling is a common example of a dynamic behaviour seen in natural systems (Gurney and Nisbet, 1998), and cyclic patterns in animal populations have long been a focus of interest (Turchin, 2003). Fluctuations in the numbers of any one species inevitably causes changes in those of others associated with it. The scientific study of population cycles commenced with the work of Charles Elton, who described the widespread existence of such periodic fluctuations in animal numbers (Elton, 1924).

Cyclic populations have been well studied, and there are many empirically reported cases. One example is the ten-year cycle of the Canada lynx, which has been studied by looking at fur catches of the Hudson's Bay Company. There are remarkably regular oscillations in numbers over a long time period (from 1821 to 1913) (Elton and Nicholson, 1942), as illustrated in Figure 1.1. Some of the best-known cases of cyclic populations are among rodents (Elton, 1927). For instance, the Norwegian lemming (*Lemmus lemmus*) population exhibits striking periodic fluctuations, with vast numbers at the population peak. The lemming cycle has been

studied extensively (Stenseth and Ims, 1993).

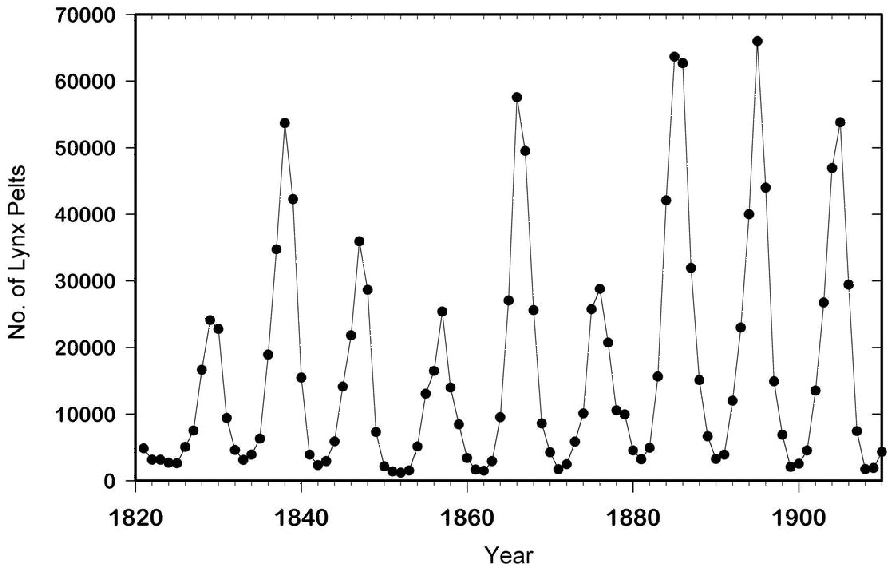

Figure 1.1: Canada lynx fur returns from the Northern Department of the Hudson's Bay Company. (The Northern Department occupied most of western Canada.) The cyclic period for these data averages 9.6 years. Figure reproduced from Krebs *et al.* (2001), published by the University of California Press, with permission. Copyright 2001 by the American Institute of Biological Sciences. Data are from Elton and Nicholson (1942).

In addition to empirical studies, mathematics has been used to investigate population oscillations. Starting with the work of Lotka (1925) and Volterra (1926), mathematical modelling has been employed in attempts to explain the causes of population cycles in animal populations.

Despite extensive research, the mechanisms involved in driving these multi-year population cycles are a subject of much debate. Elton (1924) attributed the cycles in animal abundance to climatic variations. Since then, a plethora of competing hypotheses on the factors determining the cycles have been developed (Berryman, 2002), using both empirical evidence and modelling predictions.

The hypothesis that cycles are caused by trophic interactions has received much attention (Berryman, 2002). Lotka (1924) and Volterra (1926) demonstrated that cyclic dynamics are inherent in simple predator–prey models; this led to the idea that predator effects are the cause of population oscillations. An increase in prey density results in an increase in predator density as there is plenty for the predators to eat. This then causes the prey numbers to fall. This leads to a subsequent

decline in predator numbers, allowing prey density to increase once again. Thus the relationship between prey and predator densities has the potential to cause population cycles. Similar processes can arise through other interactions. There is evidence to suggest that the interaction between herbivores and the plants they consume can generate cycles of the herbivore population (e.g. Fox and Bryant, 1989; Underwood, 1999). The interaction with pathogens has also been demonstrated as a potential driver of population cycles; Anderson and May (1981) showed that, under certain conditions, simple models of infectious disease transmission can produce host and pathogen population cycles.

In addition, it has been proposed that intrinsic factors may drive population cycles (as opposed to environmental influences). The maternal effects hypothesis argues that cycles can be caused by qualitative changes in individuals due to stress experienced by the maternal generation (Christian, 1950; Wellington, 1960). There is some theoretical evidence for this: for instance, the maternal effects model of Ginzburg and Taneyhill (1994) produces population oscillations resembling those exhibited by forest Lepidoptera. The theory that genetic effects cause cycles was proposed by Chitty (1967). This postulates that cycles result from density-dependent changes in genetic traits affecting survival and/or reproduction of individual organisms. Natural selection should favour those individuals with the 'fitness' advantage in the particular environment. This changes as density changes, and according to this argument, could promote cycles.

1.2 Density-dependent prophylaxis

In this thesis, there is a focus on two distinct cyclic systems. In the first part of the thesis, we consider the dynamical implications of density-dependent prophylaxis for an insect–pathogen system. The risk of becoming infected by a pathogen increases at high population densities. As immunity can be costly to maintain, the most efficient strategy to adopt is to tailor investment in resistance mechanisms to match the perceived risk of infection. Therefore, individuals invest more in immunity at high population densities; this phenomenon is termed density-dependent prophylaxis (DDP). DDP has been experimentally demonstrated in several insect species (e.g. Barnes and Siva-Jothy, 2000; Reeson *et al.*, 1998; Wilson *et al.*, 2002). We incorporate DDP into a model of an insect–pathogen system, and use this model to predict the impact of DDP on the likelihood of population cycles. The background details of this system are given in the introduction to Chapter 2.

1.3 Cyclic vole populations

The second topic of the thesis is an investigation into the potential drivers of cycles of vole populations. The cyclic dynamics of vole populations have been well documented and studied for a long time; indeed Elton empirically studied the fluctuations in numbers of British voles (*Microtus* and *Clethrionomys*) (Crowcroft, 1991). Our particular focus is the field vole (*Microtus agrestis*) populations of Kielder Forest, Northern UK. The voles here undergo regular population cycles of period 3–5 years, and a possible explanation for these cycles is the interaction between the voles and the grass they consume. The grass responds to herbivory by voles by increasing the silica content of its leaves. This defence mechanism reduces the nutritional quality of the grass, and therefore causes vole numbers to fall. A reduction in vole density, and hence in grazing intensity, leads to the grass silica defences relaxing. This system is discussed in more detail in Chapters 4 and 5.

Cyclic vole populations occur in a wide range of ecosystems. The population dynamics can be variable among species and geographic localities; this argues against a universal explanation of cyclicity that applies to all species at all locations (Turchin, 2003; Hanski and Henttonen, 2002). In addition to our study site at Kielder Forest, detailed studies have been performed on cyclic vole populations in Fennoscandia (e.g. Henttonen *et al.*, 1987) and in Hokkaido, Japan (e.g. Stenseth *et al.*, 2003). Not all vole populations oscillate (Turchin, 2003). Empirical data shows that the period of population cycles typically lengthens at higher latitudes and altitudes (Mackin-Rogalska and Nabaglo, 1990).

Possible factors for shaping the dynamics of fluctuating vole populations can work either separately or in combination. These are reviewed by Boonstra *et al.* (1998), Klemola *et al.* (2003), Turchin (2003) and Hanski and Henttonen (2002), and a brief outline is given here.

Firstly, there are several theories relating to the idea that intrinsic mechanisms cause vole population cycles. Intrinsic explanations assume that population dynamics are self-regulated within the population. These hypotheses consider physiological and behavioural characteristics, either of individual animals or within populations. Examples include senescence (Boonstra, 1994) and maternal effects (Inchausti and Ginzburg, 1998), and social organisation and dispersal (Krebs *et al.*, 1973). Much research has focused on the genetic changes during the vole population cycle (Krebs and Myers, 1974; Charnov and Finerty, 1980). For instance, the Chitty hypothesis, also known as the polymorphic-behaviour hypothesis, postulates that microtine cycles are mediated by natural selection operating on the genetic composition of the population (Chitty, 1967; Boonstra and Boag, 1987). However, the idea that genetic effects cause population cycles has received little empirical support and is

widely considered to be refuted (Stenseth, 1999), and intrinsic explanations in general are commonly unsupported (Akçakaya, 1992; Klemola *et al.*, 2000a; Ergon *et al.*, 2001).

Additionally, many investigations have tested the plausibility that extrinsic factors contribute to microtine population oscillations. One such theory is interactions with pathogens (Stenseth, 1985; Soveri *et al.*, 2000). For instance, the model of Smith *et al.* (2008), parameterised for cowpox virus and field vole populations of Kielder Forest, predicts disease-induced vole population cycles. Pathogen interactions are one of the least studied of the factors that could influence cyclic populations (Boonstra *et al.*, 1998).

Much data seems to suggest that trophic interactions are the major determinants of cyclic dynamics (Stenseth, 1999; Klemola *et al.*, 2003; Turchin, 2003). Vole cycles have traditionally been thought to reflect interactions with predators (Akçakaya, 1992; Korpimäki and Krebs, 1996; Klemola *et al.*, 2003), and many studies have focused on predation as the determinant of vole cycles, particularly in Fennoscandia where the theory that specialist predation causes cycles has been well developed and is richly supported (e.g. Henttonen *et al.*, 1987; Hanski *et al.*, 1993, 2001; Hanski and Henttonen, 1996, 2002). However, in other areas less of a consensus exists: for example, results of experiments conducted by Graham and Lambin (2002) indicate that predation is not sufficient to drive population cycles of field voles in the Kielder Forest. In addition, several influential reviews have concluded that predation is not driving vole oscillations (Chitty, 1960; Krebs and Myers, 1974; Taitt and Krebs, 1985). In Chapter 6 we will discuss the possibility that the difference in the mechanism causing the cycles in Kielder Forest and in Fennoscandia might have important consequences for the robustness of the cycling dynamics to climate change.

Several authors have considered the idea that interactions with food resources may play a contributing role in driving vole population processes (Lack, 1954; Hansson, 1971; Batzli, 1985, 1992; Agrell *et al.*, 1995; Högstedt *et al.*, 2005). There are two main distinct ways in which herbivore populations can be affected by interactions with the food plants. Firstly, the consumption of plant tissue may limit the quantity of food available to later-feeding herbivores. Secondly, herbivore damage may elicit inducible resistance in the plant that reduces the nutritional quality of the unconsumed tissue (Karban and Baldwin, 1997). Both of these pathways could play important roles in the long-term population dynamics of herbivores (Abbott *et al.*, 2008). If changes in food quality have significant effects on vole growth rates and reproduction output, they may impact on individual fitness and potentially population dynamics (Turchin and Batzli, 2001). Food quality is especially important for voles due to their relatively high metabolic rates, and because they have a limited

capacity to increase food consumption to compensate for poor quality diets (Zynel and Wunder, 2002). In addition, their growth rates early in development are highly dependent upon nutrient intake. Therefore, food quality has the potential to dictate the time taken to reach sexual maturity and the onset of breeding each year in voles (Krebs and Myers, 1974; Ergon *et al.*, 2001).

The significance of plant-based factors on vole populations has been examined with differing results. Agrell *et al.* (1995) conducted a manipulation of field vole (*M. agrestis*) densities within enclosed areas and it was shown that reproduction, recruitment and growth rates in introduced populations were negatively affected by previous high density. Chemical analysis of a dominating food plant indicated that herbivory at high vole density had delayed negative effects on food quality. These results are in accordance with the hypothesis that food resources are negatively affected by previous high densities (Ostfeld, 1985). However, these results are in apparent disagreement with other experiments. For instance, in a study by Ostfeld *et al.* (1993) in North America, populations of meadow voles (*Microtus pennsylvanius*) introduced to enclosures that had previously experienced high vole density and significant exploitation of the food supply, grew well and showed no negative effects. These results concur with later experimental studies on *Microtus* voles in Western Finland by Klemola *et al.* (2000a,b); there was no evidence of detrimental effects of previous grazing on population growth, reproduction or body condition of voles. Therefore, the impact of plant-based factors on the dynamics of vole populations has been the subject of some debate in ecology.

1.4 Application of delay differential equations in population dynamics

A common strand through both systems examined in this thesis is the use of delay differential equations (DDEs) to model the population dynamics. Delays are inherent in many biological processes, and hence many population models include a delay (Kuang, 1993; Smith, 2010). As an example, a simple DDE model in population dynamics is the delayed logistic (Hutchinson, 1948):

$$\frac{dN(t)}{dt} = r_0 N(t)\left[1 - \frac{N(t-\tau)}{k}\right]$$

where τ is the delay. In this model, the birth and death rates are not clearly distinguished. A more realistic model is

$$\frac{dN}{dt} = B(N(t-\tau)) - D(N(t)) \tag{1.1}$$

(Nisbet and Gurney, 1982). The death rate is a function of current population density. To represent developmental delays, the birth rate depends on the population density some time in the past. This general model is used in the investigation of Nicholson's blowflies. Nicholson's (1954, 1957) data from laboratory cultures of the sheep blowfly *Lucillia cuprina* shows population fluctuations. Model (1.1) with biologically plausible functions and parameter values predicts population cycles that are very similar to those observed by Nicholson: for instance, the 'double-peak' form of the observed cycles is captured. This example demonstrates the use of DDE models in population biology, and shows how they can realistically represent ecological systems.

1.5 Outline of thesis

Chapter 2 describes the host–pathogen model developed to determine the dynamical consequences of density-dependent prophylaxis (DDP). We examine the effects of DDP on the tendency of the system to undergo population cycles. Our results demonstrate that the delay in the onset of DDP determines its impact on the population dynamics. This chapter closes with a discussion of the biological implications of our theoretical findings. Details of the numerical method used to produce the results presented in Chapter 2 are given in Chapter 3. In addition, Chapter 3 explores the interesting dynamical behaviours that occur when the length of the delay is increased.

Chapter 4 introduces the field vole population of Kielder Forest, and the hypothesis that silica is contributing to the cyclic dynamics of the voles. This chapter is a combination of experimental and mathematical modelling work: we use the empirical findings to construct and parameterise a model for this system. Using this model, we predict cycles of a similar period to those seen in the field. We extend our model of this system to include seasonal forcing of the vole birth rate. In Chapter 5 we explore the effects of different seasonal mechanisms; specifically, we compare the impact of a variable breeding season length with a fixed birth rate within the season, with a fixed breeding season length and a variable birth rate within the season. We find that the variable season length is the more powerful driver of multi-year cycles.

In Chapter 6 we look at a vole–predator model, and examine the relative significance of a variable season length and predation in causing multi-year cycles. Our findings indicate that in this case, predation is the more significant factor.

The final chapter is a discussion that summarizes the main findings of this study and describes possible directions for future work.

Chapter 2

The population dynamical consequences of density-dependent prophylaxis

This chapter is based largely on material published in the Journal of Theoretical Biology (Reynolds *et al.*, 2011). This paper is a collaboration between Jennifer Reynolds, Andrew White, Jonathan Sherratt and Mike Boots. The model was developed by Jennifer Reynolds, Andrew White and Jonathan Sherratt, with biological input from Mike Boots. Jennifer Reynolds and Jonathan Sherratt worked together on the writing of the continuation code used to determine stability boundaries (details of which are given in Chapter 3). Jennifer Reynolds performed the model simulations and numerical analysis and wrote the paper, with comments from all co-authors.

When infectious disease transmission is density-dependent, the risk of infection will tend to increase with host population density. Since host defence mechanisms can be costly, individual hosts may benefit from increasing their investment in immunity in response to increasing population density. Such "density-dependent prophylaxis" (DDP) has now indeed been demonstrated experimentally in several species. However, it remains unclear how DDP will affect the population dynamics of the host–pathogen interaction, with previous theoretical work making conflicting predictions. We develop a general host–pathogen model and assess the role of DDP on the population dynamics. The ability of DDP to drive population cycles is critically dependent on the time delay between the change in density and the subsequent phenotypic change in the level of resistance. When the delay is absent or short, DDP destabilises the system. As the delay increases, its destabilising effect first diminishes and then DDP becomes increasingly stabilising. Our work highlights the significance of the time delay and suggests that it must be estimated experimentally

or varied in theoretical investigations in order to understand the implications of DDP for the population dynamics of particular systems.

2.1 Introduction

Given the ubiquity of parasites and pathogens in nature, and the fitness costs associated with disease, there is a clear advantage to the host in investment in defence. However, it is well established that the activation and deployment of the immune system may be costly (e.g. McKean *et al.*, 2008; Schmid-Hempel, 2003) and indeed a significant part of the disease that many infectious agents cause results from immuno-pathology (Graham *et al.*, 2005; Long *et al.*, 2008; Moret and Schmid-Hempel, 2000; Sadd and Siva-Jothy, 2006). In addition, there is good evidence that there are evolutionary costs to the maintenance of defence in the absence of parasites and pathogens (e.g. Boots and Begon, 1993; Kraaijeveld and Godfray, 1997). Hence, we would expect natural selection to favour individuals that invest more when there is the greatest threat of disease. Individuals should benefit from tailoring their allocation of resources to immunity in order to match the perceived risk of exposure to disease.

If transmission is positively density-dependent (Anderson and May, 1979; Ryder *et al.*, 2005, 2007), the risk of infection may increase at high density leading to the idea that it may be optimal to invest more in defence in crowded conditions (Barnes and Siva-Jothy, 2000; Wilson and Reeson, 1998; Wilson *et al.*, 2002). There is now experimental evidence of such "density-dependent prophylaxis" (DDP) in a number of systems, with further evidence coming from comparative studies of social and solitary species (Barnes and Siva-Jothy, 2000; Cotter *et al.*, 2004; Hochberg, 1991a; Reeson *et al.*, 1998; Wilson and Reeson, 1998; Wilson *et al.*, 2002). For example, larvae of both the Oriental armyworm *Mythimna separata* and the African armyworm *Spodoptera exempta* show increased viral resistance when reared at high population densities (Kunimi and Yamada, 1990; Reeson *et al.*, 1998). Mealworm beetles (*Tenebrio molitor*) reared at high larval densities show lower mortality when exposed to a generalist entomopathogenic fungus, compared to those reared singly (Barnes and Siva-Jothy, 2000). Similarly, Wilson *et al.* (2002) found that desert locusts (*Schistocerca gregaria*) reared under crowded conditions were significantly more resistant to an entomopathogenic fungus than solitary locusts. Furthermore, a recent study on adult bumble-bee workers (*Bombus terrestris*) concluded that there is rapid plasticity in immunity levels dependent on social context (Ruiz-González *et al.*, 2009). This demonstration of DDP in adults suggests that it may be a widespread phenomenon, and considerably broadens its potential significance. It is therefore important to examine the impact that DDP may have on the population

dynamics of both the host and the parasite.

There has been some theoretical examination of the effect of DDP on host–parasite population dynamics. White and Wilson (1999) used a discrete-time model, representing non-overlapping insect generations, and found that if the density-dependent effect is sufficiently small, it stabilises the dynamics. Reilly and Hajek (2008) developed a framework with a continuous-time model for host and pathogen within the season and a discrete-time map between seasons with a model structure related to gypsy moth–virus interactions. In contrast to White and Wilson (1999), they reported that DDP has a destabilising effect on the population. Here, we present a general continuous-time model framework that allows the effects of DDP to be understood in more detail. There is a well established literature on continuous models (e.g. Anderson and May, 1981; Bowers *et al.*, 1993; White *et al.*, 1996), so a continuous framework is used here to ensure that comparisons can be drawn with other studies. Our model enables us to produce specific and widely applicable conclusions. The aim is to thoroughly examine the implications of DDP for population dynamics and reconcile the current differences in the predictions of the theoretical studies.

2.2 The model

Our aim is to produce a general theoretical framework and we therefore choose a classic model framework for representing hosts infected by free-living stages. Much of the evidence for DDP has been found in invertebrate systems and therefore we use a baseline model without acquired immunity. We examine the effects of DDP on the stability of the system by examining the likelihood of population cycles. Our framework is an extension of Anderson and May's (1981) Model G that includes self-regulation of the host (Bowers *et al.*, 1993). The Bowers *et al.* (1993) model was developed to investigate the possible role of pathogens in the cyclic dynamics of forest insect pests. We consider a system in which the host population is composed of susceptibles, with density X, and infecteds, with density Y (total density $H = X + Y$), and with a free-living pathogen with density of infective stages W. The dynamics are represented by the following system of differential equations:

$$\frac{dH}{dt} = rH\left(1 - \frac{H}{K}\right) - \alpha Y \tag{2.1}$$

$$\frac{dY}{dt} = \beta W(H - Y) - (\alpha + b)Y \tag{2.2}$$

$$\frac{dW}{dt} = \lambda Y - \mu W. \tag{2.3}$$

Here we choose to use the differential equation for total host density (equation (2.1)), but we could interchange this with one for the susceptible host density (equation (2.4) below). For clarity, the model in terms of X, Y and W consists of equations (2.2) and (2.3) together with:

$$\frac{dX}{dt} = (r+b)(X+Y) - bX - r\frac{(X+Y)^2}{K} - \beta WX. \tag{2.4}$$

The model assumes that host self-regulation acts on birth rate and that both susceptible and infected hosts can die naturally. Susceptible hosts can become infected through contact with free-living infective stages of the pathogen, and once infected experience additional mortality due to the disease. Infected hosts also release infective stages at a constant rate and these stages are lost through natural decay. Descriptions of the parameters in the model are given in Table 2.1. We have used as our reference parameter values those from Bowers *et al.* (1993). The effective rate of production of infective stages, λ, is large in relation to the other rate parameters because pathogens are typically highly productive (Anderson and May, 1981). Throughout this study, units of time are years and units of abundance are individuals per unit area.

Parameter	**Meaning**
r	Intrinsic rate of net increase of the host (birth rate − death rate b)
K	Host carrying capacity
α	Rate of disease-induced mortality
β	Transmission coefficient of the disease
b	Natural host death rate
γ	Recovery rate of the host (included in an extension of the model: see Discussion)
λ	Rate at which an infected host produces infective stages of the pathogen
μ	Decay rate of the infective stages of the pathogen
p	Measure of the reduction in β caused by DDP
β_0	Transmission coefficient of the disease when there is no DDP
τ	Delay in onset of DDP, as a proportion of the average host lifespan ($1/b$)

Table 2.1: Model parameter definitions. Values of the parameters that remain unchanged for all figures are: $r = 1$, $K = 1$ and $\beta_0 = 0.0001$. Units of time are years and units of abundance are individuals per unit area; see Bowers *et al.* (1993) for details.

Under DDP, when host density H is high, individuals invest more in resistance mechanisms, and therefore the transmission rate of the disease is reduced. To represent this density-dependent response, we modify the above model by changing β

from a constant parameter to a density-dependent term. For simplicity, we take β to be a simple linear function that decreases as $H(t)$ increases:

$$\beta = \beta_0 \left(1 - \frac{p}{100K} H(t)\right). \tag{2.5}$$

Here β_0 is a constant and p represents the percentage reduction in β caused by the prophylactic response when $H(t) = K$. For example, when $p = 20$, there is a 20% reduction in β at $H(t) = K$ (see Figure 2.1). Note that as $H(t) \leq K$, the function β is always non-negative.

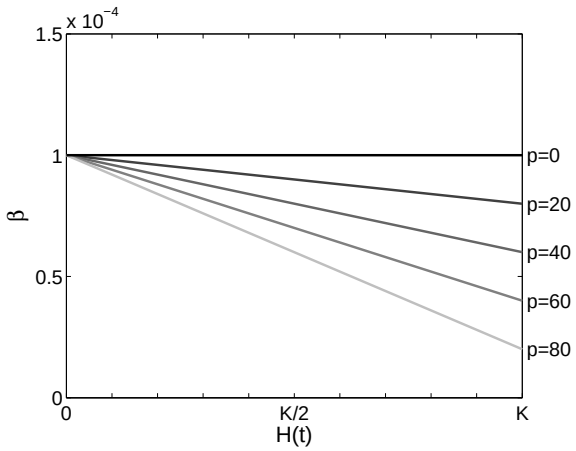

Figure 2.1: The disease transmission rate β is a function of $H(t)$. This figure shows β for DDP of varying strengths, i.e. different p values. The horizontal line ($p = 0$) represents no prophylactic response.

2.3 Population dynamics

The model framework (equations (2.1)–(2.3)) has three steady states: the trivial state ($H = 0$, $Y = 0$, $W = 0$), which is always unstable since we assume $r > 0$, the disease-free state ($H = K$, $Y = 0$, $W = 0$) and an infected state (H^*, Y^*, W^*) where

$$\begin{aligned} Y^* &= \frac{r}{\alpha} H^* \left(1 - \frac{H^*}{K}\right) \\ W^* &= \frac{\lambda}{\mu} Y^* \end{aligned}$$

and H^* is a solution to the cubic equation

$$(H^*)^3\left(\frac{pr}{100\alpha K^2}\right)-(H^*)^2\left(\frac{r}{\alpha K}+\frac{pr}{100\alpha K}-\frac{p}{100K}\right)+H^*\left(\frac{r}{\alpha}-1\right)+\frac{\mu(\alpha+b)}{\lambda\beta_0}=0. \tag{2.6}$$

This cubic equation always has one negative root, which is not ecologically relevant. The two roots that remain can both be complex, in which case there is pathogen extinction. Otherwise there are two positive, real roots. In most cases, one is less than K and one is greater than K, the latter not being relevant. Both can be greater than K, so neither is relevant: in this case pathogen extinction occurs. For some parameters, both roots are less than K. This means that both are potentially relevant to ecological applications. However, the larger root corresponds to a steady state that is always unstable. We focus on the smaller of the two roots when this case arises (see Appendix A for further discussion).

The basic reproduction rate of the pathogen is

$$R(X)=\frac{\lambda\beta_0\left(1-\frac{p}{100}\frac{X}{K}\right)X}{\mu(\alpha+b)}.$$

The maximum of this, denoted by R_{max}, depends on the strength of DDP as follows:

$$R_{max}=\begin{cases} R(X=K) & \text{for} \quad p<50 \\ R(X=50K/p) & \text{for} \quad p\geq 50. \end{cases}$$

Pathogen extinction occurs for $R_{max}<1$. R_{max} decreases as p increases, so DDP makes it more difficult for the disease to persist. (See Appendix A for further details.)

For certain parameter values the infected state is unstable, and then one expects population cycles of host and pathogen to occur (Anderson and May, 1981; Bowers *et al.*, 1993; White *et al.*, 1996). To investigate the effect of DDP on the population dynamics, we explore the boundary in parameter space between the occurrence of cycles and the endemic equilibrium being stable.

2.4 Results

We examine how DDP affects the propensity of cycles in disease parameter space. Figure 2.2(a) shows $\alpha-\lambda$ parameter space partitioned into the regions where cycles and no cycles occur. Parameters α and λ are key to the characterisation of the disease, since α is the disease-induced mortality rate, and λ is the rate at which an infected host produces infective stages of the disease. When there is no DDP ($p=0$), the boundary is equivalent to that calculated in Bowers *et al.* (1993).

As the strength of the prophylactic response increases (p increases), the parameter region giving cycles becomes larger, and so the system is destabilised. We therefore conclude that DDP that depends on current host density acts to induce cycles.

2.4.1 Delay in onset of DDP

Thus far we have incorporated DDP by setting the transmission rate of the disease to be a function of current host density. In reality, there is likely to be a delay between the assessment of density and the subsequent adjustment in the investment in defence. Experimental evidence indicates that this delay may be short, with DDP being elicited rapidly in adults (Ruiz-González *et al.*, 2009), or relatively long, with early instar density determining the level of defence in later instars or adults (e.g. Reeson *et al.*, 1998). Previous theoretical studies (White and Wilson, 1999; Reilly and Hajek, 2008) include a delay (implicitly or explicitly), but only consider a single fixed delay length. Our aim is to examine in detail how the delay may affect the population dynamics. To include the delay in DDP in our model, we change the dependence on $H(t)$ in equation (2.5) to a dependence on $H(t-\tau/b)$, with delay τ/b. Here, the parameter τ represents the delay as a proportion of the average lifespan of the host ($1/b$), and is therefore between 0 and 1.

Figure 2.2(b) shows the results when the proportional time delay $\tau = 0.99$. At this time delay, increases in the strength of DDP act to reduce the size of the region of parameter space that gives rise to population cycles, and therefore DDP stabilises the system. As the time delay is increased there is a transition from the situation where DDP has a destabilising effect (Figure 2.2(a)) to one where DDP has a stabilising effect (Figure 2.2(b)). A change in the time delay can cause the effect of DDP to be reversed. Therefore a key new result is that the effect of DDP depends critically on the length of the delay.

In order to examine the effects of changing the time delay in more detail, we look at the interactions between τ and other parameters in the model. Non-dimensionalisation reveals that there are only three independent parameter groupings, in addition to p and τ. Variations in these parameter groupings can be considered via changes in α, μ and λ (see Appendix B for mathematical details). Figures 2.3 and 2.4 show the boundaries in parameter space between regions of cycles and no cycles, for different parameter combinations and different strengths of the DDP response. Cycles occur for low values of the pathogen decay rate (Figure 2.3(a)) and for high values of the rate at which infected hosts produce infective stages of the pathogen (Figure 2.3(b)). These results support previous findings that did not involve a prophylactic response or a time delay (Anderson and May, 1981; Bowers *et al.*, 1993; White *et al.*, 1996), but also emphasize how the region of parameter

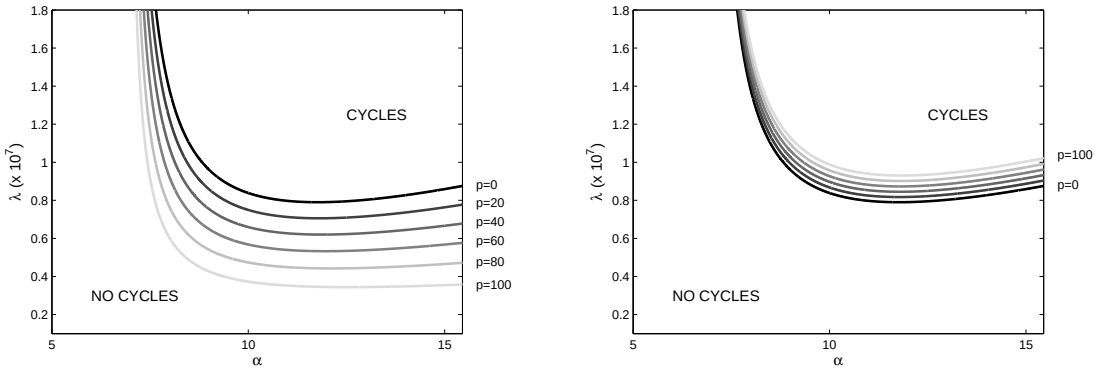

(a) (b)

Figure 2.2: The divisions in $\alpha - \lambda$ parameter space between cyclic behaviour and no cycling, for a series of p values. In (a) there is no delay ($\tau = 0$); in (b) there is a within generational delay ($\tau = 0.99$). For the $p = 0$ case, as we have no delay term, we can find the boundary between the two regions by consideration of the Routh–Hurwitz stability criteria. (With the characteristic equation in the form $z^3 + Az^2 + Bz + C = 0$, cycles occur when $AB - C < 0$; this partitions parameter space.) However, with $p \neq 0$, the model comprises delay differential equations, and the characteristic equation can no longer be solved algebraically. Instead, we take a point on the $p = 0$ curve and use this as a starting point for numerical continuation in p up to a particular value of p, for instance $p = 20$, tracking the passing of eigenvalues across the imaginary axis. Once a point on the $p = 20$ boundary curve is obtained, we change to numerical continuation in α, keeping p fixed. In this way, we can trace the stability boundary curves through parameter space. In this figure, $b = 3.3$ and $\mu = 3$.

space giving rise to cycles is modified by DDP. Additionally, intermediate values of disease-induced mortality favour cycles, provided the time delay before the onset of DDP is not large (Figure 2.4).

Figures 2.3 and 2.4 additionally allow an examination of the effects of the delay τ on the population dynamics. There is a consistent trend that as the time delay τ increases, the parameter region in which cycles are produced diminishes. Thus increasing the delay stabilises the system. These figures also clarify the effects of increasing the strength of DDP (increasing p). The value of the delay at which the lines where $p = 20$ and $p = 80$ intersect is significant. When τ is below this value, an increase in the DDP strength p destabilises the population; when τ is above the intersection value, an increase in p stabilises the population. This corresponds to a transition from a pattern such as that seen in Figure 2.2(a) to that in Figure 2.2(b). The delay at which the curves intersect does have a very slight dependence on the p values chosen, but this is negligible for practical purposes (less than 0.2%).

In summary, for short delays, an increase in the strength of DDP is destabilising,

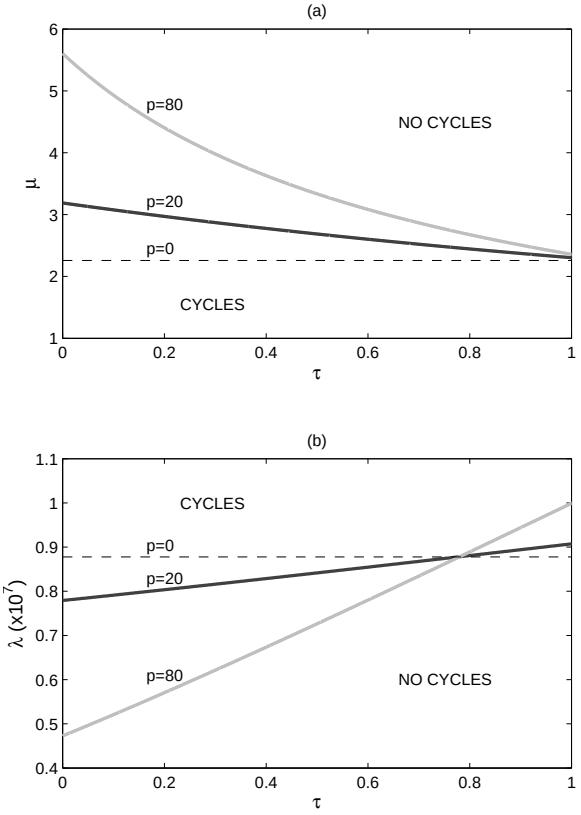

Figure 2.3: The effects of the parameters (a) μ and (b) λ on the transition to cyclic dynamics. For each figure, one parameter is varied and others are fixed. Reference values: $\lambda = 8 \times 10^6$, $\mu = 3$, $\alpha = 15.5$ and $b = 3.3$. In each plot, the curves for two values of p are depicted, plus the curve for $p = 0$. In this way, the effects of changing both p and τ are shown, so that conclusions can be drawn about how both the strength of prophylaxis and the length of delay affect the population dynamics. In (a), there are cycles below each line and no cycles above; in (b), there are cycles above each line and no cycles below. The time delay τ is expressed as a proportion of the average lifespan of the host, $(1/b)$.

and can significantly expand the parameter region over which population cycles are exhibited. As the delay increases, this destabilising effect of DDP is reduced, until a critical delay is reached. For delays longer than this critical value, an increase in the strength of DDP is stabilising. As the delay increases, the extent of this stabilising effect increases.

Figure 2.4 indicates how the dynamics are affected by changing underlying model parameters. As pathogen production λ increases, the parameter region giving cycles becomes larger, for both p values (compare Figure 2.4 (a)–(c)). In contrast, as pathogen decay μ increases, the region giving cycles becomes smaller (compare Figure 2.4 (d), (b) and (f)). Therefore, increasing the rate at which an infected host produces infective stages of the pathogen destabilises the dynamics, whereas

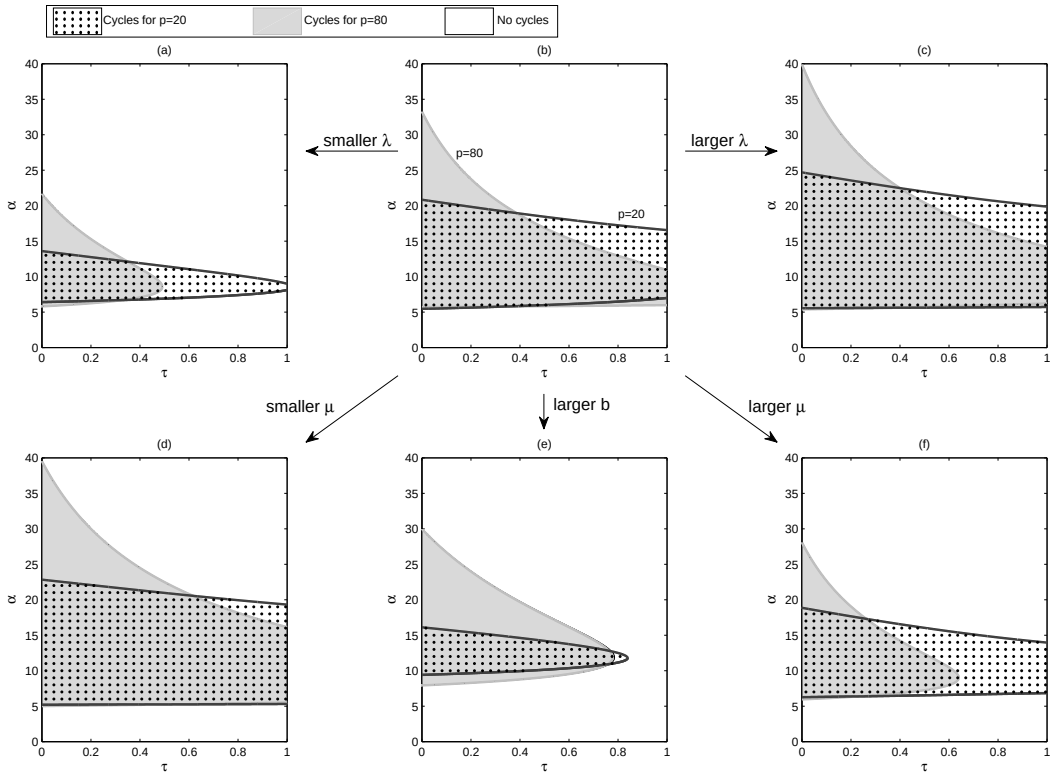

Figure 2.4: The effects of parameter α on the transition to cyclic dynamics, and how these change when other parameters are varied. For (b) the fixed parameters are $\mu = 3$, $\lambda = 8 \times 10^6$ and $b = 1.65$. The remaining panels show the results of changing each of these parameters in turn from this reference parameter set. Parameter values: (a) $\lambda = 5 \times 10^6$; (c) $\lambda = 10 \times 10^6$; (d) $\mu = 2$; (e) $b = 3.3$; (f) $\mu = 4$. Note that the value of b in (e) is the value used in previous figures. The time delay τ is expressed as a proportion of the average lifespan of the host, $(1/b)$. The regions of cycles for $p = 20$ are dotted black and the regions of cycles for $p = 80$ are shaded grey.

increasing the pathogen decay rate is stabilising. In addition to studying the effects of changing the disease parameters, we also look at changing the natural host death rate b. Increasing b reduces the average lifespan of the host. As the host death rate increases, the region of cycles becomes smaller, and therefore the system is stabilised (compare Figure 2.4 (b) and (e)). This figure shows that the critical point where the $p = 20$ and $p = 80$ lines intersect is parameter-dependent: it increases as b gets larger and as μ gets smaller. However, it is relatively insensitive to changes in λ. The implication of this is that for high pathogen decay rates and small host death rates (i.e. long lifespan), the effect of increasing the strength of DDP reverses at time delays that are relatively short as a proportion of the average host lifespan.

Typical population dynamics for parameters in the cycling region are shown in Figure 2.5. Cycles arise because as host density increases, an epidemic is triggered, and there is a rapid increase in pathogen numbers. This causes an increase in

infection, and a subsequent fall in host density. This leads to a decline in pathogen numbers, allowing host density to increase once again. For a fixed parameter set, an increase in the level of DDP can change the nature of the cycles generated (Figure 2.5). For all other parameters fixed, changing the DDP strength p moves

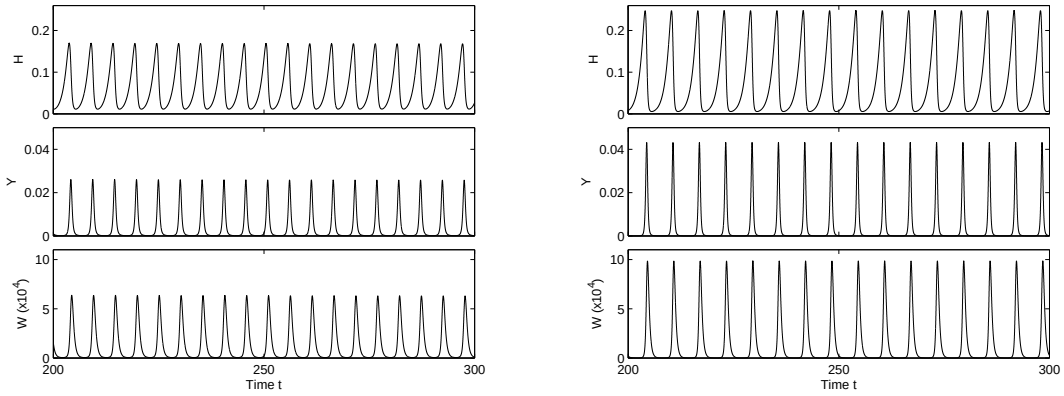

(a) (b)

Figure 2.5: Cyclic dynamics at equilibrium. Parameter values: $\tau = 0.33$, $\alpha = 14$, $\lambda = 1 \times 10^7$, $b = 3.3$, $\mu = 3$ and (a) $p = 20$, (b) $p = 80$. The cycles in (b) are of higher amplitude and have a longer period. These simulations are produced by MATLAB using the delay differential equation solver dde23. Solutions are shown after running for 200 time units to ensure decay of transients. The initial conditions were $H = 0.2$, $Y = 0.01$ and $W = 1 \times 10^2$, but the long-term dynamics shown are not sensitive to initial conditions.

the boundary of cycles. Changing the boundary so the point in parameter spaces lies deeper within the cycle region tends to increase both the period and amplitude of the cycles (Anderson and May, 1981).

2.5 Discussion

Density-dependent prophylaxis (DDP) is hypothesised to be a widespread phenomenon in natural systems (Wilson and Reeson, 1998). However, the impact of DDP on the population behaviour of outbreaking species is yet to be critically evaluated (Klemola *et al.*, 2007). In this study we develop a theoretical framework to explore the population dynamical impact of DDP. We have shown that increasing the strength of the prophylactic response can be either stabilising and destabilising, depending on the delay between the assessment of density and the adjustment in resistance. When the delay is absent or short, DDP is destabilising; as the de-

lay increases, its destabilising effect diminishes and, once a threshold in the delay is exceeded, it becomes increasingly stabilising. This highlights the importance of the delay and indicates that it is essential to either estimate the delay in natural / laboratory systems or vary the delay in mathematical models to understand the influence of DDP on population dynamics in any given system.

Previous theoretical studies that have examined DDP have (implicitly or explicitly) considered a single fixed delay for the onset of DDP (White and Wilson, 1999; Reilly and Hajek, 2008). These studies report conflicting findings for the impact of DDP, with it either stabilising (White and Wilson, 1999) or destabilising (Reilly and Hajek, 2008) the population behaviour. Our analysis shows that the dynamical outcomes depend critically on the delay length and this could explain the apparent contradiction between these studies.

DDP is most commonly reported in insect–pathogen systems in which the infection is often lethal and therefore in the above analysis we considered a model without recovery from infection. However, to test the generality of our findings, we also studied an extension of our model framework that includes recovery (γ) (see legend to Figure 2.6 for details). Our conclusions are unaffected by the inclusion of recovery: there is a parameter-dependent delay value below which an increase in the strength of DDP is destabilising, and above which such an increase is stabilising (Figure 2.6). Recovery decreases the size of the region of $\alpha - \lambda$ parameter space where cycles arise (Figure 2.6) and therefore increasing recovery is generally stabilising. This agrees with our intuition and is consistent with previous findings that indicate that recovery, in the absence of DDP effects, reduces the likelihood of cycles (Norman *et al.*, 1994).

It has been postulated that DDP is likely to be manifested particularly in insect species exhibiting population cycles and / or outbreaks (Wilson and Reeson, 1998). Indeed, several of the species for which DDP has been experimentally demonstrated are prone to outbreaks which can cause widespread damage to natural vegetation and crops, for example the desert locust *Schistocerca gregaria* (Wilson *et al.*, 2002), the African armyworm *Spodoptera exempta* (Reeson *et al.*, 1998) and the Oriental armyworm *Mythimna separata* (Kunimi and Yamada, 1990). Changes in disease-transmission rate due to density-dependence are known to strongly influence population dynamics (Hochberg, 1991b), and it has been predicted that the lower rates of transmission among high-density populations caused by DDP may destabilise host–pathogen interactions and contribute to the large outbreaks characteristic of the insect populations concerned (Reeson *et al.*, 1998). Our findings confirm that DDP does have a significant impact on the population dynamics, and could be a key factor driving outbreaks and cycles, providing the delay in its onset is sufficiently small. When the time until the onset of DDP is short, individuals can rapidly in-

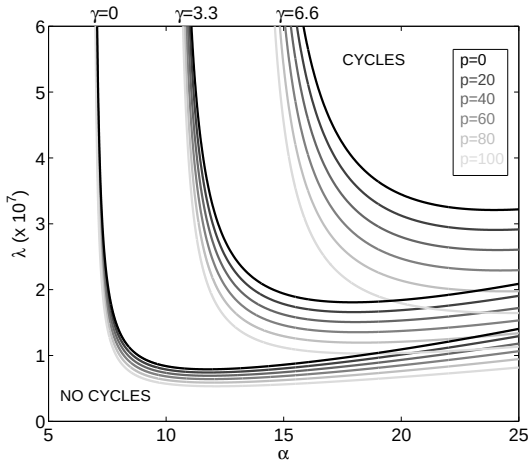

(a)

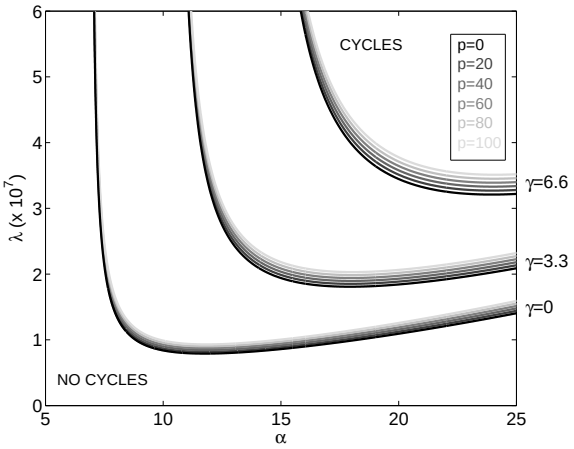

(b)

Figure 2.6: Recovery γ stabilises the disease dynamics. (a) shows the results for delay $\tau = 0.33$ and (b) for $\tau = 0.99$. To add recovery to the model, we add a $-\gamma Y$ term to equation (2.2), giving $dY/dt = \beta W(H - Y) - (\alpha + b + \gamma)Y$. Curves are shown for two non-zero values of recovery: $\gamma = 3.3$ and $\gamma = 6.6$, and for a range of p values. As γ increases, the cycling region is reduced. Increasing p gives the same trends for $\gamma > 0$ as for $\gamma = 0$. In this figure, $b = 3.3$ and $\mu = 3$ and the time delay τ is expressed as a proportion of the average lifespan of the host, $(1/b)$.

crease resistance at high host densities, resulting in lower than expected rates of transmission and reducing the capacity for the pathogen to regulate the population. This destabilises the host–pathogen interaction and may contribute to the boom-and-bust nature of the population dynamics (Reeson *et al.*, 1998). Furthermore, our results indicate that the peak and period of population cycles are affected by the extent of DDP. Therefore, DDP may have important implications for the duration and size of outbreaks and will need to be considered when developing biological control strategies to manage pest species.

Pathogens are important agents in the regulation of host populations and there has been extensive debate into their role in driving and modulating host outbreaks (e.g. Berryman, 1996; Klemola *et al.*, 2007; Sherratt and Smith, 2008). For cyclic insect populations it has been suggested that although pathogens may promote population oscillations they are unlikely to be the sole driver of cycles since in model systems the population density at the peak of the oscillations is well below outbreak levels (Bowers *et al.*, 1993; White *et al.*, 1996). Extensions to these models that include a time delay in host self-regulation or include additional model complexity to better represent insect–pathogen systems show an increased propensity to cycle (Bonsall *et al.*, 1999, Xiao *et al.*, 2009). Our findings show that the inclusion of DDP could operate in a similar manner. In particular, provided the delay before the onset of DDP is short, we predict an increase in the parameter regions over which cycles are exhibited and an increase in the amplitude of population oscillations.

Our key result is that the time delay between the assessment of population density and the change in host defence is critical in determining the influence of DDP on population dynamics. It would be relatively straightforward to design laboratory experiments to estimate this delay. We propose a possible experimental protocol with a population of an insect species and an appropriate virus. Prior to the experiment, the insect population is kept at low density. At the start of the experiment, half of the population is transferred to high density conditions and half kept at low density. At regular time intervals, a number of individuals from each set are challenged with the virus and the proportion of those that become infected is recorded. Initially the proportion infected in the low and high regimes should be similar, but once the DDP effect is induced (after the delay τ/b) the individuals in the high regime will have an increased level of resistance and therefore a decreased prevalence of infection should be observed (see Figure 2.7). This would allow the delay parameter to be estimated and could feedback to theoretical assessments of population dynamics. This would be highly informative: quantitative predictions could be made about the impact of DDP and this would further inform the debate on the role of pathogens in driving population cycles.

Outbreak pest species continue to cause major economic problems and one of the best studied examples of DDP is in a classic outbreak pest species, the locust (Wilson *et al.*, 2002). It is of great importance to understand whether their natural parasites through processes such as DDP help to generate their unstable population dynamics. Furthermore, pathogens are increasingly proposed as control agents for insect pests where there is the need for stable control. What our work emphasises is that it is the delay between increases in density and increased investment in immunity that is critical. Where it is not possible to measure this delay experimentally, any models built to assess the role of parasites and pathogenic control agents in specific systems

need to assess the role of the delay. We have found that DDP can be stabilising or destabilising. Short-lived host species faced with long-lived free-living parasites are most likely to be destabilised by DDP, but the delay is critical to the outcome.

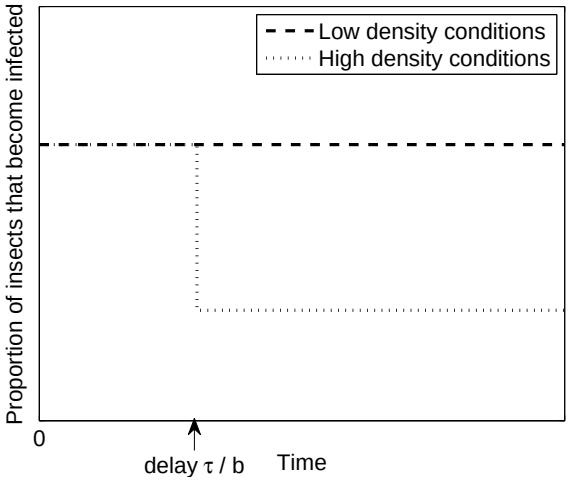

Figure 2.7: Expected outcome of the experimental procedure outlined in the Discussion. The delay τ/b could be read off from experimental data as indicated.

2.6 Appendix A

In this appendix we explain the conditions under which there is pathogen extinction. For the model *without* DDP, the basic reproductive rate, R, of the pathogen is

$$R(X) = \frac{\lambda\beta X}{\mu(\alpha + b)}$$

where β is constant. When $R < 1$ the disease cannot persist (the disease-free steady state is stable). In the absence of DDP, disease persistence is determined by assessing R in a disease-free population at the host carrying capacity, $R_0 = R(K)$. Disease extinction occurs if $R_0 < 1$.

For our model, with density-dependent β, R can be written

$$R(X) = \frac{\lambda\beta_0 \left(1 - \frac{p}{100}\frac{X}{K}\right) X}{\mu(\alpha + b)}.$$

To determine when $R < 1$ holds, we seek the largest value of $R(X)$, which we denote R_{max}. In the absence of DDP this occurred when $X = K$, however with a density-

dependent β the maximum need not occur at the carrying capacity. We differentiate R with respect to X and set to zero to give

$$X = \frac{50K}{p}.$$

For $p \geq 50$, $50K/p$ is on $X = [0, K]$. So

$$R_{max} = R(X = 50K/p) \text{ for } p \geq 50.$$

(Note for $p = 50$, $50K/p = K$.) For $p < 50$, $50K/p > K$, which is not relevant. The maximum on $X = [0, K]$ is at $X = K$ (see Figure 2.8), so

$$R_{max} = R(X = K) \text{ for } p < 50.$$

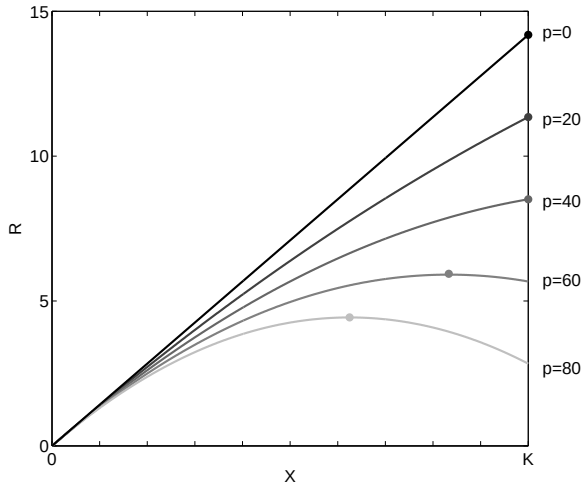

Figure 2.8: The basic reproductive rate of the infection (R) needs to be calculated at different values of the density of susceptible hosts (X) depending on the strength of DDP (i.e. the value of p). This figure shows function $R(X)$ for different values of p, for representative parameter values, which are $\lambda = 8 \times 10^6$, $\mu = 3$, $\alpha = 15.5$ and $b = 3.3$. For $p < 50$, the maximum of $R(X)$ occurs for $X > K$, which is not relevant. So we take $R_{max} = R(K)$ as this is the maximum within $X = [0, K]$. For $p \geq 50$, the maximum of $R(X)$ lies within $X = [0, K]$ at $X = 50K/p$. The R_{max} value for each p is indicated with a dot.

Figure 2.8 shows that for any given X, $R(X)$ decreases as p increases, making pathogen extinction more likely. Thus DDP acts to make disease persistence more difficult.

For sufficiently large p, and for appropriate values of the other parameters, a

stable disease-free steady state coexists with an ecologically relevant infected steady state. This links to the roots of cubic equation (2.6): this case occurs when there are two positive roots less than K. The cubic equation always has one negative root; Figure 2.9 illustrates all possible cases for the two remaining roots. In the

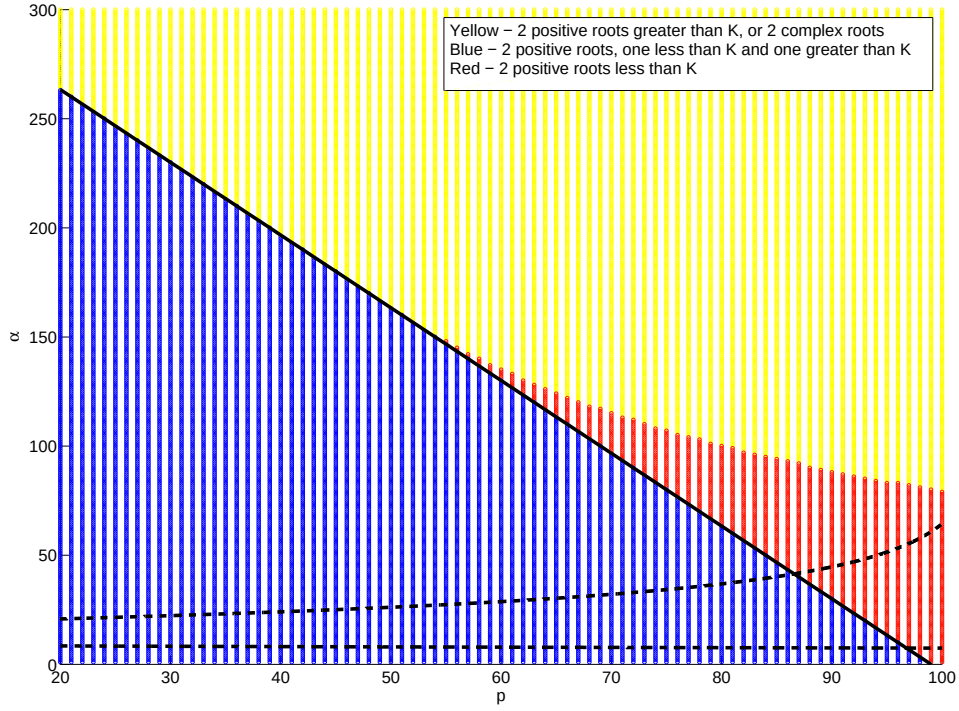

Figure 2.9: Division of $p-\alpha$ parameter space into three coloured regions depending on the nature of the roots of the cubic equation (2.6). The cubic always has one negative root. The remaining roots can either be both complex or both real and positive. When both are real and positive, there are distinct cases: both roots greater than K; one greater than K and one less than K; both less than K. When complex or greater than K, a root is not ecologically relevant. Above and to the right of the solid black line, the disease-free steady state ($H = K, Y = 0, W = 0$) is stable. Below and to the left of the solid black line, this steady state is unstable. Between the dashed black lines, the infected steady state is unstable (cycles are produced). We use $p-\alpha$ parameter space in which all three regions are clearly depicted.

yellow region of Figure 2.9, pathogen extinction occurs; there is no other relevant steady state and the disease-free steady state is stable. In the blue region, there is just one relevant infected equilibrium, the stability of which is discussed as the main topic of this chapter. The disease-free steady state is unstable here. Further analysis is required in the case where there are two potentially relevant infected

steady states, i.e. two roots less than K. This occurs for parameter values in the red region. The larger of the two roots corresponds to a steady state which is always unstable, while the equilibrium corresponding to the smaller root can be either stable or unstable (giving cycles). The disease-free steady state is stable in this region, and for certain initial population densities, the population tends to the disease-free steady state. Numerical studies suggest that there is a separatrix in phase space, passing through the (unstable) steady state which corresponds to the larger cubic root. This separatrix divides phase space and determines the basins of attraction for the two steady states. We are interested in the dynamics when disease is present, so we focus on this region of phase space, rather than on behaviour in the basin of attraction of the disease-free steady state.

2.7 Appendix B

In this appendix, mathematical details of the non-dimensionalisation of the model (equations (2.1)–(2.3)) are given. This non-dimensionalisation is used to determine which parameters should be varied when undertaking a sensitivity analysis of the findings.

We first set the following dimensionless variables:

$$H' = H/H_s,\ Y' = Y/Y_s,\ W' = W/W_s \text{ and } t' = t/t_s.$$

So

$$\begin{aligned}\frac{dH}{dt} &= \frac{d(H'H_s)}{d(t't_s)} = \frac{H_s}{t_s}\frac{dH'}{dt'} \\ &= rH'H_s(1 - \frac{H'H_s}{K}) - \alpha Y'Y_s\end{aligned}$$

and multiplying by t_s/H_s gives

$$\frac{dH'}{dt'} = rH't_s\left(1 - \frac{H'H_s}{K}\right) - \frac{\alpha Y'Y_s t_s}{H_s}.$$

Similarly,

$$\begin{aligned}\frac{dY}{dt} &= \frac{d(Y'Y_s)}{d(t't_s)} = \frac{Y_s}{t_s}\frac{dY'}{dt'} \\ &= \beta W'W_s(H'H_s - Y'Y_s) - (\alpha + b)Y'Y_s\end{aligned}$$

and multiplying by t_s/Y_s gives

$$\frac{dY'}{dt'} = \frac{\beta W' W_s t_s}{Y_s}(H'H_s - Y'Y_s) - (\alpha + b)Y't_s.$$

Also,

$$\begin{aligned}\frac{dW}{dt} &= \frac{d(W'W_s)}{d(t't_s)} = \frac{W_s}{t_s}\frac{dW'}{dt'} \\ &= \lambda Y'Y_s - \mu W'W_s\end{aligned}$$

and multiplying by t_s/W_s gives

$$\frac{dW'}{dt'} = \frac{\lambda Y'Y_s t_s}{W_s} - \mu W't_s.$$

We can thus re-express the model equations.

Parameters can be eliminated by an appropriate selection of t_s, H_s, Y_s and W_s. Choosing

$$t_s = 1/r,\ H_s = Y_s = K \text{ and } W_s = r/\beta$$

gives

$$\begin{aligned}\frac{dH'}{dt} &= H'(1 - H') - \frac{\alpha}{r}Y' \\ \frac{dY'}{dt'} &= W'(H' - Y') - \frac{(\alpha + b)}{r}Y' \\ \frac{dW'}{dt'} &= \frac{\lambda K \beta}{r^2}Y' - \frac{\mu}{r}W'.\end{aligned}$$

This dimensionless form shows that there are four independent parameter groupings:

$$\alpha/r,\ b/r,\ \mu/r \text{ and } \lambda K\beta/r^2.$$

To cover all cases, it is therefore enough to consider variations in α, b, μ and λ. Note that in the Discussion, we comment on an extended model which includes recovery γ. Changing γ is akin to changing b and keeping r constant. Thus, since we look at the effects of changing γ, we are left with only three other parameters that we need to vary: α, λ and μ.

Chapter 3

Further exploration of the density-dependent prophylaxis model

This chapter gives further details on the host–pathogen model developed in Chapter 2 to represent density-dependent prophylaxis (DDP). The first section describes the numerical method used to determine the stability boundaries presented in Chapter 2, and gives some background information on delay differential equations. In Section 3.2 we explore the population dynamical consequences of increasing the delay term in the model. The complex structure of the parameter space giving cycles for long delays is described and discussed.

3.1 Details of the continuation method

In this section, details are given of the numerical technique used in Chapter 2. The model developed in Chapter 2 to represent DDP is as follows:

$$\frac{dH(t)}{dt} = rH(t)\left(1-\frac{H(t)}{K}\right) - \alpha Y(t) \tag{3.1}$$

$$\frac{dY(t)}{dt} = \beta_0\left(1-\frac{p}{100K}H(t-\tau/b)\right)W(t)(H(t)-Y(t)) - (\alpha+b)Y(t) \tag{3.2}$$

$$\frac{dW(t)}{dt} = \lambda Y(t) - \mu W(t). \tag{3.3}$$

Here H is the total host population density, within which Y is the density of susceptible individuals, and W is the density of free-living stages of the pathogen population. The parameters in the model are all positive, and τ/b is the delay. We aim to assess the stability of the non-trivial steady state (H^*, Y^*, W^*), given in Chapter 2. (Note

that the equilibrium value H^* is a solution of a cubic equation (2.6).) A continuation method is used to trace stability boundaries in parameter space, coded using the mathematical software Maple.

We commence with some background information on delay differential equations (DDEs). As with ordinary differential equations (ODEs), stability properties of linear DDEs can be characterised and analysed by studying their characteristic equations. However, with DDEs this is more complicated, as the characteristic equations typically have infinitely many roots. As a simple example, consider the DDE

$$\frac{dy(t)}{dt} = y(t-T) + 2y(t).$$

We want to determine the stability of the steady state at the origin ($y = 0$). We seek solutions of the form $y(t) = e^{Et}$. Substituting this into the DDE gives first

$$Ee^{Et} = e^{Et-ET} + 2e^{Et},$$

which leads to the characteristic equation

$$e^{-ET} + 2 - E = 0.$$

Note that the eigenvalue E appears in the exponent of the first term, causing the characteristic equation to possess an infinite number of roots.

In general, for a linear DDE of the form

$$\frac{d\mathbf{x}(t)}{dt} = A_0\mathbf{x}(t) + A_1\mathbf{x}(t-T),$$

where A_0 and A_1 are matrices, the associated characteristic equation is

$$\det(-EI + A_0 + A_1e^{-TE}) = 0 \tag{3.4}$$

where I is the identity matrix. The roots E of the characteristic equation (3.4) are called *characteristic roots*.

An important point to note is that while there are an infinite number of characteristic roots, there are only a finite number of roots located to the right of any vertical line in the complex plane. Formally, given $\sigma \in \mathcal{R}$, there are at most finitely many characteristic roots satisfying $\mathrm{Re}(E) > \sigma$. (See Smith (2010, p46) for a proof.)

For a non-linear system of DDEs, like equations (3.1)–(3.3) above, one can determine linear stability by firstly linearizing the system about the equilibrium, and then analyzing the characteristic equation of the associated linear system. If all characteristic roots have negative real parts, i.e. if all roots satisfy $\mathrm{Re}(E) \leq \delta < 0$, then the equilibrium is a linearly stable steady state of the original DDE; if $\mathrm{Re}(E) > 0$ for

some characteristic root, then the equilibrium is unstable. (See Hale and Verduyn Lunel (1993) for the proof.)

We employ a numerical method to determine regions in parameter space where the equilibrium of our DDP model (equations (3.1)–(3.3)) is unstable, in which case the solutions are cyclic, and the regions where it is stable. We consider perturbations away from the infected equilibrium such that $H(t) = H^* + \epsilon\hat{H}e^{Et}$, $Y(t) = Y^* + \epsilon\hat{Y}e^{Et}$ and $W(t) = W^* + \epsilon\hat{W}e^{Et}$, where ϵ is small. We linearise about the steady state (H^*, Y^*, W^*). We are interested in tracking the point in parameter space where E cross the imaginary axis, i.e. when $\mathrm{Re}(E) = 0$. We therefore substitute $E = i\omega$ into the Jacobian matrix, and then take the determinant, in order to find points in parameter space at which there is a change of stability.

The following equations need to be solved together:

- real part of the determinant = 0;
- imaginary part of the determinant = 0;
- cubic equation (2.6) (to give H^*).

An appropriate starting guess is required for this calculation: we can use the case when $p = 0$ (no DDP and no delay), as the stability boundary can be determined algebraically for this case. In the first instance, we aim to find the stability boundary for some p, say $p = 20$ for example, in $\alpha - \lambda$ parameter space. We fix α and look for the λ value for a point on the stability boundary. We start at $p = 0$ and, using sufficiently small step sizes, we perform numerical continuation in parameter p, to locate a point on the boundary for $p = 20$. In this computation, at each step the solution for the previous step is used as the starting guess. Once a point on the stability boundary is located, one then fixes p and varies the parameter α. Using sufficiently small step sizes in α, one can trace through parameter space along the stability boundary.

In this continuation calculation, one needs to provide starting guesses for H^*, λ and ω. We can easily find starting guesses for H^* and λ from the $p = 0$ case. A starting guess for ω when $p = 0$ can also be obtained. In this case, there is no delay, and so the characteristic equation can be written $E^3 + AE^2 + BE + C = 0$. Substituting $E = i\omega$ gives $-i\omega^3 A - B\omega^2 + Ci\omega + D = 0$ and hence $\omega = \sqrt{D/B}$. Explicit formulae for the constants B and D can easily be found.

The stability boundary can also be determined in different parameter spaces, using the same numerical continuation procedure.

3.2 Extending the range of delays considered

In Chapter 2 we explored the implications of density-dependent prophylaxis (DDP) for the population dynamics of a host–pathogen system. We found that the delay was critical in determining whether DDP is stabilising or destabilising. We looked specifically at delays within the average host lifespan ($0 < \tau/b < 1/b$). In this section, we explore what happens when we extend the delay to values higher than $1/b$. We find that complex and interesting dynamics occur with this lengthened delay.

Note that $1/b$ is only the *average* host lifespan, and therefore could be exceeded to some extent in real systems. However, our exploration of this extended parameter space is motivated by mathematical rather than biological interest.

We focus on the model of host–pathogen densities described in Chapter 2 (equations (3.1)–(3.3)). Recall that parameter τ represents the delay as a proportion of the average lifespan of the host ($1/b$), and so in this section we consider values of τ above 1.

In Chapter 2 we found that increasing the delay reduces the region in parameter space where the solutions are cyclic, and thus stabilises the system. However, when extending the delay to $\tau > 1$, increasing the delay is not always stabilising (Figure 3.1). An increase in the delay can lead to an expansion of the parameter region where solutions are cyclic. Therefore, an increase in the delay can destabilise the dynamics.

To illustrate this behaviour more clearly, we look at $\lambda - \tau$ parameter space, with a fixed value of α. Figure 3.2 shows the stability boundary for $p = 20$: the boundary between the stable and unstable regions oscillates as the delay increases. Increasing the delay changes between being stabilising and destabilising. In addition, comparison of the $p = 0$ line (black) with the $p = 20$ curve (red) shows that the effect of DDP switches between being stabilising and destabilising as the delay changes.

The pattern becomes more complex as the strength of the prophylactic response (p) increases (Figure 3.3); the oscillatory pattern of the stability curves becomes more irregular, and there are increasingly elongated extensions of the lower part of the stability boundary. The population dynamics of the system become more complicated with a longer delay and with a stronger prophylactic response.

Next, for completeness, we look at $\alpha - \tau$ parameter space, with fixed λ. The results depend on the value of λ. For relatively large λ, the stability boundaries are as shown in Figure 3.4: there are two boundary curves, with the parameter region giving cycles between them. In this figure, $\lambda = 5 \times 10^7$. If extended, the stability boundary curves of Figure 3.1 would cross the line $\lambda = 5 \times 10^7$ twice. These two crossings correspond to the two stability boundary curves in Figure 3.4. In contrast,

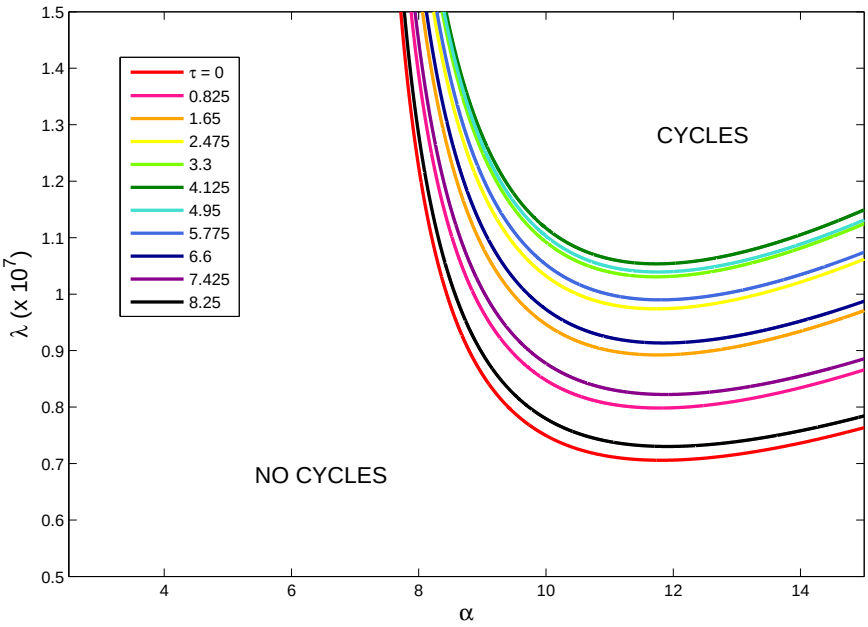

Figure 3.1: Stability boundary curves for different τ values, for a fixed p ($p = 20$), showing that increasing the delay is not consistently stabilising when extended beyond the average host lifespan. Delay values are $\tau = 0 : 0.825 : 8.25$, and an increasing τ is represented by a change in colour from red to black. Values of τ above 1 represent those that are longer than the average host lifespan. As the delay increases, firstly the cycling parameter region diminishes, and then it expands.

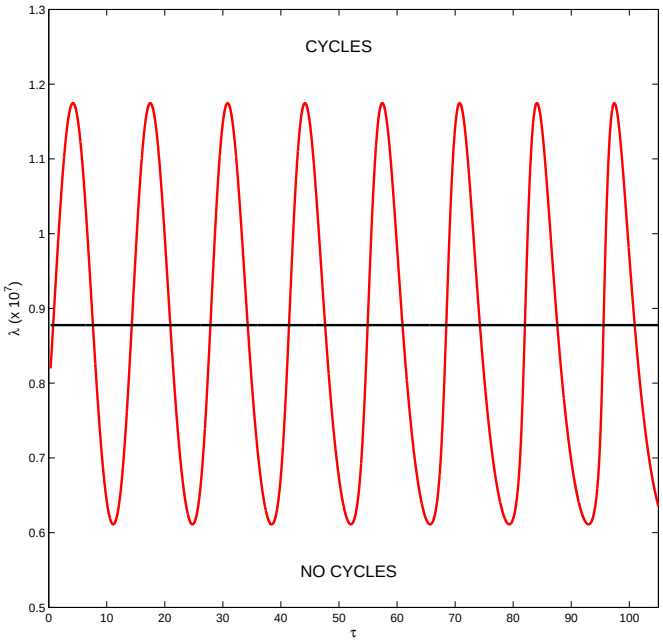

Figure 3.2: Stability boundary curve for $p = 20$ (red) in $\lambda - \tau$ parameter space, showing an oscillatory pattern. The curve for $p = 0$ (black) is also shown for comparison. Below the lines, there are no cycles; above the lines, there are cycles. In this figure, $\alpha = 15.5$.

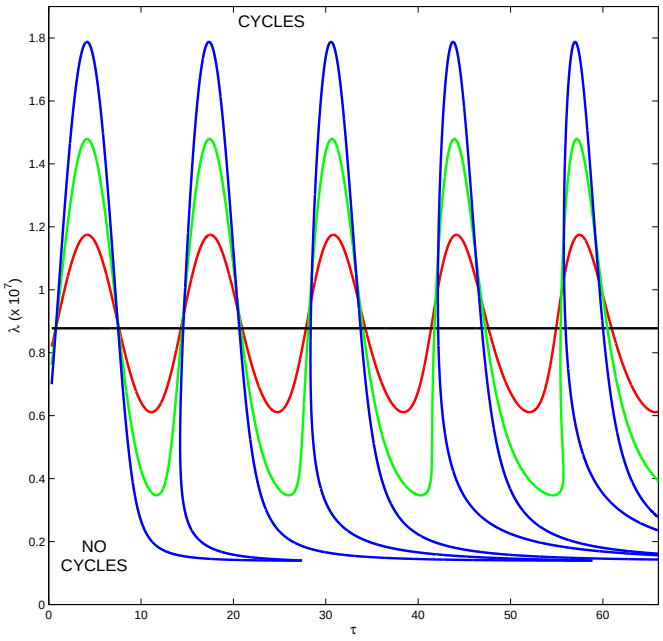

Figure 3.3: Stability boundary curves for $p = 20$ (red), $p = 40$ (green) and $p = 60$ (blue) in $\lambda - \tau$ parameter space. The curve for $p = 0$ (black) is also shown for comparison. Below the lines, there are no cycles; above the lines, there are cycles. In this figure, $\alpha = 15.5$. Note that the oscillations are not periodic.

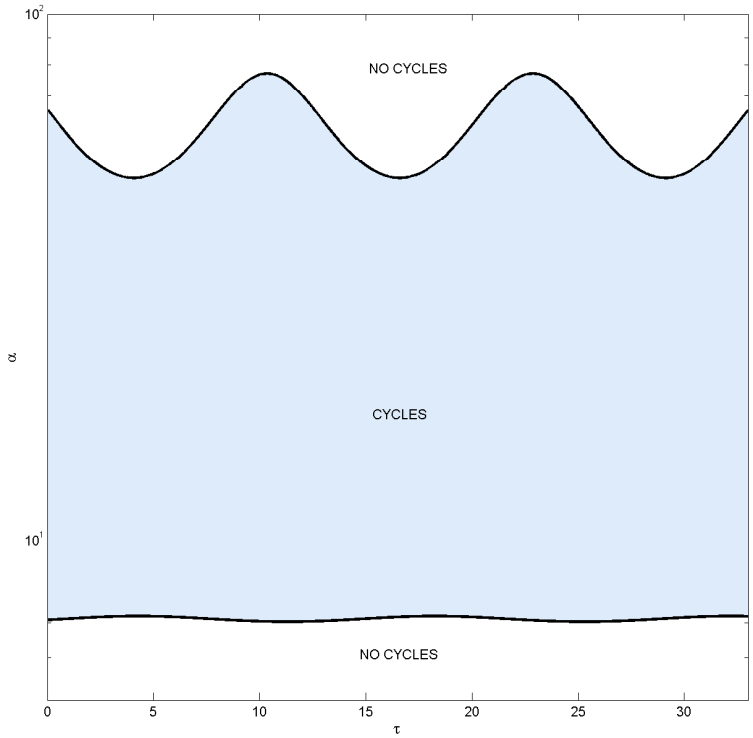

Figure 3.4: Stability boundary curves for $p = 20$ in $\alpha - \tau$ parameter space, for 'large' λ. In this figure, $\lambda = 5 \times 10^7$. There are two curves, and cycles are generated for parameters lying between them. Note that for clarity, a log scale is used for the vertical axis.

for relatively small λ, the boundaries are as shown in Figure 3.5. Here we find that there are a series of distinct regions in parameter space in which cycles are generated. The value of λ here is 0.8×10^7. To understand this behaviour, one can observe that in Figure 3.1, some stability boundary curves cross the line $\lambda = 0.8 \times 10^7$, while others do not. So for some delays, there are no cycles for any value of α.

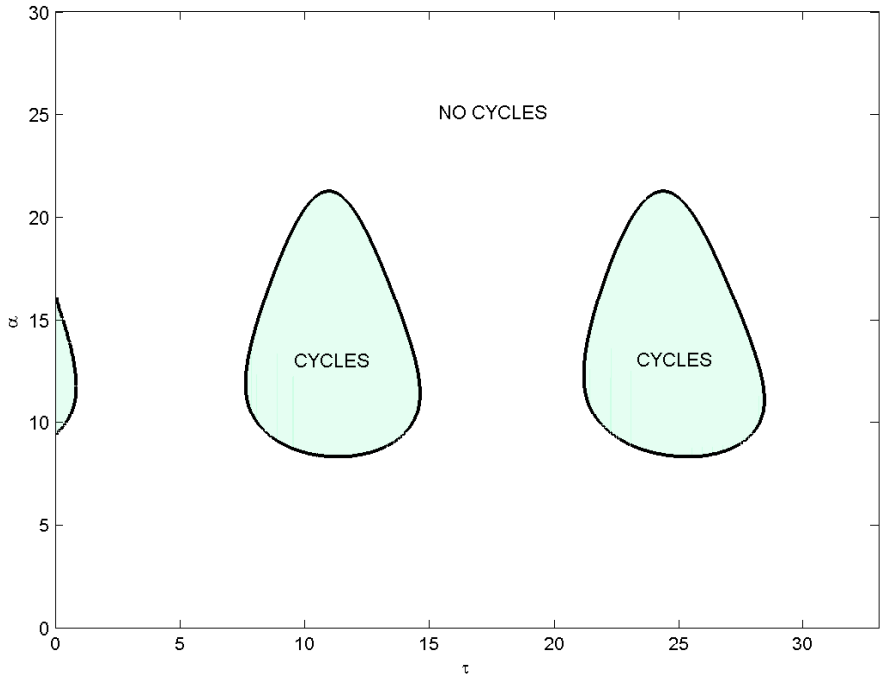

Figure 3.5: Stability boundary curves for $p = 20$ in $\alpha - \tau$ parameter space, for 'small' λ. In this figure, $\lambda = 0.8 \times 10^7$. In this case, the curves form 'islands', and cycles are generated for parameters within these islands.

It can be seen from Figures 3.2 and 3.3 that for certain values of λ there are multiple stability switches as the time delay increases. These are illustrated by the simulations shown in Figure 3.6; as the delay increases, the long-term dynamical behaviour switches between non-cyclic and cyclic. There are also stability switches for certain values of α as the delay increases (Figures 3.4 and 3.5). Multiple stability switches as the delay increases are also reported by Xiao *et al.* (2009), who extend Model G of Anderson and May (1981) by including delayed host self-regulation.

It is possible to analytically confirm the switches of stability shown by our nu-

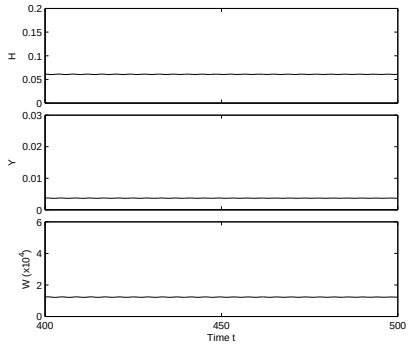

(a) $\tau = 3.96$

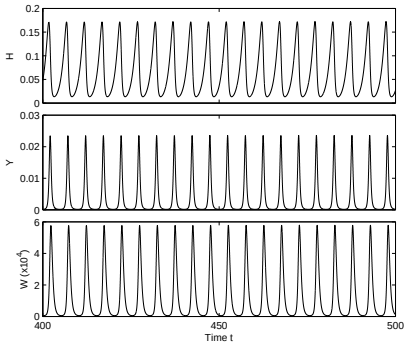

(b) $\tau = 10.56$

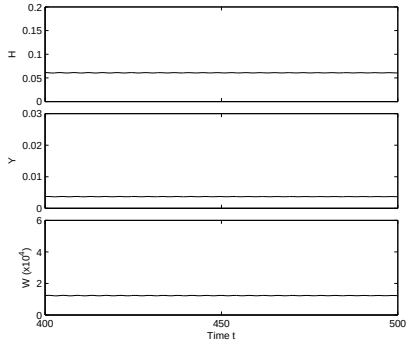

(c) $\tau = 17.16$

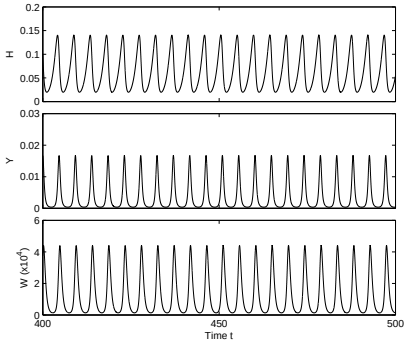

(d) $\tau = 23.76$

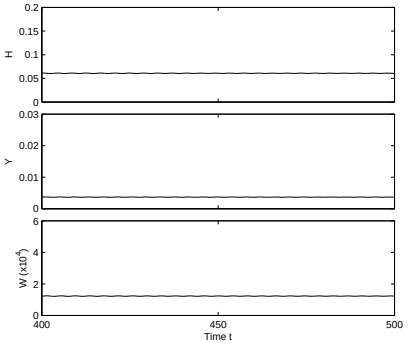

(e) $\tau = 30.36$

Figure 3.6: Numerical simulations of equations (3.1)–(3.3) to illustrate the stability switches as the delay τ increases. Times series are shown for 5 different values of τ. All other parameter values are the same for all plots, and are as follows: $r = 1$, $K = 1$, $\alpha = 15.5$, $b = 3.3$, $\mu = 3$, $\lambda = 1 \times 10^7$, $p = 20$ and $\beta_0 = 0.0001$. The dynamical behaviour at equilibrium switches between cyclic and non-cyclic. These simulations are produced by MATLAB using the delay differential equation solver dde23, which is based on an explicit Runge-Kutta $(2, 3)$ pair. Solutions are shown after running for 400 time units to ensure decay of transients.

merical method. The characteristic equation of equations (3.1)–(3.3) can be written

$$C_0 + C_1 E + C_2 E^2 + E^3 - \alpha(\mu + E)\Upsilon e^{-\tau/bE} = 0 \tag{3.5}$$

where Υ, C_0, C_1 and C_2 depend on the model parameters as follows:

$$\begin{aligned}
\Upsilon &= \frac{\beta_0 p}{100K} W^*(H^* - Y^*), \\
C_0 &= \alpha\mu\Gamma + r\left(\frac{2H^*}{K} - 1\right)\left(\Gamma\mu + \alpha\mu + b\mu - \frac{\lambda\Gamma(H^* - Y^*)}{W^*}\right), \\
C_1 &= r\left(\frac{2H^*}{K} - 1\right)(\mu + \Gamma + \alpha + b) + \Gamma\alpha + \Gamma\mu + \alpha\mu + b\mu - \frac{\lambda\Gamma(H^* - Y^*)}{W^*}, \\
C_2 &= r\left(\frac{2H^*}{K} - 1\right) + \mu + \Gamma + \alpha + b,
\end{aligned}$$

with

$$\Gamma = \beta_0\left(1 - \frac{p}{100K}H^*\right)W^*.$$

At a stability change, an eigenvalue E has zero real part. This corresponds to an eigenvalue crossing the imaginary axis. Setting $E = i\omega$ (with ω real) and equating real and imaginary parts of equation (3.5) gives

$$C_0 - C_2\omega^2 = -\Upsilon\alpha\left[\mu\cos\left(\frac{\tau}{b}\omega\right) + \omega\sin\left(\frac{\tau}{b}\omega\right)\right] \tag{3.6}$$

$$C_1\omega - \omega^3 = -\Upsilon\alpha\left[\omega\cos\left(\frac{\tau}{b}\omega\right) - \mu\sin\left(\frac{\tau}{b}\omega\right)\right]. \tag{3.7}$$

It can be seen that for any solution ω of equations (3.6) and (3.7), $-\omega$ also satisfies the equations: if any eigenvalue crosses the imaginary axis, so too does its conjugate. Moreover, $\omega = 0$ cannot satisfy (3.6), so that the origin cannot be an eigenvalue. Thus at a stability change, two eigenvalues (a complex conjugate pair) cross the imaginary axis.

Writing $\theta = \omega\frac{\tau}{b}$ and defining a new parameter ϕ by setting $\frac{\mu}{\sqrt{\mu^2+\omega^2}} = \cos\phi$ and hence $\frac{\omega}{\sqrt{\mu^2+\omega^2}} = \sin\phi$, where $\phi \in [0, 2\pi)$, gives

$$C_0 - C_2\omega^2 = -\Upsilon\alpha\sqrt{\mu^2 + \omega^2}\cos(\phi - \theta) \tag{3.8}$$

$$C_1\omega - \omega^3 = -\Upsilon\alpha\sqrt{\mu^2 + \omega^2}\sin(\phi - \theta). \tag{3.9}$$

We seek values of the delay for which these equations hold. We have

$$\begin{aligned}
\cos(\phi - \theta) &= -\frac{C_0 - C_2\omega^2}{\Upsilon\alpha\sqrt{\mu^2+\omega^2}} \\
\Rightarrow \theta &= \phi - \cos^{-1}\left(\frac{C_2\omega^2 - C_0}{\Upsilon\alpha\sqrt{\mu^2+\omega^2}}\right) \\
\Rightarrow \tau &= \frac{b}{\omega}\phi - \frac{b}{\omega}\cos^{-1}\left(\frac{C_2\omega^2 - C_0}{\Upsilon\alpha\sqrt{\mu^2+\omega^2}}\right).
\end{aligned}$$

Using the definition of ϕ, this leads to the following expression for the delay τ:

$$\tau = \frac{b}{\omega}\cos^{-1}\left(\frac{\mu}{\sqrt{\mu^2+\omega^2}}\right) - \frac{b}{\omega}\cos^{-1}\left(\frac{C_2\omega^2 - C_0}{\Upsilon\alpha\sqrt{\mu^2+\omega^2}}\right). \tag{3.10}$$

It follows from equation (3.10) that for each real value of ω, the corresponding eigenvalue crosses the imaginary axis an infinite number of times as τ increases. It also follows that the difference in τ between each crossing is

$$\Delta\tau = 2\pi\left(\frac{b}{\omega}\right). \tag{3.11}$$

This is verified by the stability boundary curves generated numerically.

There may be multiple values of ω for any given parameter set. The values of ω can be found from:

$$\frac{(C_0 - C_2\omega^2)^2 + \omega^2(C_1 - \omega^2)^2}{\Upsilon^2\alpha^2(\mu^2+\omega^2)} = 1, \tag{3.12}$$

which follows from equations (3.8) and (3.9). This is a cubic equation in ω^2, and there are hence six possible values of ω. However, only real values are relevant. In addition, since a stability change involves a complex conjugate pair of eigenvalues crossing the imaginary axis, we can restrict our attention without loss of generality to cases where $\omega > 0$.

In order to determine the type of stability changes (if any) that occur when an eigenvalue pair crosses the imaginary axis, one can determine the direction of the crossing. For this, we use parts of a proof by Cooke and van den Driessche (1986) (also given in Kuang (1993)), with added steps for clarity. Firstly, the characteristic equation (3.5) can be written in the form

$$P(E) + Q(E)e^{-ET} = 0 \tag{3.13}$$

(where $P(E) = C_0 + C_1E + C_2E^2 + E^3$, $Q(E) = -\alpha(\mu + E)\Upsilon$ and $T = \tau/b$). We

regard the characteristic root $E(T) = x(T) + i\omega(T)$ as a function of T, and we try to determine the direction of motion of $x(T)$ as T is varied, i.e. we determine

$$S = \text{sign}\left(\frac{d}{dT}(\text{Re}E(T))|_{E=i\omega}\right) = \text{sign}\left[\text{Re}\left(\frac{dE(T)}{dT}\Big|_{E=i\omega}\right)\right].$$

Differentiating (3.13) with respect to T yields

$$\frac{dE}{dT} = \frac{EQ(E)}{P'(E)e^{ET} + Q'(E) - TQ(E)} \tag{3.14}$$

and, since from (3.13) $e^{-ET} = -P(E)/Q(E)$, then we obtain

$$\left(\frac{dE}{dT}\right)^{-1} = -\frac{P'(E)}{EP(E)} + \frac{Q'(E)}{EQ(E)} - \frac{T}{E}, \tag{3.15}$$

which holds at any simple root of (3.13). Hence,

$$\begin{aligned} S &= \text{sign}\left(\text{Re}\left(\frac{dE}{dT}\right)^{-1}\Big|_{E=i\omega}\right) \\ &= \text{sign Re}\left[-\frac{P'(i\omega)}{i\omega P(i\omega)} + \frac{Q'(i\omega)}{i\omega Q(i\omega)} - \frac{T}{i\omega}\right] = \text{sign Re}\left[-\frac{P'(i\omega)}{i\omega P(i\omega)} + \frac{Q'(i\omega)}{i\omega Q(i\omega)}\right] \\ &= -\text{ sign Im}\left[\frac{P'(i\omega)}{\omega P(i\omega)} - \frac{Q'(i\omega)}{\omega Q(i\omega)}\right]. \end{aligned} \tag{3.16}$$

From this, we can see that the sign depends on ω, and is independent of the delay value. It can be shown that the crossing at two adjacent ω values are in opposite directions (Kuang, 1993). One will correspond to a crossing of the imaginary axis from left to right; the next will correspond to a crossing from right to left.

To demonstrate this, let us take as an example case $\lambda = 0.6 \times 10^7$ with $p = 40$, and all other parameters as for Figure 3.3. For $\tau = 0$, there are three eigenvalues: one negative and a complex conjugate pair with negative real parts; the dynamics are stable. We aim to determine what happens with $\tau > 0$. Values of ω can be calculated using equation (3.12), and this gives four real values: ± 1.485 and ± 1.547 (correct to three decimal places). Without loss of generality, we can just consider positive ω, and we write $\omega_1 = 1.485$ and $\omega_2 = 1.547$. From equation (3.16), ω_1 corresponds to a crossing of the imaginary axis from right to left, and ω_2 to a crossing in the opposite direction. As the delay increases from zero, the dynamics will switch between unstable (with one pair of eigenvalues with positive real part) and stable (with all eigenvalues with negative real part), as eigenvalues cross back and forth. As a result, there are stability switches as the delay increases, shown in

our figure.

However, there is only a finite number of these stability switches. The difference in τ between switches is dependent on ω (from equation (3.10)). The difference in τ between switches with $\omega = \omega_1$ is larger than the difference with $\omega = \omega_2$ (see Figure 3.7). Thus, as τ increases, eventually there will be two consecutive switches with $\omega = \omega_2$, leading to two pairs of eigenvalues with positive real parts. For all values of τ above this, the equilibrium is unstable; there will always be eigenvalues with positive real parts.

This underlying behaviour causes the shapes shown in Figure 3.3. The ω values depend on λ and other parameters. Values of ω_1 and ω_2 become further apart as parameter p increases, so there will be fewer stability switches before the dynamics become unstable.

We conclude with a comment about numerical continuation of the stability boundary. Our basic method for this calculation is described in Section 3.1. However, the procedure has been slightly modified in order to cope with the additional complexity of these new patterns. In earlier figures, it was possible to perform numerical continuation in one parameter only. For instance, the curves of Figure 2.6 are produced through parameter continuation in α, i.e. α is either decreased or increased, and if the step sizes are sufficiently small, this can be continued through all required values of α. However, with a larger delay, this cannot be achieved in some cases. Figure 3.8 shows an example. In this case, the curve is not always monotonic in τ, and as a result, numerical continuation via increasing τ will fail. When this occurs, we switch to numerical continuation in λ (results shown in red), in order to continue the curve. A more sophisticated approach would be to use arclength continuation (Doedel, 1981) but in practice the simpler method of parameter continuation with parameter switching works well.

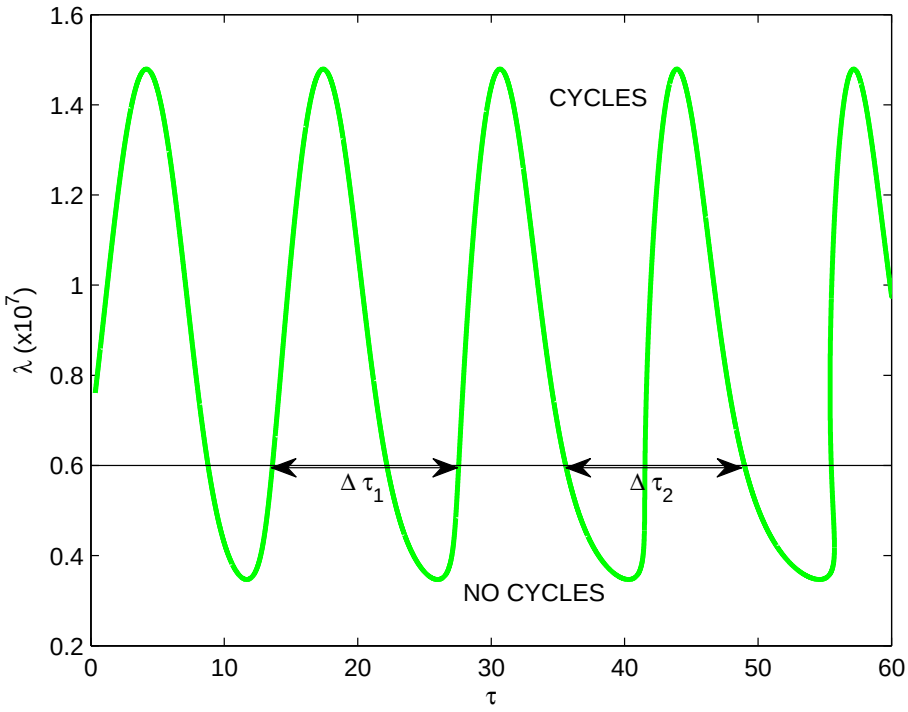

Figure 3.7: Stability boundary curve for $p = 40$: an example to demonstrate properties of the stability switches. For $\lambda = 0.6 \times 10^7$, there are stability switches between unstable (cycles) and stable (no cycles). The switches from unstable to stable correspond to a crossing of a pair of eigenvalues across the imaginary axis from right to left. The value of ω for these switches is ω_1. The switches from stable to unstable correspond to a crossing of a pair of eigenvalues from left to right. The value of ω for these switches is ω_2. From result (3.11), for ω_1, the difference in τ between crossings of the imaginary axis is $\Delta\tau_1 = 2\pi(\frac{b}{\omega_1}) = 13.963$. Similarly, for ω_2, the difference is $\Delta\tau_2 = 2\pi(\frac{b}{\omega_2}) = 13.403$. These agree with measurements on the numerically calculated stability boundary illustrated in this figure. Since $\omega_1 < \omega_2$, $\Delta\tau_1 > \Delta\tau_2$, and therefore as τ increases, there will eventually be two consecutive switches with ω_2. For values of the delay above this, the dynamics will be unstable, as there will always be eigenvalues with positive real part. One can calculate the number of oscillations that occur before this. For this example case, there will be 15 oscillations before the equilibrium becomes unstable for all larger τ; this is dependent on the value of λ.

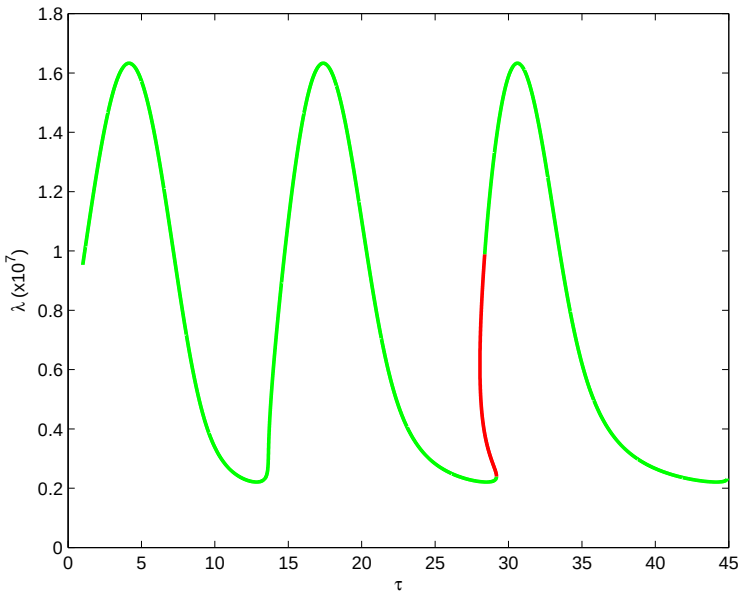

Figure 3.8: An example stability boundary curve to demonstrate the need to switch from continuation in τ to continuation in λ. The section shown in red has been produced by continuation in λ. During the continuation process, if the loop fails prematurely, a smaller parameter step size is attempted first. If this does not work, then the continuation is switched to the alternative parameter in order to continue the curve. Note that the oscillations presented here are not periodic.

Chapter 4

Delayed induced silica defences in grasses and their potential for destabilising herbivore population dynamics

This chapter is based on material submitted as a manuscript to be published (Reynolds *et al.*, submitted, a), which is a collaboration between Jennifer Reynolds, Fergus Massey, Xavier Lambin, Stefan Reidinger, Jonathan Sherratt, Matthew Smith, Andrew White and Sue Hartley. Fergus Massey, Xavier Lambin and Sue Hartley conceived and designed the greenhouse experiment, and Fergus Massey and Stefan Reidinger performed the experimental work; much of the experimental detail included in the manuscript has been omitted in this thesis. Fergus Massey, Xavier Lambin, Jennifer Reynolds, Jonathan Sherratt and Andrew White analysed the data. Jennifer Reynolds, Jonathan Sherratt, Andrew White and Matthew Smith developed the mathematical models. Jennifer Reynolds performed the model simulations and conducted the statistical work and sensitivity analysis. All authors contributed to writing and editing the manuscript.

Some grass species mount a defensive response to grazing by increasing their rate of uptake of silica from the soil and depositing it as abrasive granules in their leaves. Increased plant silica levels reduce food quality for herbivores that feed on these grasses. Here we provide empirical evidence that a principal food species of an herbivorous rodent exhibits a delayed defensive response to grazing by increasing silica content, and present theoretical modelling that predicts that such a response alone could lead to the population cycles observed in some herbivore populations.

Experiments under greenhouse conditions revealed that the rate of deposition of silica defences in the grass *Deschampsia caespitosa* is a time-lagged, nonlinear

function of grazing intensity and that, upon cessation of grazing, these defences take around 1 year to decay to within 5% of control levels. Simple coupled grass–herbivore population models incorporating this functional response, and parameterized with empirical data, consistently predict population cycles for a wide range of realistic parameter values for a (*Microtus*) vole–grass system. Our results support the hypothesis that induced silica defences have the potential to strongly affect the population dynamics of their herbivores. Specifically, the feedback response we observed could be a driving mechanism behind the observed population cycles in graminivorous herbivores, in cases where grazing levels in the field become sufficiently large and sustained to trigger an induced silica defence response.

4.1 Introduction

Unstable consumer–resource interactions are hypothesized to drive multi-year population cycles (Turchin, 2003), such as those observed in some populations of moths, hares and rodents (Turchin and Batzli, 2001). The general consensus is that, unlike predator–prey or host–parasite interactions, plant–herbivore interactions alone are unlikely to be the cause of the delayed density dependence that characterizes such cycles. A sufficiently strong and time-lagged negative feedback is required for coupled trophic interactions alone to generate population cycles (Berryman, 2002; Turchin, 2003) and, to date, there has been a general lack of empirical support to suggest that the negative feedback between density-dependent grazing intensity and grazing-dependent food availability meets this requirement (Turchin and Batzli, 2001). Previous studies examining whether grazing-induced changes in food quantity provide a potential negative feedback mechanism have rarely observed a sufficient depletion of plant biomass and many plant species regrow rapidly following grazing (e.g. Krebs and Myers, 1974; Ostfeld and Canham, 1993), although there are some possible exceptions, such as studies of Norwegian and brown lemmings in colder climates feeding on slow growing mosses (Turchin *et al.*, 2000; Krebs *et al.*, 2010). Hence the quantity of food available is currently believed to play a secondary role in shaping the population cycles of herbivores, being limited to interactions with other destabilizing mechanisms, such as physiological condition or susceptibility to predators or pathogens (Huitu *et al.*, 2003; Boonstra and Krebs, 2006).

However, a decrease in plant biomass is not the only way food can become limiting for herbivores (Batzli, 1992): in addition, the availability of high quality food can be reduced by the production of grazing-induced plant defences. Increases in the levels of plant defences following grazing have been demonstrated in many plant species (Karban and Baldwin, 1997). There are also a substantial number of theoretical studies suggesting that grazing-induced plant defences may provide a

sufficient negative feedback to drive population cycles. These mostly involve generic models (Edelstein-Keshet and Rausher, 1989; Lundberg *et al.*, 1994; Underwood, 1999; Turchin, 2003), although a few have been parameterized for particular insect systems (Haukioja, 1980; Underwood and Rausher, 2002). This theoretical work has highlighted the characteristics of a negative feedback between grazing intensity and levels of induced defences that could potentially generate population cycles. These include: (a) the time elapsing between herbivore damage and the onset of induction relative to the potential rate of increase of the herbivore population in that time (Haukioja, 1980; Bryant, 1981; Myers and Williams, 1984; Haukioja, 1991a) and (b) the magnitude (in terms of demographic impact on the herbivore) and persistence of the induced response (in terms of decay rate or 'relaxation') (Edelstein-Keshet and Rausher, 1989; Turchin and Taylor, 1992; Lundberg *et al.*, 1994; Underwood, 1999; Underwood and Rausher, 2002). Several inducible defence mechanisms of a magnitude and persistence that is appropriate to give them the potential to generate cycles have been considered (Karban and Baldwin, 1997), some of which, known as delayed inducible resistance mechanisms, can occur over timescales of months or even years (Haukioja, 1991a). Despite this, it has proven difficult to demonstrate empirically that induced defences affect herbivore population cycles (e.g. Haukioja, 1980; Underwood, 1999; Klemola *et al.*, 2000a; Ruohomaki *et al.*, 2000; Turchin, 2003; Huitu *et al.*, 2003; Kent *et al.*, 2005).

Current explanations for population cycles of voles in Fennoscandia invoke a predator–prey interaction between voles of the genus *Microtus* and their specialist predators, with other small mammal species, including *Myodes* folivorous voles, being entrained by 'spill over' predation (Hanski and Henttonen, 2002; Oksanen *et al.*, 2000). In these systems, induced plant defences do not seem to play a role in driving the cycles of folivorous voles. Indeed several studies have provided convincing evidence against the induction of plant defences in response to grazing by those rodents. For example, ericaceous plants subjected to grazing by *Myodes* voles in northern Fennoscandia (Oksanen *et al.*, 1987; Rammul *et al.*, 2007) showed no inducible defences, and the sedge *Carex bigelowii* showed no induced defensive response to simulated grazing by lemmings (*Lemmus lemmus*) (Lindgren *et al.*, 2007). However, there may be important contrasts between populations in Fennoscandia and other regions, and between forb and grass-feeding species. Although no populations of forb-eating *Myodes* voles display cyclic dynamics outside Fennoscandia and in allopatry with graminivorous *Microtus* voles (Oksanen *et al.*, 2000), numerous grass-eating *Microtus* vole populations display cyclic dynamics outside Fennoscandia (Lambin *et al.*, 2006; Lambin *et al.*, 2000; Mackin-Rogalska and Nabaglo, 1990; Tkadlec and Stenseth, 2001).

Grasses are the main food for several herbivores exhibiting cyclic populations,

including *Microtus* vole populations across much of Europe. Unlike the *Myodes* vole populations mentioned above, some of the *Microtus* vole populations reach sufficiently high densities to significantly damage grasses through sustained grazing, especially in winter (Jedrzejewska and Jedrzejewski, 1998; Lambin *et al.*, 2006; Lambin *et al.*, 2000; Myllymäki, 1977; Tkadlec and Stenseth, 2001). Despite using similar experimental designs, three previous studies using *Microtus* voles reached contradictory conclusions on the impact of past grazing on herbivore population performance. Through manipulation of vole densities within enclosed wet meadow areas, Agrell *et al.* (1995) observed that reproduction, recruitment, and body growth rate in introduced *Microtus agrestis* populations were negatively affected by high previous density. In contrast, working with the same species in abandoned farmland colonised by grasses, Klemola *et al.* (2000b) only found weak delayed effects of past overgrazing on vole reproduction and no effect on population growth rates. A third study with meadow voles (*Microtus pennsylvanicus*) in old fields, detected effects of past density on adult survival rates but not on other traits (Ostfeld and Canham, 1995). The indices of plant quality (sugar, fibre and protein content) measured in the two former studies were also inconclusive.

Traditionally, it has been thought unlikely that induced defences in grasses would affect population growth rates of grazing herbivores, because, particularly in comparison to woody plants (Bryant *et al.*, 1983), grasses were thought to respond to herbivory by rapid regrowth from their basal meristems rather than investing in chemical defence (McNaughton, 1979). Many of the plant defences involved in delayed induced resistance in trees, such as some types of phenolic compounds, resins and tannins (Bryant *et al.*, 1983; Kaitaniemi *et al.*, 1998), are not present in grasses. However, it has long been suggested that grasses may in fact 'fight back' (Vicari and Bazely, 1993). Grasses contain silica-based physical defences, which have been shown to be an effective deterrent against mammalian herbivores (Gali-Muhtasib *et al.*, 1992; Cotterill *et al.*, 2007; but see Vicari and Bazely, 1993). Silica (SiO_2) is taken up from the soil as silicic acid and deposited in the leaves as hard granules known as phytoliths, which make grasses abrasive. Concentrations of silica are related to previous grazing history (McNaughton *et al.*, 1985; Brizuela *et al.*, 1986), and so are potentially inducible.

Recent empirical studies in greenhouse conditions have demonstrated silica induction experimentally (Massey *et al.*, 2007a) and suggested that inducible silica-based defences in grasses could have important consequences for the dynamics of herbivore populations. The presence of silica in plants can alter both the preference and performance of mammalian herbivores (Massey and Hartley, 2006; Massey *et al.*, 2007b; Massey *et al.*, 2009). For example, silica-enriched grass has been shown to be poorly digested by field voles (*Microtus agrestis*), leading to a decline in the

growth rate of both adults and juveniles, particularly on winter forage (Massey and Hartley, 2006; Massey *et al.*, 2008). In addition, there is both laboratory and field evidence that grasses vary their uptake of silica in response to sustained grazing, indicating the potential for reciprocal feedback between herbivores and their food (Massey *et al.*, 2007a; Massey *et al.*, 2008). Despite this, we still lack sufficient data on the nature of the response to test whether inducible silica defences could play a role in generating the population cycles observed in some herbivore populations. Specifically, previous work has only generated a relatively imprecise estimate (between 3 and 14 months) of the rate of silica induction in grasses in response to grazing (Massey *et al.*, 2007a), and to date we have no knowledge about whether, and for how long, such a response persists once grazing is removed.

The effect that inducible silica-based defences in grasses have on the population dynamics of herbivores is therefore akin to a jigsaw puzzle in which some of the pieces are already in place: silica is an inducible defence; grazing can trigger this induction; and the silica level in grass does affect the performance of mammalian herbivores. However, two vital pieces of this jigsaw puzzle are currently missing, both related to the timescale of silica-based defences, which is crucial to their potential to cause cycles. Firstly, what is the time scale of silica induction after grazing in grasses and how quickly do these defences 'relax' once grazing has stopped? And secondly, is the time scale of induction and relaxation compatible with the generation of herbivore population cycles?

In this chapter we answer the first of these questions by a greenhouse experiment that yields, for the first time, specific data on silica induction and relaxation in a grass species (tufted hair grass, *Deschampsia caespitosa* (L.) P. Beauv.). We then address the second question by using our data to parameterize models for the specific case of field voles (*Microtus agrestis*) in Kielder Forest (Northern UK), whose diet is dominated by *D. caespitosa* (Stenseth *et al.*, 1977; Klemola *et al.*, 2000a). Like many other *Microtus* voles, populations of *M. agrestis* are renowned for exhibiting large amplitude cycles in abundance (Lambin *et al.*, 2000) and in some cases these cycles can occur in the absence of obvious top down regulation (Ergon *et al.*, 2001; Graham and Lambin, 2002). Our results suggest that silica-based defences in grasses may be a key causal factor for the cycles in such cases.

4.2 Materials and methods

Note: Much of the experimental detail included in the submitted manuscript has been omitted in this thesis as I did not perform the experiments: only a summary is given here.

4.2.1 Timing and nature of silica defence induction and relaxation

Seeds of *D. caespitosa* were grown under greenhouse conditions and watered *ad libitum* for six months prior to the experiment. Plants were then randomly allocated to one of three damage treatments: 1) approximately 5% of leaves eaten by voles per month; 2) approximately 20% of leaves eaten by voles per month; 3) undamaged control. Damage levels were achieved by placing wire mesh exclosures over each plant, then pulling the desired proportion of the total number of leaves through the mesh so that they were exposed to voles. Control plants were treated in the same manner; however, no foliage was pulled through the mesh.

The experiment was conducted in two parts: defence induction and then defence relaxation. For the defence induction phase, each plant was damaged monthly by voles in accordance with the specific damage treatment for six months. Following this, all damage events were stopped but each plant retained its treatment identity. Plants were grown for a further six months to test for a defence relaxation phase: the time required following the last damage event for a plant to cease producing elevated levels of silica. During both phases, samples of newly expanded leaves from plants of each treatment were removed at monthly intervals.

4.2.2 Calibration procedure

The silica concentration of the plant samples was measured. To account for seasonal variation in silica levels which was unrelated to damage treatments (see control data in Figure 4.1(a),(b)) we subtracted the mean silica concentration of control plants from both other treatments at each time point, prior to analysis. The resulting silica concentrations (Figure 4.1(c)) were thus those resulting directly from the damage treatments imposed, rather than the date in the growing season.

4.3 Experimental results

Concentrations of silica in young *D. caespitosa* leaves exposed to the high grazing treatment (20% leaf area removed per month) increased non-linearly with time (Figure 4.1). In contrast, the low grazing treatment (5% leaf area removed per month) did not induce a persistent increase in silica over the 6 month period, although the data imply that there might have been an initial small increase in silica concentrations by month 4, relative to the control (Figure 4.1), which subsequently ceased. Following the cessation of the grazing treatments, silica concentrations in the newly expanded leaves from plants in the high damage treatment decreased over the sub-

sequent 7 month period. However, even after 7 months without damage, the higher silica concentrations in new leaves in the high grazing treatment imply that the relaxation of past induction was not complete (Figure 4.1). Silica concentrations in the low grazing treatments remained at control levels over the same period.

4.4 Theoretical modelling of silica dynamics

We developed a simple mechanistic model of grazing-induced silica defences, with relaxation in the absence of grazing, and fitted it to our empirical data. We assumed that silica induction is an increasing saturating function of damage (implied from Figure 4.1), but that there is some time delay in this response (Figure 4.1), presumably related to the time required for leaf re-growth, between damage and the occurrence of elevated silica levels in new leaves. We also assumed that after cessation of damage, silica concentrations decay exponentially back to their pre-treatment levels (strongly suggested by Figure 4.1). To enable us to later combine this model with a model of vole population dynamics, we made the simple assumption that the levels of damage by voles in a given area are directly proportional to vole density, and used vole density to represent grazing rate. Denoting by $V(t)$ and $S(t)$ the vole density (voles per hectare) and silica concentration (% dry mass) at time t (years), respectively, our model is

$$\begin{aligned} \frac{dS}{dt} &= \text{induction} - \text{decay} \\ &= \frac{KV(t-T)^n}{V_0^n + V(t-T)^n} - c(S(t) - S_{control}) \end{aligned} \tag{4.1}$$

where $S_{control}$ is the mean silica concentration in the absence of damage, $(cS_{control} + K)$ is the maximum possible rate of silica production (yr^{-1}), n (the Hill coefficient, unitless) scales the shape of the functional response of silica induction rate to vole density (grazing intensity), V_0 is the vole density at which damage-induced production is half of the maximum possible (ha^{-1}), T is the time delay in silica induction (years), and c scales the background exponential decay rate of silica (yr^{-1}).

4.4.1 Parameterising the model

Our measurements of the silica concentrations in control plants (see Figure 4.1(a),(b)) were used to estimate $S_{control} = 2.54\%$ dry mass. We assumed that the two damage treatments corresponded to two different values of V in the first 5 months of the experiment; specifically, we assume a direct proportionality between vole density and grazing intensity. Equation (4.1) is linear in S, and so it can easily be rewritten

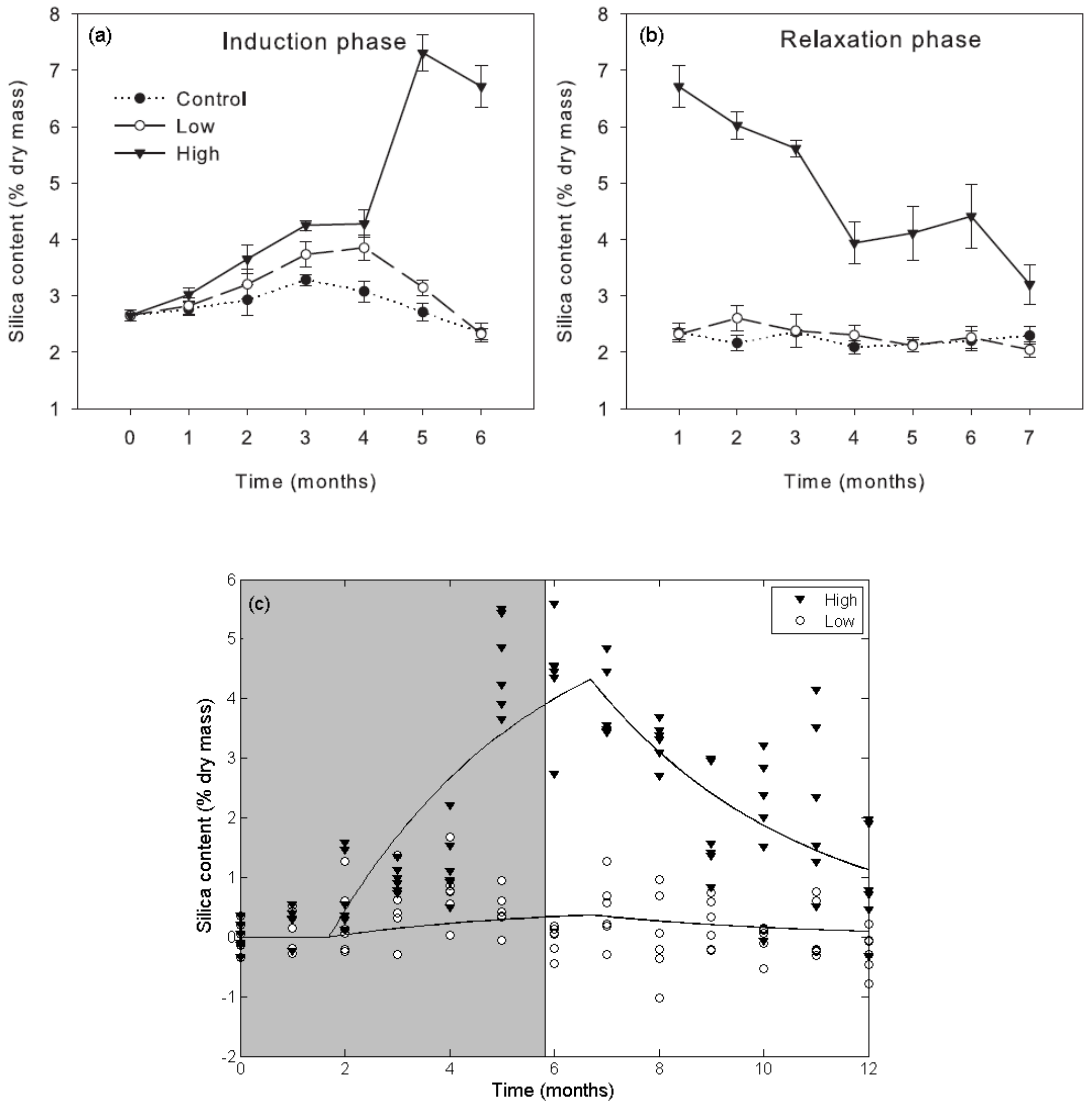

Figure 4.1: (a,b) Silica concentrations (mean ± SE) in *D. caespitosa* leaves from plants under three damage treatments (low: 5% leaf area removed per month; high: 20% leaf area removed per month; undamaged controls) plotted against (a) time since starting monthly damage events (defence induction phase), and (b) time since cessation of monthly damage events (defence relaxation phase). Note that the data at 6 months in the induction phase are the same as those at 1 month of the relaxation phase. (c) Silica concentrations of individual *D. caespitosa* leaves under the same treatments (after subtracting control means from each data point) compared to our fitted solutions of equation (4.1) for the two damage regimes, with parameter values as given in the main text. Note, the 'Induction phase' and the 'Relaxation phase' are shown together here. In the grey shaded region the leaves were exposed to monthly damage events. We assessed the fit between the model and the data by analyzing the standardized residuals (one for each data point). Visual inspection of residuals plotted against time indicated no bias, making a chi-squared goodness of fit test appropriate. With 20 goodness of fit bins, this gave a significance probability of 0.33.

in terms of $S^*(t) = S(t) - S_{control}$:

$$\frac{dS^*}{dt} = -cS^*(t) + 0, \qquad 0 < t < T \text{ and } t > T + 5 \text{ months} \tag{4.2a}$$

$$\frac{dS^*}{dt} = -cS^*(t) + P_{low}, \ T < t < T + 5 \text{ months, low damage (low V)} \tag{4.2b}$$

$$\frac{dS^*}{dt} = -cS^*(t) + P_{high}, \ T < t < T + 5 \text{ months, high damage (high V).} \tag{4.2c}$$

Here P_{low} and P_{high} are the production rates of silica at low and high levels of vole damage respectively; they depend on K, V_0, n, and the two damage levels. To fit the four parameters c, T, P_{low} and P_{high}, we minimized the sum of the squared differences between the numerical solution of (4.2a–4.2c) and the empirical data: both the model solutions and the minimization were done using the software package MATLAB (www.mathworks.com). This gives $c = 3.0$ per year, $T = 1.7$ months, $P_{low} = 1.6\%$ dry mass per year, $P_{high} = 18.4\%$ dry mass per year. From the fitted values of P_{low} and P_{high}, we must determine K, V_0 and n. Positivity of K and V_0 requires $n > 1.8$, implying that silica induction is fundamentally a threshold phenomenon. However, beyond this constraint there are insufficient data to independently determine all three parameters, and we fix $n = 2$ (but examine the sensitivity of the results to changes in n later); this allows us to obtain values for K and V_0, in terms of the effective vole densities in the two treatment regimes.

4.4.2 Model solutions

We superimposed the solution of equation (4.1) on the empirical data (Figure 4.1(c)) using parameters obtained from our experiments via non-linear least squares regression, with vole densities corresponding to the experimental damage treatments. We assessed the fit between the model and the data using statistical analysis. Inspection of the standardized residuals showed no evidence of bias, making a chi-squared goodness of fit test appropriate. With 20 goodness of fit bins, this gave a significance probability of 0.33. The predictions of this fitted model are consistent with the empirical data. Overall, this model clearly captures the qualitative dynamics of the induction and decay phases of the silica dynamics under both high and low grazing treatments. The fitted parameters imply that there is a time lag of around 1.7 months in the response of silica to grazing, that the silica induction response is a saturating (sigmoidal) function of cumulative vole grazing intensity and that there is a background exponential decay rate of induced defences of 3 yr^{-1}, which translates to a decay of around 22% per month, or 95% per year.

4.4.3 Model extension: Incorporating vole dynamics

The next stage in our study was to couple the silica induction and decay model, fitted to our experimental results, with a simple model of *M. agrestis* population dynamics, to investigate whether the feedback between the functional response and the rodent population dynamics is sufficient to generate population cycles, if silica affects vole reproductive rate only. We modelled the vole population dynamics using

$$\begin{aligned} \frac{dV}{dt} &= \text{birth} - \text{death} \\ &= [B_{min} + (B_{max} - B_{min})F(S(t))]V(t) - dV(t) \end{aligned} \tag{4.3}$$

where d is the vole death rate, assumed constant and independent of silica, and B_{min} and B_{max} are the minimum and maximum vole birth rates. In the absence of relevant data, we took $B_{min} = 0.1B_{max}$, but the precise scaling between the minimum and the maximum birth rates only affects the quantitative details of the results. The function $F(S(t))$ is the functional response of vole birth rates to silica concentrations. Caged voles fed on a controlled diet start to lose weight rather than gain it at a silica level of 6.6% dry mass (Massey *et al.*, 2008). Therefore we took $F = 0$ for $S > 6.6\%$ dry mass, with $F = 1$ for $S < S_{control}$ and with a linear decrease between these two levels (see Figure 4.2(a)). We parameterized d and B_{max} for the *M. agrestis* populations in Kielder Forest, the site of our long term field studies on vole populations in Northern UK. At this upland site voles show 3–5 year population cycles and live in grass dominated clear cuts within large stands of spruce plantation. In a previous study at Kielder, an association between silica concentrations in *D. caespitosa* plants and the rate of change of the rodent populations was detected (Massey *et al.*, 2008) and it has also been demonstrated that changes in the timing of reproduction, rather than survival, co-vary strongly with past vole density (Ergon *et al.*, 2011). Monthly survival probabilities implied by field data (Graham and Lambin, 2002; Burthe *et al.*, 2008) led us to estimate a death rate of $d = 2.7$ per year (Smith *et al.*, 2006). The maximum per capita birth rate of voles, B_{max}, is a more difficult parameter to estimate. Time series data from Kielder imply a maximum per capita birth rate of at least 4.1 per year (Smith *et al.*, 2006), whereas trapping data implies a figure of 10.6 (Smith *et al.*, 2008) and studies of similar rodent taxa have suggested values of 13.8, or even as high as 16 (Turchin and Ostfeld, 1997). We therefore regarded the maximum birth rate as a free parameter and investigated the form of model solutions as it was varied. With a value of 4.1 per year, the model predicts constant population levels. However, at maximum birth rates above 8.4 per year, population cycles occur (Figure 4.3).

The key driver for these cycles is the delayed nonlinear induction of silica due

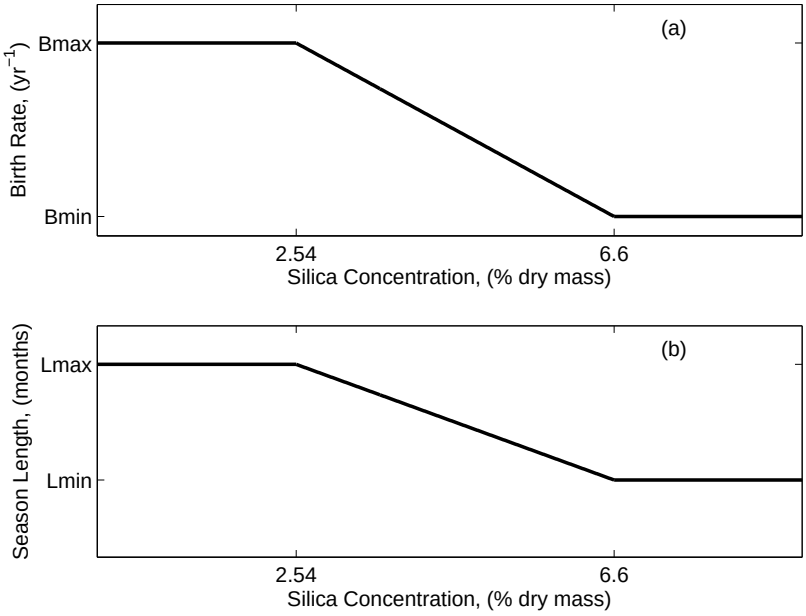

Figure 4.2: The relationship between (a) the birth rate, which equals $[B_{min}+(B_{max}-B_{min})F(S(t))]$, and silica concentration for the non-seasonal model: coupling equations (4.1) and (4.3) and (b) the season length, which equals $[L_{min} + (L_{max} - L_{min})F(S(t^*))]$, and silica concentration for the seasonal model: coupling equations (4.1) and (4.4).

to grazing (see equation (4.1)). Figure 4.4 illustrates the sensitivity of the vole dynamics to changes in the four parameters that determine this induction term and also to the silica decay rate. We varied each parameter by $+/-70\%$ of the values used in Figure 4.3, with the other parameters fixed. Throughout this range, changes in the parameter values mainly have quantitative effects on the amplitude of the population cycles, with changes in the value of the delay parameter, T, and the Hill coefficient, n, having the largest effects. In addition, a qualitative difference in the dynamics is predicted for sufficiently small values of T, n, and K, which is proportional to the maximum rate of silica production. Specifically, the dynamics change from cyclic to non-cyclic when T, n and K are decreased by 41%, 40% and 69% of their reference values, respectively. Cyclic behaviour is lost when c is increased by 192% of its reference value; we have never found non-cyclic behaviour when changing V_0.

4.4.4 Further model extension: Incorporating seasonality

Given the known destabilizing role of seasonality on trophic interactions (Hanski and Korpimäki, 1995; Altizer *et al.*, 2006), we investigated coupling our silica induction and decay model to an alternative model of vole population dynamics in which

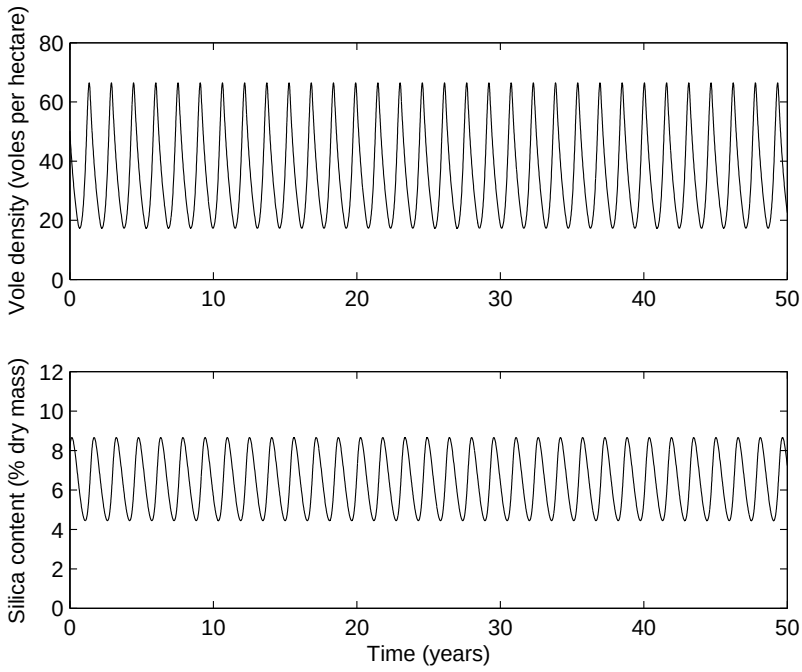

Figure 4.3: Vole population cycles driven by silica induction in grass, as predicted by the non-seasonal model: coupling equations (4.1) and (4.3). We assumed a maximum birth rate of 12.0 yr^{-1}; other parameters are as given in the main text. Solutions are shown after 50 years, which removes the effects of our initial conditions ($S = 5\%$ dry mass, $V = 25$ ha^{-1} for $t \leq 0$). In order to label the vole density axis, it is necessary to assign a value to V_{high}, the effective vole density corresponding to the high damage level, and we use $V_{high} = 50$ ha^{-1}. This implies that the effective vole density corresponding to the low damage level is $V_{low} = 50/4 = 12.5$ ha^{-1}. (These values of V_{high} and V_{low} give parameter values $K = 65.0$ yr^{-1} and $V_0 = 79.8$ ha^{-1}.)

each year was divided into a reproductive and non-reproductive season, with plant silica concentration determining the relative lengths of those seasons. Field studies have shown that the timing of seasonal reproduction in over-wintered female rodents can vary in a delayed density-dependent manner in some cyclic populations (Ergon *et al.*, 2011) and theoretical studies have provided evidence that the phenomenon of delayed density-dependent reproductive timing can generate population cycles (Smith *et al.*, 2006). Thus, it is hypothesized that, rather than the birth rate being modified by silica levels, it is the onset of reproduction that is delayed as a result of a high silica diet and this affects the total births in a season by reducing the breeding season length (Smith *et al.*, 2006). We therefore explored whether making the onset of the reproductive season a function of past silica concentrations could lead to cyclic dynamics. To do this we replaced the silica-dependent birth rate with a rate that is constant over a breeding season and incorporated seasonality by setting the breeding season length (in months) to be a function of the silica level in

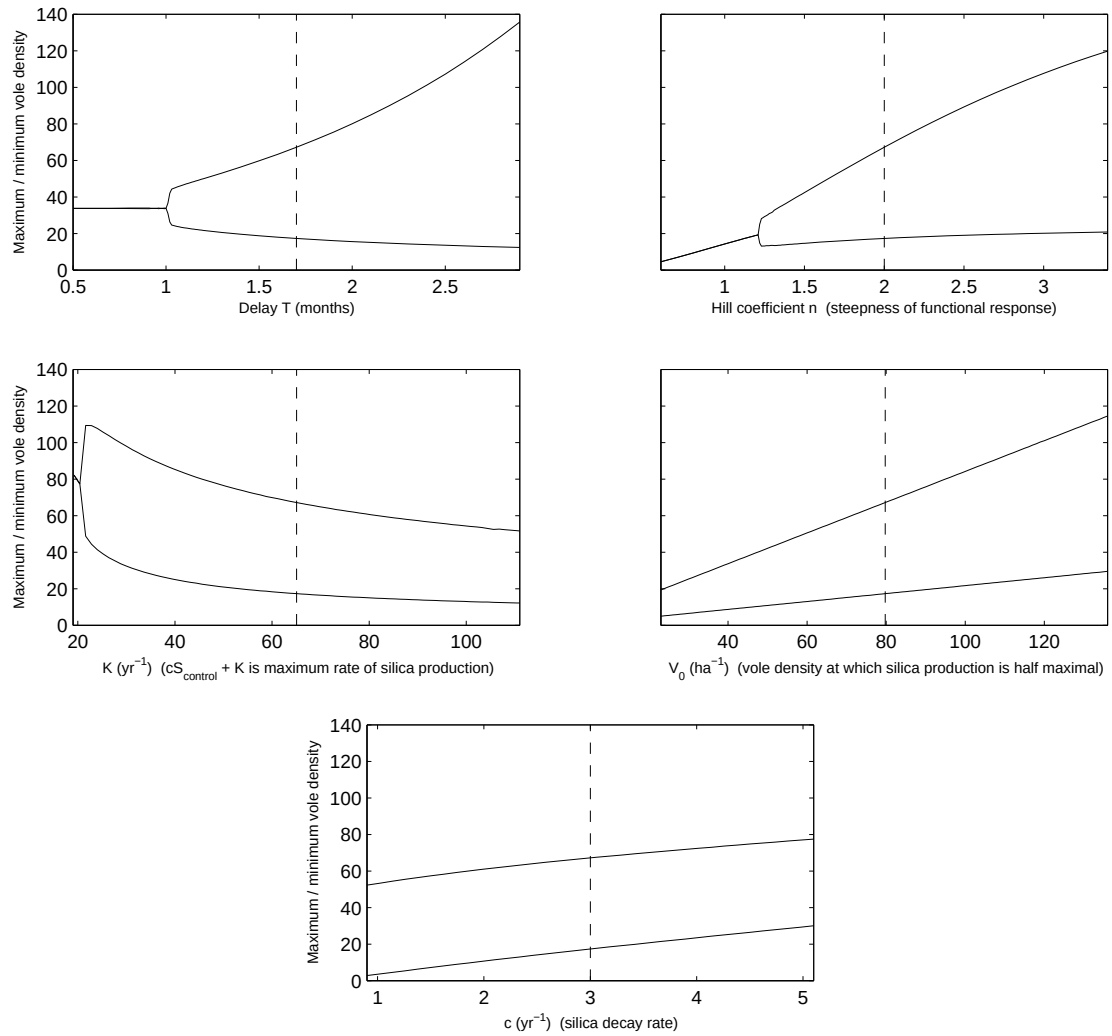

Figure 4.4: Sensitivity of vole population cycles to changes in the parameters in the silica equation (4.1). The five parameters are T, n, K, V_0 and c. In each panel we fix four of the five parameters at the values used in Figure 4.3, and vary the fifth by $+/-70\%$ (chosen arbitrarily). For a sequence of values of the varying parameter, we solved the non-seasonal model equations (4.1) and (4.3) for 500 years starting from initial conditions as in Figure 4.3, and then recorded the maxima and minima of the solutions over the next 100 years. Cases for which these two curves coincide correspond to non-cyclic dynamics. The dashed lines indicate the reference values of the five parameters, i.e. the values used in Figure 4.3.

the early spring. Therefore we modelled the vole population dynamics as

$$\frac{dV}{dt} = B_{max}V(t) - dV(t) \text{ in the breeding season} \quad (4.4a)$$

$$\frac{dV}{dt} = -dV(t) \text{ in the non-breeding season.} \quad (4.4b)$$

We assumed that the date of onset of the breeding season is a simple function of the plant silica concentration at the beginning of spring, of the form season length $= L_{min} + (L_{max} - L_{min})F(S(t^*))$, where $L_{min} = 4$ months and $L_{max} = 10$ months are the shortest and longest possible breeding seasons respectively (Smith *et al.*, 2006; Ergon *et al.*, 2011). We assumed $F = 1$ when $S < S_{control}$, and $F = 0$ when $S > 6.6\%$ dry mass, with F decreasing linearly as a function of silica between these two levels (see Figure 4.2(b)). Here t^* is a fixed 'census point', and represents the earliest possible start to breeding (in spring). Thus the breeding season starts at time $t^* + (L_{max} - L_{min})[1 - F(S(t^*))]$ and ends at time $t^* + L_{max}$.

The non-seasonal model framework and sensitivity analysis outlined above highlights the potential for silica effects on reproduction to drive cycles in natural systems. The seasonal model, more reflective of our particular vole system, predicts multi-year population cycles for lower and more realistic birth rates than the previous model (above 5.2 per year) and emphasises that the results are robust to the manner in which the silica effect is represented. The model solutions show intervals of irregular cycles separating periodic behaviour (Figure 4.5); dynamics of this type are characteristic of systems on the edge of chaos. The cycle periods are typically 3 or 4 years, with the breeding season lengths implied by the silica solutions varying between 4 and 7.5 months. Both of these properties and also the overall form of the simulated dynamics are highly reminiscent of field data on vole population cycles in general, and of the *M. agrestis* populations in Kielder Forest in particular (Lambin *et al.*, 2000).

4.5 Discussion

In this study we have empirically characterized the induction of silica-based defences in *Deschampsia caespitosa* following grazing. Furthermore, we have provided theoretical evidence that if this response alone is driving vole population dynamics through its impact on reproduction, then it could generate multi-year cycles in their populations. We restricted ourselves to a minimalist model grounded in empirical evidence: a variety of other factors are also likely to influence the delayed-density dependence even if induced silica defences are found to be a key mechanism driving cycles in some herbivore populations. For example, silica induced reductions in the

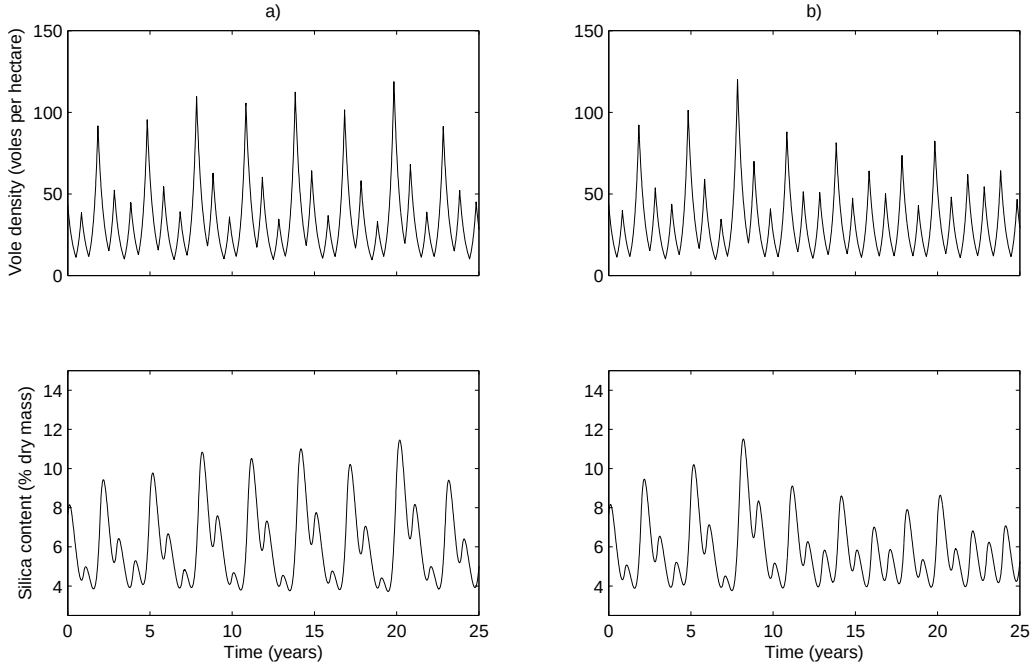

Figure 4.5: Vole population cycles driven by silica induction in grass, as predicted by the seasonal model: coupling equations (4.1) and (4.4). We assumed a birth rate of 6.42 yr^{-1} in (a) and 6.48 yr^{-1} in (b); other parameters are as given in the main text. Solutions are shown after 960 years, which removes the effects of our initial conditions. The initial conditions, and the assumed value of V_{high}, are as for Figure 4.3. In both (a) and (b), the breeding season length varies between 4 months and 7.5 months, in line with field data (Ergon *et al.*, 2011).

assimilation of nutrients by voles, which we hypothesize would delay reproduction further, could also reduce survivorship, fecundity, immune responses (Kapari *et al.*, 2006) and/or susceptibility to predators. It is important to note that silica defence induced cycles, if they do occur, are likely to be restricted to herbivores in which grasses form an important component of their diet, either as a dominant source of nutrition in general, or at specific time periods (e.g. over the winter). There is little empirical evidence for such induced plant defences operating in forb-eating cyclic *Myodes* vole populations in Fennoscandia. However, in the specific field study system modelled here, and in a wide range of other herbivore populations, grasses form a major component of the diet and may become the only source of nutrition during the winter. For example, Hansson (1971) found that grasses and graminoids were the dominant food source (together between 44 and 60% of the annual intake) for *Microtus agrestis* voles in Sweden. Whilst we have characterised the induced silica responses of just one grass species, itself an important food source for *Microtus* voles, Massey *et al.* (2007a, 2007b) demonstrated that several other grasses eaten by voles, e.g. *Festuca*, induce silica in response to vole grazing and that silica level was

the most important determinant of vole preference in experiments using 18 different grass species. Therefore, even if several different grasses are eaten in the field, as reported by Hansson (1971), we believe it is highly likely that silica defences are present in many of them and will be induced if herbivory is sustained.

While our model predictions are general, when parameterized by empirical data they are similar to multi-annual cyclic population trajectories observed at least in the southern European cyclic *Microtus* vole populations (where both peak and trough densities are higher than in Fennoscandia). Similarities include cycle period length, the variable breeding season length, and associated summer declines in density following extended non-breeding seasons, a feature shared by virtually all cyclic vole populations (Hansson and Henttonen, 1985). Moreover, both in model predictions and in field data from Kielder Forest, vole abundance in the trough of the cycles is relatively high, a feature that makes vole cycles in this location unlikely to be caused by predator–prey interactions.

There are four features of the observed functional response of *D. caespitosa* to grazing that we predict would contribute to it having a destabilizing effect on rodent population dynamics: (i) the time lag between initial damage and an induced response; (ii) the nonlinear response of the rate of silica induction to grazing intensity; (iii) the relatively slow relaxation rate of the response in the absence of grazing; (iv) the overall magnitude of the silica response and the assumed associated impact on vole reproduction. Our sensitivity analysis (Figure 4.4) describes how variation in each of these features might influence the interaction and also suggests that the cycles predicted by our models are not restricted to narrow, nor unrealistic, ranges of parameter values.

The time lag between initial damage and the observed induced response in our experiments is within the (wide) range of induced physical responses seen in other plant species (e.g. Molano-Flores, 2001; Dalin and Bjorkman, 2003), but is slow relative to the induction of many chemical defences (e.g. Hartley and Firn, 1989; Underwood, 1998). On that basis we predict that induced physical defences are more likely to have a destabilizing effect on herbivore populations than most types of chemical defences. The shape of the functional response of silica induction to grazing intensity implies some mechanism through which, above a threshold level of cumulative grazing, plants rapidly increase silica uptake and deposition. This is consistent with a previous study using two other grass species, in which repeated damage was required for silica induction and a single high damage event had no detectable effects on silica concentration in re-growth tissues (Massey *et al.*, 2007a). Overall, this finding implies that the grazing-induced silica defence mechanism is an active response which can be 'switched on' by some stimulus induced by sufficient grazing. Our theoretical findings confirm that the existence of this threshold-like

induced silica response significantly increases the likelihood of an unstable plant–herbivore interaction (Figure 4.4).

The observed relaxation of silica defences after the cessation of grazing occurs over a relatively long period of time, being predicted to take around a year to decline to within 5% of control levels. This rate is likely to be significantly slower under colder field conditions because the rate of silica uptake is affected by temperature (as are many other transport processes in plants; Tamai and Ma, 2003); also leaf lifetime is likely to be longer in the field than under greenhouse conditions. Once silica is deposited as phytoliths within the leaves it is highly immobile and likely to remain there for the lifetime of the leaf (Epstein, 1999). Furthermore, in perennial grasses like *D. caespitosa*, which have relatively slow leaf turnover, much of the standing leaf biomass will retain the 'memory' of past induction, although old leaves may only be eaten by voles at times of acute food stress. Similar slow relaxation rates in physical defences have been observed in other systems (Bryant *et al.*, 1985; but see Sinclair *et al.*, 1988, Huntzinger *et al.*, 2004). We only measured silica concentration in regrowth tissue so we do not know whether silica deposition also takes place in extant leaves that survive herbivore damage events, or whether induction is restricted to the plant growing season. Further, the mechanistic links between silica induction responses and population dynamics in field conditions remain untested.

Although silica has long been thought to be a potentially inducible defence mechanism in grasses (McNaughton and Tarrants, 1983), the main mechanism by which silica was thought to deter herbivores was a constitutive one, namely increased abrasion and physical resistance by phytoliths (Reynolds *et al.*, 2009). Attempts to demonstrate that silica is inducible by experimental damage have produced conflicting results (Kindomihou *et al.*, 2006), possibly because many studies use artificial defoliation which does not cause the same defence induction response as real herbivory (Massey *et al.*, 2007a). This distinction between plant responses to real and artificial herbivory is long established (e.g. Hartley and Firn, 1989) and the mechanisms responsible are now elucidated (Halitschke *et al.*, 2001). Here we demonstrate a more dynamic aspect of silica defences, whereby herbivory itself is shown to alter the rate of silica uptake by the plant and this response decays once herbivory stops. Our work clearly indicates that physical defences should no longer be viewed as static and unresponsive. Rather, it adds to a growing body of evidence that plants may adapt their physical defences in response to external stimuli in a similar way to many inducible chemical ones, adding a new dimension to our understanding of the evolution of plant defences.

In conclusion, our study provides clear evidence that a principal food species of an herbivorous rodent exhibits a delayed defensive response to grazing, and provides the first empirical data on the details of this induction and of the subsequent relax-

ation. Our modelling further predicts that this induction–relaxation response alone is sufficient to drive the population cycles both in the specific system of *M. agrestis* voles in Kielder Forest, and more generally in other graminivorous rodent populations in which populations reach sufficiently high densities so as to induce silica defences in their food supply. These results argue strongly for a more widespread assessment of the extent and role of silica defences in natural communities, in particular those with cyclic populations of herbivores.

Chapter 5

A comparison of the dynamical impact of seasonal mechanisms in a herbivore–plant defence system

This chapter largely contains material submitted for publication (Reynolds *et al.*, submitted, b). This is a collaboration between Jennifer Reynolds, Jonathan Sherratt, Andrew White and Xavier Lambin. Jennifer Reynolds, Jonathan Sherratt and Andrew White developed the mathematical models, and Xavier Lambin provided biological insights. Jennifer Reynolds performed the model simulations and analysis. Jennifer Reynolds wrote the paper, with comments from all co-authors.

Plant defences can reduce herbivore fitness and may promote population cycles in some herbivore systems. In this study, we model the interaction between plant defences and herbivores, and include seasonal forcing, a ubiquitous environmental influence in natural systems. We compare the impacts of two different seasonal mechanisms on the dynamics of the herbivore–plant defence model. The first mechanism involves a fixed breeding season length and a variable birth rate within the breeding season; the second involves a variable breeding season length and a fixed birth rate within the breeding season. When parameterised for a specific cyclic system, namely field voles and silica, our model predicts that a variable season length gives multi-year cycles for a larger region in parameter space than a variable birth rate. Our results highlight the complexity of the dynamical effects of seasonal forcing, and that these effects are strongly dependent on the type of seasonal mechanism.

5.1 Introduction

Cyclic patterns in animal populations have long been a focus of scientific interest (Elton, 1924; Turchin, 2003). Despite extensive research, the mechanisms under-

pinning these multi-year population cycles are a subject of much debate (Krebs, 1996; Turchin, 2003). Elton (1924) described the widespread existence of periodic fluctuations in animal abundance and attributed this to climatic variations. Since then, many hypotheses concerning the factors determining population cycles have been developed. However, firm evidence for causality is rare and the elucidation of the processes driving population cycles is a key topic of interest in population ecology. Also, it is becoming increasingly recognised that different and/or multiple mechanisms may operate in different systems (Turchin, 2003).

One hypothesis is that interactions with food resources can cause population cycles (Lack, 1954). This includes classical studies that focus on predator–prey interactions (Lotka, 1925; Volterra, 1926; May, 1972) but also includes plant–herbivore interactions. There are two main distinct ways in which herbivore populations can be affected by interactions with the food plants. Firstly, the consumption of plant tissue may limit the quantity of food available to later-feeding herbivores; secondly, herbivore damage may elicit inducible resistance in the plant, thereby reducing the nutritional quality of the plant tissue (Karban and Baldwin, 1997). Both of these pathways could play important roles in the long-term population dynamics of herbivores (Abbott *et al.*, 2008). Changes in the abundance of food is thought unlikely to cause cycling, because a sufficient depletion of plant biomass is rarely observed, with many plant species recovering rapidly after grazing (e.g. Krebs *et al.*, 1986; Desy and Batzli, 1989; Boonstra *et al.*, 1998). However, there is significant evidence that in some systems, population cycles are related to the deterioration in the quality of food due to induced defences of the plant in response to intense grazing at the population peak.

In many plants, damage by herbivory induces changes in the composition of the foliage (Fowler and Lawton, 1985). Many plant characteristics, ranging from secondary chemistry to physical features such as thorn density, can change in response to herbivore damage (Karban and Baldwin, 1997). These inducible defences have been shown to adversely affect herbivore growth and/or reproduction (e.g. Bryant, 1981; Schultz and Baldwin, 1982; Karban and Carey, 1984; Massey *et al.*, 2006; Massey and Hartley, 2006). As a result, inducible defences are predicted to significantly influence the dynamics of herbivore populations. Indeed it has been argued that inducible defences contribute to driving cyclic fluctuations in a number of herbivore populations (Benz, 1974; Haukioja, 1980; Fox and Bryant, 1984; Haukioja, 1991b). For example, Fox and Bryant (1984) demonstrate that the responses of Alaskan woody plants could account for the oscillatory nature of the snowshoe hare population. Benz (1974) shows that the larch tree responds to high levels of feeding by the larch budmoth by growing short needles of reduced nutritional quality. This causes a decrease in budmoth population density. This interaction is claimed to con-

tribute to the population cycles of the larch budmoth. It should be noted that there is also evidence contrary to the hypothesis that inducible defences cause cycles; for example, the findings of Sinclair *et al.* (1988) suggest that inducible changes in the levels of plant secondary compounds do not cause the cyclic population dynamics of the snowshoe hare.

There is also a growing body of theoretical evidence that grazing-induced plant defences contribute to cyclicity (Lundberg *et al.*, 1994; Underwood, 1999). Underwood (1999) developed a model framework that focuses on the impact of induced resistance due to herbivorous insect populations. Lundberg *et al.* (1994) model herbivore population density and the plant population, stratified into discrete classes to represent the different plant defence levels that result from the grazing intensity the plant has been subject to. The model is applied to understand the changes in abundance observed in lemmings. These studies provide theoretical support for the idea that inducible defences in plants can cause fluctuations. In contrast, Edelstein-Keshet and Rausher (1989) develop a general mathematical framework and find that inducible defences cause persistent fluctuations only under unusual conditions. Lundberg *et al.* (1994) conclude that inducible defence may be an important factor for explaining the cyclic dynamics of herbivore populations, but their model does not generate stable limit cycles. They believe that seasonal perturbations may maintain the cycles, although no evidence for this is given. The aim of this chapter is to investigate in detail the way in which seasonal forcing affects the dynamics of a herbivore population regulated by inducible plant defences. We develop a simple model to represent the herbivore–plant interaction, and examine the effects on the population dynamics of adding seasonality.

Understanding seasonality in ecological systems is of great importance since natural populations are embedded in periodically varying environments. Imposing periodic forcing on a biological system can lead to major changes in system behaviour: it has long been established that unforced systems with simple dynamic behaviour can become very complex when periodically forced (Guckenheimer and Holmes, 1986). Identifying the role played by seasonal forcing in driving dynamical behaviours is therefore a key issue.

Despite the ubiquitous nature of seasonality, exploring its consequences for population dynamics poses a challenge. Seasonal mechanisms can be difficult to pinpoint empirically and can give rise to complex population fluctuations (Altizer *et al.*, 2006). One area where the effects of seasonality on population dynamics has been relatively well explored is in infectious diseases. Seasonality has been incorporated into epidemiological models in the areas of childhood diseases (Dietz, 1982; Schwartz and Smith, 1983; Keeling *et al.*, 2001) and wildlife diseases (Roberts and Kao, 1998; Ireland *et al.*, 2004; Smith *et al.*, 2008). If the underlying non-seasonal

model has periodic solutions, then the dynamics once seasonal forcing is imposed can become more complex; the seasonality can interact with underlying oscillations, resonate, and result in a range of complex behaviours including chaos (Ireland *et al.*, 2007). If the non-seasonal model does not have periodic solutions, the application of seasonality can, in some cases, cause oscillations with period an integer multiple of the forcing period (Schwartz and Smith, 1983; Greenman *et al.*, 2004). In addition, there have been a number of studies on seasonality in predator–prey systems (Kuznetsov *et al.*, 1992; Rinaldi *et al.*, 1993; Gakkhar *et al.*, 2009). These models show a rich variety of behaviour, including stable and unstable periodic solutions of various periods, quasi-periodicity and chaos. Moreover, the behaviours can be transitory, for example windows of periodicity can be observed. This confirms that seasonality has the power to transform simple ecosystems into complex ones. These examples illustrate the complexity of the role of seasonality in shaping population dynamics. Adding seasonality can lead to interesting and biologically important dynamics, and can help to explain complex empirical data.

In strategic theoretical studies, seasonal forcing is typically incorporated by setting a specific model life history parameter to periodically vary in time, for instance by simple sinusoidal variation of the parameter (e.g. Rinaldi *et al.*, 1993; Greenman *et al.*, 2004; Greenman and Norman, 2007; Ireland *et al.*, 2007). Alternatively, seasonal variation is incorporated in a manner motivated by the biological reality of the specific system being studied: for example, models of childhood diseases incorporate seasonal variation in contact rates by imposing an increased rate during school terms compared to school holidays (Keeling *et al.*, 2001). Many natural systems have defined breeding seasons and therefore seasonality can be applied to the birth rate by defining a distinct reproductive and non-reproductive season (Smith *et al.*, 2008).

In this chapter, we apply seasonal forcing to the herbivore birth rate in a simple plant defence–herbivore model. We examine the effects of two different seasonal mechanisms to explore the role of seasonality in driving population fluctuations. The first seasonal mechanism involves a birth rate dependent on the level of plant defence, with a fixed breeding season length. The second involves a breeding season length dependent on the plant defence, with a constant birth rate in the breeding season. We undertake a comparison of these two types of seasonal forcing and their effects on the herbivore population dynamics. In order for a full investigation to be carried out, we choose a specific system as a case study, namely the interaction between voles and the silica content of the grass they consume.

5.2 Model

We use a general model framework to represent the interaction between herbivores and an inducible plant defence:

$$\frac{dH}{dt} = a(S(t),t)H(t) - bH(t) \tag{5.1}$$

$$\frac{dS}{dt} = \frac{K(H(t-\tau))^2}{H_0^2 + (H(t-\tau))^2} + cS_0 - cS(t) \tag{5.2}$$

where $H(t)$ is the herbivore density and $S(t)$ the level of plant defence at time t. Inducible plant defences have been shown to affect growth or reproduction in individual herbivores adversely (e.g. Bryant, 1981; Schultz and Baldwin, 1982; Karban and Carey, 1984; Massey *et al.*, 2006; Massey and Hartley, 2006); in line with this evidence, we take the herbivore birth rate a to be a function of the level of the inducible factor. Parameter b is the herbivore death rate. We denote by cS_0 the background level of plant defence production; here S_0 is the background level of the inducible factor, i.e. its level in the absence of herbivory. The induction rate depends on the herbivore density, with a sigmoidal functional form. By definition, the induction level drops to zero in the absence of herbivores, and physiological constraints mean that its production must saturate at high levels of herbivory. H_0 is the herbivore density at which induction is half of the maximum possible, and $K + cS_0$ is the maximum possible rate of production of the inducible factor. The time delay τ represents the time taken for the inducible factor to be produced after herbivory occurs. Parameter c is the decay rate of the inducible factor. The plant defences decay when herbivory diminishes; Rhoades (1983) argues that this is because inducible defences are costly to a plant and are therefore not likely to be maintained unless a need for them exists.

We denote by a_{max} and a_{min} the maximum and minimum birth rates respectively. We make the assumption that for $S < S_0$ there is no effect of the plant defence on the herbivore, so the birth rate is at its maximum. Above inducible factor levels of S_0, the birth rate decreases linearly with concentration.

In reality, many animal species have seasonal birth rates, so we impose a seasonally forced herbivore birth rate by introducing a breeding season and non-breeding season each year. This is typical of the life-history of many herbivore species in temperate climates. We let the length of the breeding season be denoted by l. In the non-breeding season, the herbivore birth rate a is taken to be zero.

We consider two different seasonal mechanisms, both affecting the herbivore birth rate. Firstly, the birth rate a in the breeding season is dependent on the concentration of inducible factor, and secondly, the breeding season length l is dependent

on the concentration of inducible factor. We denote by l_{max} the maximum breeding season length, and by l_{min} the minimum breeding season length. The addition of seasonal forcing typically complicates and potentially destabilises the population dynamics of a system. By examining two different mechanisms, we intend to test whether the way seasonality is manifested influences its effects on the population dynamics.

5.3 Case study

In order to analyse this model, we focus on a specific case study. Our aim is to compare two different seasonal mechanisms operating on the herbivore birth rate. We therefore focus on a particular ecological system where both mechanisms can potentially operate, namely the interaction between voles and the silica content of the grass they consume. The choice of voles as the herbivore species is a natural one due to the abundance of literature on the potential causes of vole population cycles.

Silica (silicon dioxide, SiO_2) in the tissues of grasses acts as an antiherbivore defence strategy to reduce levels of grazing by both vertebrate (McNaughton and Tarrants, 1983; Gali-Muhtasib *et al.*, 1992; Massey and Hartley, 2006) and invertebrate herbivores (O'Reagain and Mentis, 1989; Vicari and Bazely, 1993; Massey *et al.*, 2006). Silicification is the most widespread characteristic of grasses thought to play a role in herbivore resistance. For plants that cannot respond to grazing damage by compensatory shoot growth, production of toxins can have an adaptive advantage at the individual level, by reducing the depletion of plant tissue by herbivory.

Silica has been proposed as the primary defence in many grasses (Massey *et al.*, 2007b). There is evidence that it has a range of detrimental effects on herbivores that ingest it (Jones and Handreck, 1967). Silica reduces foliage digestibility, leading to reductions in herbivore growth rates (Massey *et al.*, 2006; Massey and Hartley, 2006; Massey *et al.*, 2008). In addition, silica increases the abrasiveness of grass, deterring feeding by herbivores (Massey *et al.*, 2006; Massey and Hartley, 2006; Massey *et al.*, 2007b). Therefore silica acts to reduce the quality of the plant as food for herbivores. Food quality is especially important for voles due to their relatively high metabolic rates, and because they have a limited capacity to increase food consumption to compensate for poor quality diets (Zynel and Wunder, 2002). In addition, their growth rates early in development are highly dependent upon nutrient intake. Therefore, vole food quality has the potential to dictate the time taken to reach sexual maturity and the onset of breeding each year (Krebs and Myers, 1974; Ergon *et al.*, 2001).

Silica defences in grasses are induced by herbivore grazing (McNaughton and

Tarrants, 1983; Massey *et al.*, 2007a). The induction of defences in response to herbivore damage is widely recognized as an effective plant defence strategy, particularly in cases where defences are costly or the threat of herbivore attack is intermittent (Karban and Baldwin, 1997). It has been shown that silica can be induced by vole grazing to levels sufficient to deter further feeding and also affect herbivore performance (Massey and Hartley, 2006).

To parameterise this model, we use the particular case of field voles (*Microtus agrestis*) in Kielder Forest, Northern UK. This vole population fluctuates cyclically over a range of about 20–700 voles/hectare in optimal habitats with a characteristic period of 3–5 years (see Lambin *et al.* (2000) for details). There are long term data sets on vole populations, and intensive studies on the field vole, its predators and its food plants have been conducted. The roles of predation by the common weasel, a vole specialist, and intrinsic mechanisms (e.g. maternal effects) have been tested and rejected as causal mechanisms for vole population cycles in this area (Ergon *et al.*, 2001; Graham and Lambin, 2002). In contrast, grazing induced changes in plant quality, affecting vole nutrition and their ability to reach reproductive status in the spring, could offer a plausible explanation.

In Kielder Forest, the grass species *Deschampsia caespitosa* is the dominant food plant for voles, and in winter and early spring, when energetic demands for voles are at their highest, there is no significant alternative food source. There is growing evidence that, in this area, silica levels in the grass may be a determinant of cyclic population patterns. A correlation between vole population density, and therefore grazing intensity, and grass silica content has been noted in the field (Massey *et al.*, 2008): in sites where vole population density was high, silica levels in grass leaves collected several months later were also high, and vole populations subsequently declined; in sites where vole population density was low, silica levels were low and population density subsequently increased. These findings highlight the potential importance of interactions between silica defences and vole abundance, and suggest that, for this specific population, silica-based defences in grasses may play an important role in driving vole population cycles.

We take the inducible factor S in equations (5.1) and (5.2) to be silica (% dry mass), and the herbivore density H to be the density of field voles (per hectare). Using a least squares method, we have previously derived parameter estimates for K, H_0, S_0, c and τ using greenhouse data (Reynolds *et al.*, submitted, a). Field data (Graham and Lambin, 2002; Burthe, 2005) give monthly survival probabilities, which lead to an estimate for the vole death rate of $b = 0.22$ per month (corresponding to a monthly survival of about 80%) (Smith *et al.*, 2006). These parameter values are shown in Table 5.1. (Note that the estimates of parameters K and H_0 are chosen in order to set an absolute scale for the population densities.)

Parameter	Value
K	5.42 per month
H_0	79.77 per hectare
S_0	2.54% dry mass
c	0.25 per month
b	0.22 per month
τ	1.7 months

Table 5.1: Parameter estimates for the case study.

We assume that the birth rate is at its minimum value (i.e. silica has its maximum effect) for silica levels of 6.6 and above. This value is taken from experimental data of Massey *et al.* (2008): a vole growth rate of 0 corresponds to a silica content of 6.6% dry mass. Between silica levels of 2.54 (the background level of silica, S_0) and 6.6, we assume the birth rate decreases linearly with silica. Figure 5.1(a) illustrates the vole birth rate function used in our model.

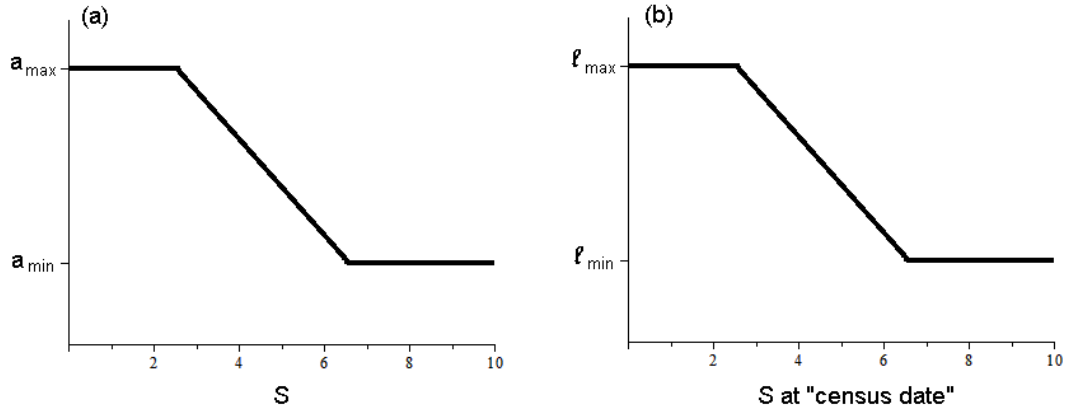

Figure 5.1: (a) Vole birth rate a and (b) vole breeding season length l as functions of silica S. For (a), the birth rate is dependent on silica at the present time, whereas for (b), the breeding season length is dependent on silica at the "census date".

There is a significant variation in the available estimates for the maximum birth rate of voles, a_{max}. Time series data from Kielder Forest imply a value of at least 0.3 per month (Smith *et al.*, 2006), whereas trapping data imply a figure of 0.9 (Smith *et al.*, 2008). Studies of similar rodent taxa have suggested values of 1.2 and 1.3 (Turchin and Ostfeld, 1997). We therefore regard this parameter as variable, and

investigate the effects on the model solutions of changing a_{max}.

5.4 Seasonal models

We consider two different seasonal models.

Seasonal model 1: The breeding season length is fixed; we denote it by l_{max}. During this part of the year, the birth rate is given by the function $a(S(t))$ (illustrated in Figure 5.1(a)), and in the remainder of the year the birth rate is set to zero.

The timing of spring reproduction shows substantial variation in Kielder Forest (Ergon *et al.*, 2011); the onset of the breeding season varies from mid-March to early June in different years. To test the possible effects of this on the population dynamics, we develop a second seasonal model. In this model, silica affects vole breeding through the regulation of the season length:

Seasonal model 2: The breeding season length l depends on silica as depicted in Figure 5.1(b). We assign a "census date" at the earliest possible time in the year at which the breeding season can start, and it is the silica level at this date that determines the breeding season length for that year. The birth rate in the breeding season is always fixed at its maximum value a_{max}. The birth rate is zero in the non-breeding season.

The underlying silica-dependent functional form is the same for both models (Figure 5.1); the season length in model 2 depends on silica in the same way as the birth rate depends on silica in the first seasonal model. For low silica levels (i.e. less than or equal to 2.54% dry mass) the two models become equivalent: there is a birth rate of a_{max} for l_{max} months. We impose these conditions to allow us to compare the two models in an effective way.

5.5 Results

Our aim is to compare the effects of the two different seasonal mechanisms on the population dynamics. There are two steady states: the trivial $(H, S) = (0, S_0)$ and another with non-zero H. We can determine for which parameter values the trivial steady state is stable using Floquet theory (see Appendix A). When the trivial steady state is unstable, the non-trivial steady state is relevant. The seasonal forcing means that any solution will be cyclic, displaying either annual or multi-year cycles. The annual cyclic behaviour is due simply to the dynamics being entrained to the

annual seasonal forcing. Our focus is an investigation of the causes of multi-year cycles, which here refer to repeated oscillations in abundance with a cycle period longer than one year.

To compare the two seasonal models, we initially set $a_{min} = l_{min} = 0$. The maximum reproductive season length for field voles in Kielder Forest is 10 months (Ergon *et al.*, 2001), so we set $l_{max} = 10$ here. Figure 5.2 shows the cycles generated for both models for three different values of the maximum herbivore birth rate, a_{max}. This figure shows that as a_{max} increases, cycles change from annual to multi-year. We find that seasonal model 2 gives multi-year cycles for lower values of the maximum herbivore birth rate than seasonal model 1. Specifically, model 1 generates multi-year cycles for a_{max} values of 0.73 per month and above; model 2 generates multi-year cycles for values of 0.44 per month and above. So model 2 has the largest region in parameter space where there are multi-year cycles.

We can compare the results of these seasonal models with the results of the model *without* seasonality. By definition, the non-seasonal model does not have distinct non-breeding and breeding seasons; rather, breeding occurs throughout the year, with the birth rate depending on silica as shown in Figure 5.1(a). Due to the absence of seasonality, there is no underlying annual cycling for this non-seasonal framework. The non-seasonal model predicts cycles for a_{max} values of 0.70 per month and above. Below this value, the solutions are non-cyclic. Therefore, the seasonality mechanism in model 1 actually slightly reduces the region in parameter space where there are multi-year cycles. In contrast, this parameter region is significantly larger for seasonal model 2. Note that in order to make a comparison between the seasonal and non-seasonal models, we scale the birth rate for the non-seasonal model, so that over one year the birth rate is equivalent to that of the seasonal models.

A delay term is known to be a potentially destabilising factor (Haberman, 1977). The data used to parameterise the model for the vole–silica system clearly indicates a short delay (of 1.7 months) between herbivore damage and plant response (Reynolds *et al.*, submitted, a). Moreover, other theoretical studies modelling herbivore–plant defence interactions also include a delay term (Underwood, 1999). However, from the viewpoint of generality to other systems, it is important to explore the effects of changing the delay length τ, including the particular case of no delay. Figure 5.3 shows the lowest maximum birth rates for which multi-year cycles are generated (as opposed to annual cycles) for both seasonal models, for a range of τ values, including $\tau = 0$. Seasonal model 2 consistently predicts multi-year cycling for a larger region in parameter space. Therefore our main conclusion remains the same regardless of the value of the delay term: seasonal model 2 generates multi-year cycles for lower values of a_{max} than seasonal model 1. For $\tau = 0$, values above 0.47 per month give multi-year cycles for model 2; the corresponding threshold value is 3.76 per month

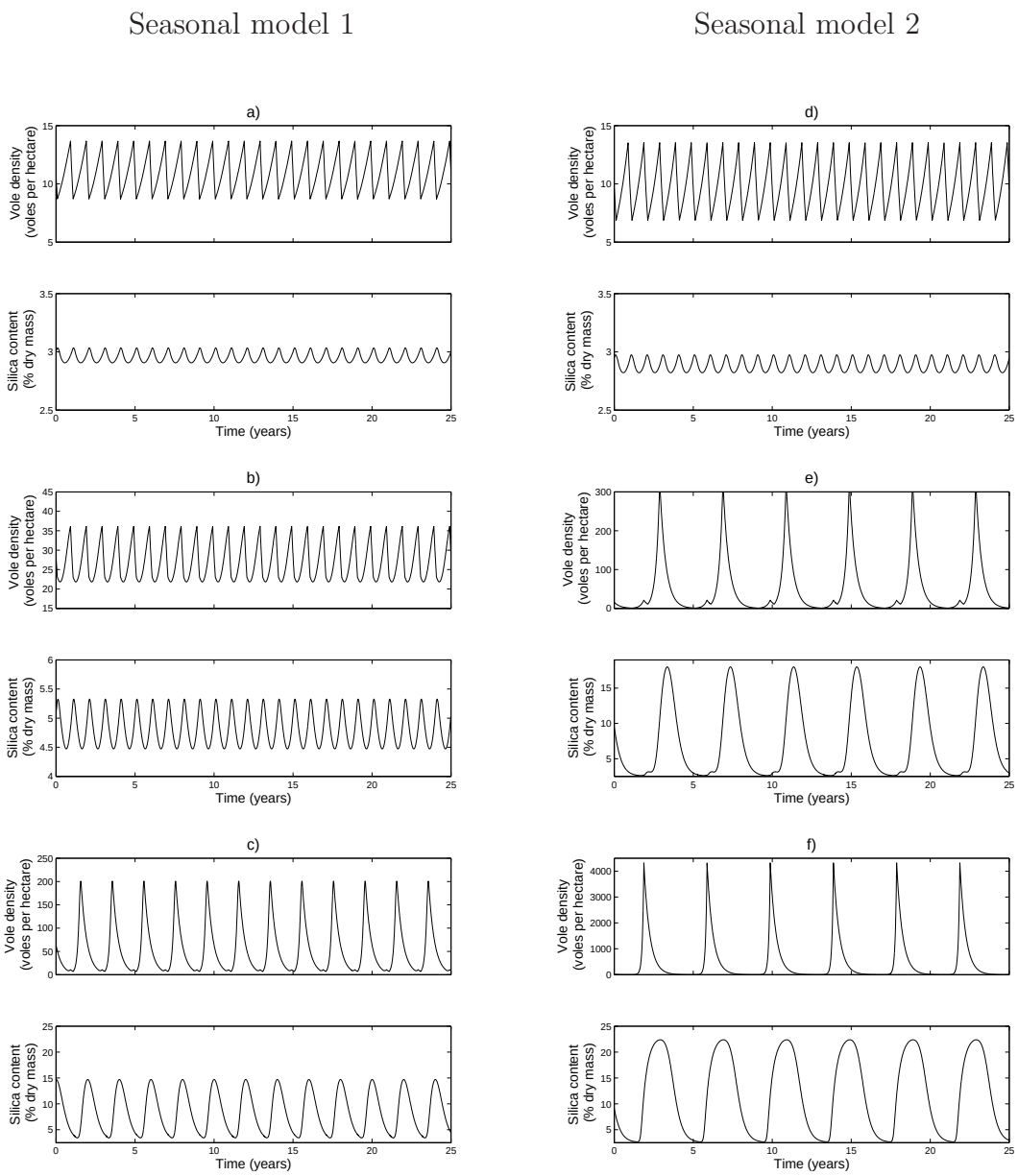

Figure 5.2: Cycles generated for seasonal model 1 and seasonal model 2 for three different values of a_{max}, the maximum birth rate. $a_{max} = 0.3$ (per month) for (a) and (d); $a_{max} = 0.6$ for (b) and (e); $a_{max} = 1.2$ for (c) and (f). Here $a_{min} = l_{min} = 0$, and $l_{max} = 10$ as explained in the main text. These simulations are produced by MATLAB using the delay differential equation solver dde23. Initial conditions are: $S = 5\%$ dry mass and $H = 25$ per hectare for $t \leq 0$. Solutions are shown after 450 years. Note that in order for the cycles to be seen clearly, the scales on the y-axes are not all the same. Seasonal model 2 has a greater tendency to produce multi-year cycles.

for model 1. It can be seen from these results that the delay plays an important role in the generation of multi-year cycles for seasonal model 1; the value of the maximum birth rate has to be increased significantly to give multi-year cycles in the case with no delay. However, for seasonal model 2, the delay has relatively little effect on the population dynamics.

Figure 5.3 also shows the lowest maximum birth rate values for which the corresponding non-seasonal model generates cycles. For this model, below the line the solutions are non-cyclic. This line is above that for seasonal model 2 for all values of the delay considered, but its relation to the line for seasonal model 1 is dependent on the delay value. The non-seasonal model does not produce cycles without the delay.

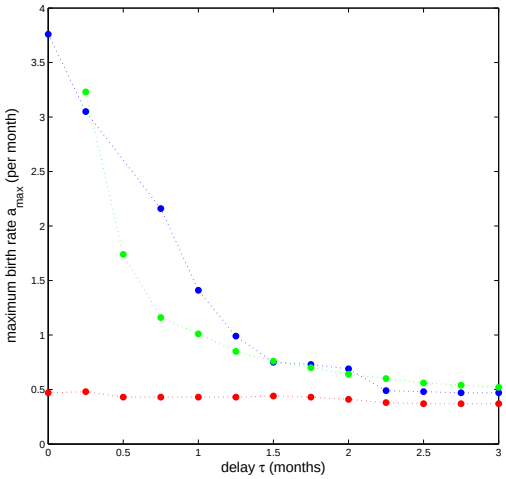

Figure 5.3: The lowest maximum birth rates for which there are multi-year cycles, for varying values of the delay τ. Results are shown for both seasonal models and also for the non-seasonal framework as explained in the main text. Blue line: seasonal model 1; red line: seasonal model 2; green line: non-seasonal model. For the seasonal models, below the lines there are annual cycles. For the non-seasonal model, below the line the solutions are non-cyclic.

We can conclude that the seasonal mechanism of model 2 drives multi-year cycles more strongly than that of model 1. That is, a variable season length produces multi-year cycles for a larger range of parameters than a variable birth rate. This result holds irrespective of the value of the delay. Therefore, within the context of our model framework, a variable season length is more powerfully destabilising than a variable birth rate. One mechanism causes a significantly greater tendency to cycle than the other, indicating that the way seasonality is incorporated into a model is highly important. This emphasises that the way seasonality operates can have

important implications for the population dynamics.

5.5.1 Combining seasonal mechanisms

Above we study the two seasonal mechanisms in isolation. We now consider a model where a combination of both seasonal mechanisms is possible. We introduce two new parameters in order to characterise the combination of the seasonal mechanisms: p_{birth} and p_{length} defined such that

$$\begin{aligned} a_{min} &= a_{max}(1 - p_{birth}) \\ l_{min} &= l_{max}(1 - p_{length}). \end{aligned}$$

Parameter p_{birth} denotes the strength of the silica effect on birth rate. Similarly, p_{length} denotes the strength of the silica effect on the season length. Both parameters take values in the range $[0, 1]$. For low silica levels, the breeding season length and birth rate are both at their maximum values, independent of p_{birth} and p_{length}. (Seasonal model 1 of the above analysis is recovered when $p_{birth} = 1$ and $p_{length} = 0$. Similarly, seasonal model 2 is recovered when $p_{birth} = 0$ and $p_{length} = 1$.)

In our model framework we assume that any regulation of the birth rate and breeding season is due entirely to silica. This is because we want to examine the silica effect alone. A consequence of this is that for low values of p_{length} and p_{birth} (i.e. weak silica effects), there is insufficient control on the population, leading to an unbounded increase in vole density. (This is an obviously unrealistic outcome; see Appendix B for more details.) In practice, population pressure is manifested in many different ways, and other forms of regulation will limit growth at high densities.

Our aim is to assess the role of different types of seasonal forcing in driving multi-year cycles. We therefore look at the division in parameter space between annual and non-annual cycles, and also the behaviour of the non-annual cycles. Figure 5.4 shows the dominant periods of the cycles generated for a range of a_{max} and l_{max} values. It can be concluded that an increase in the maximum birth rate or the maximum breeding season length induces multi-year cycles in general: as a_{max} or l_{max} is increased, there are fewer annual cycles (dark blue dots) and more multi-year cycles, and greater cycle periods are attained. In addition, the cycles with the longest periods are for high p_{length} and low p_{birth}, i.e. when the silica has a strong effect on the season length and a weak effect on the birth rate. Parameter p_{length} is more likely to promote multi-year cycles than p_{birth}. Combining the two seasonal mechanisms has confirmed that variability in the season length is a more powerful driver of cycles than variability in the birth rate.

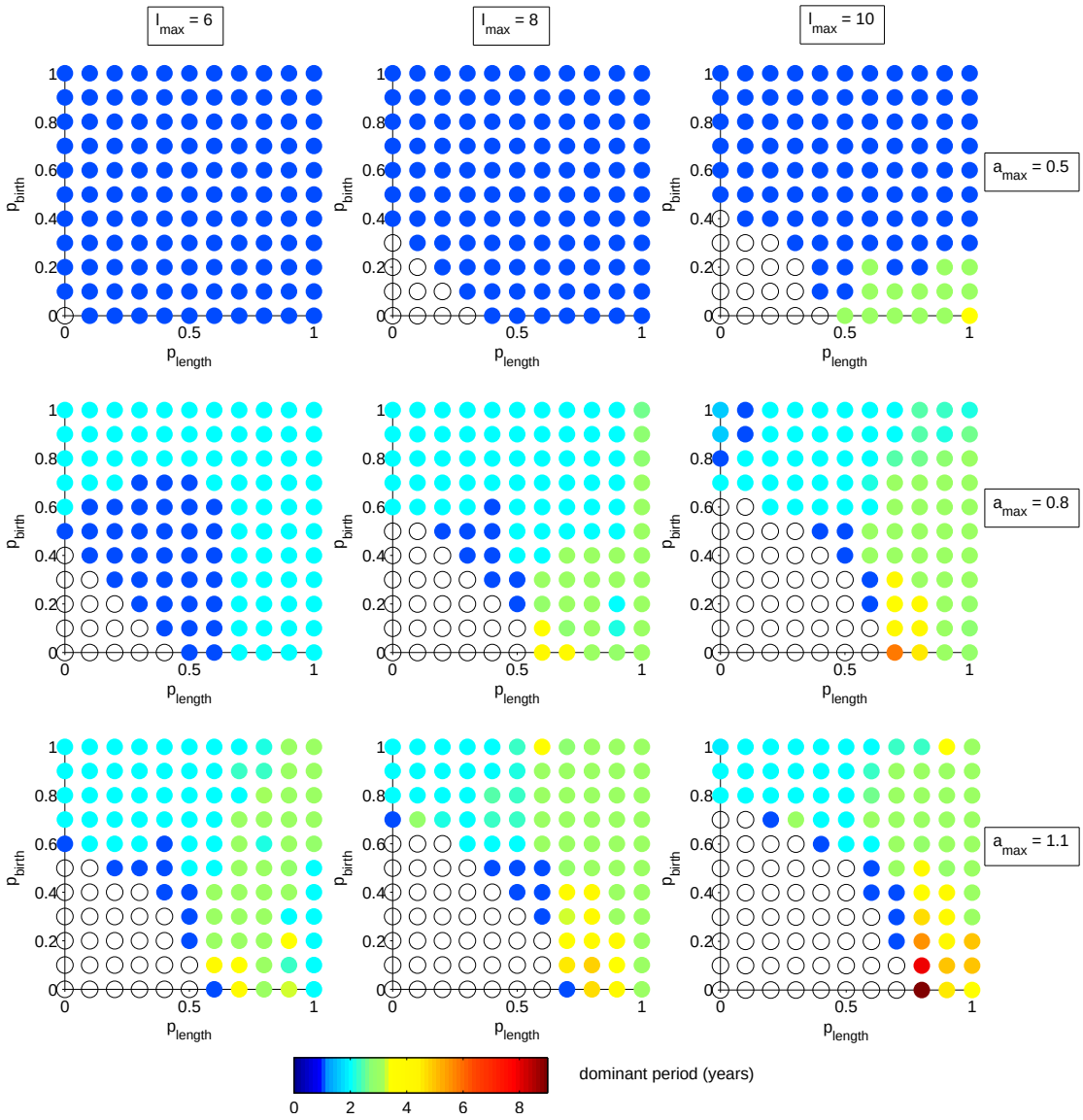

Figure 5.4: Dominant periods of the population cycles, for different parameter combinations. The uncoloured dots denote when the vole density increases without bound (due to lack of regulation by silica; see Appendix B). After 490 years, the densities are assessed at yearly intervals over 10 years. The difference between the maximum and minimum densities is compared to 5% (chosen arbitrarily) of the mean density. If the difference is smaller, then the cycles are deemed annual (dark blue dots); if larger, they are non-annual. For the non-annual cycles, fast Fourier transform is used to generate power spectra, from which the dominant period is established. The periods considered are restricted to those that are factors of the length of the time series data set processed. Therefore, in order to accurately capture the cyclic nature of the time series, we consider a range of different lengths of data. We record the period with the largest associated power value for each data length. These power values are scaled so that they can be compared, and the period corresponding to the largest power value (after scaling) across all the range is said to be the dominant period. Initial conditions are as for Figure 5.2.

In order to establish the dominant period of the multi-year time series predicted by the model, we use fast Fourier transform (this procedure is described in the legend to Figure 5.4). Some examples of the cycles generated by the model are shown in Figure 5.5. Each corresponds to a specific point from the grids of Figure 5.4. Figure 5.5(a) shows typical annual cycles (period = 1), and the other plots show multi-year cycles of various periods. The fast Fourier transform procedure gives non-integer periods for certain points, because it assigns an 'average' period. An example of this is shown in 5.5(d). In this case there is a repeating pattern of a cycle of period 2 followed by a cycle of period 3. The repeating pattern is not exact, and so the cycles are not of period 5. The average period of 2.5 represents / quantifies the cyclic behaviour generated in this instance.

5.5.2 Extensions to the model

From the results described above we can conclude that variability in the breeding season length (controlled by parameter p_{length}) is a more significant driver of cycles than variability in the herbivore birth rate (controlled by parameter p_{birth}). The season length is dependent on S at a given "census date", and the birth rate is dependent on S at the present time. In an attempt to elucidate the reasons behind our results, we consider an alternative seasonal model, where we set the birth rate to depend on the inducible defence level S at the "census date". Note that this modification is not motivated by biological realism, but is done to further our understanding of the model. Parameters p_{birth} and p_{length} are defined in the same manner as for the original seasonal model.

With this new framework, parameter p_{birth} has a similar effect to that of parameter p_{length}. Figure 5.6 displays the dynamical predictions of this amended model in $p_{length} - p_{birth}$ parameter space. Comparing this figure to the corresponding (bottom middle) panel of Figure 5.4, one can see that the pattern is more symmetric for the new model: there is a similar variation in both directions. To compare the effects of the seasonal mechanisms in isolation, we compare the results of the model with $p_{birth} = 0$ and $p_{length} = 1$ to those with $p_{length} = 0$ and $p_{birth} = 1$. Both cases give multi-year cycles for similar values of the maximum birth rate, a_{max}. This confirms that in this new model set-up, a variable season length and a variable birth rate have a similar impact on the cyclic behaviour of the system; parameter p_{length} is no longer the dominant driver of multi-year cycles.

These findings suggest that the mechanism by which the season length is determined is the important destabilising factor. The season length is dependent on the inducible factor at a specific date, and is fixed for that year. When the birth rate is defined in the same way, then it becomes a similarly powerful driver of multi-year

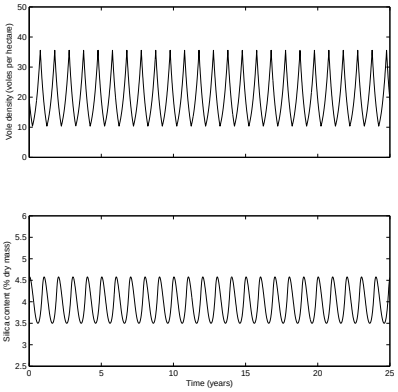

(a) Annual cycles. Parameters: $p_{birth} = 0.6$, $p_{length} = 0.7$, $a_{max} = 0.5$ and $l_{max} = 10$.

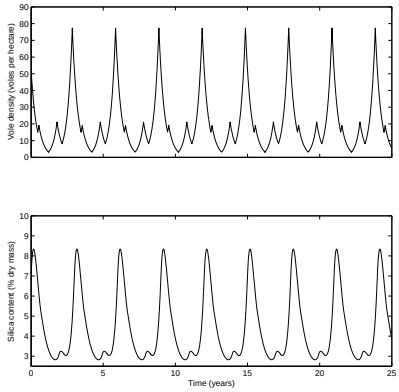

(b) Average period: 3. Parameters: $p_{birth} = 0.1$, $p_{length} = 0.9$, $a_{max} = 0.5$ and $l_{max} = 10$.

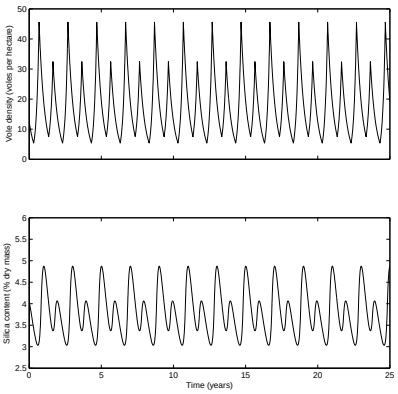

(c) Average period: 2. Parameters: $p_{birth} = 0.8$, $p_{length} = 0.7$, $a_{max} = 0.8$ and $l_{max} = 6$.

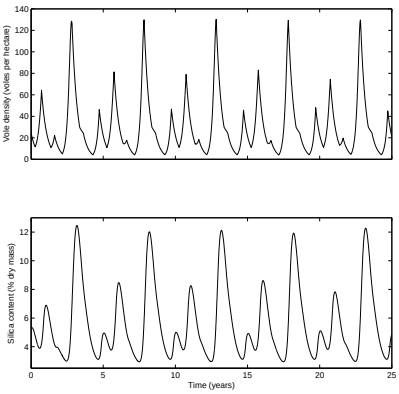

(d) Average period: 2.5. Parameters: $p_{birth} = 0.8$, $p_{length} = 0.7$, $a_{max} = 0.8$ and $l_{max} = 10$.

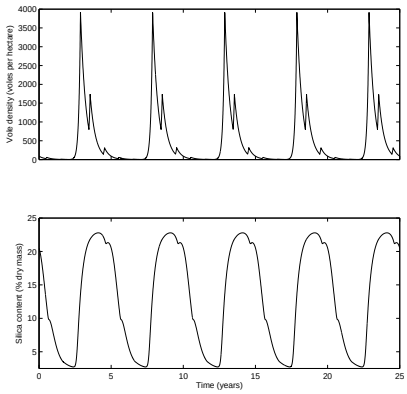

(e) Average period: 5. Parameters: $p_{birth} = 0.1$, $p_{length} = 0.9$, $a_{max} = 1.1$ and $l_{max} = 10$.

Figure 5.5: Examples of cyclic behaviour predicted by the model for different values of the parameters p_{birth} and p_{length} (characterising the strength of the silica effect), a_{max} (the maximum herbivore birth rate) and l_{max} (the maximum breeding season length). Each example corresponds to a particular point on the grids of Figure 5.4. Initial conditions are as for Figure 5.2 and solutions are shown after 450 years.

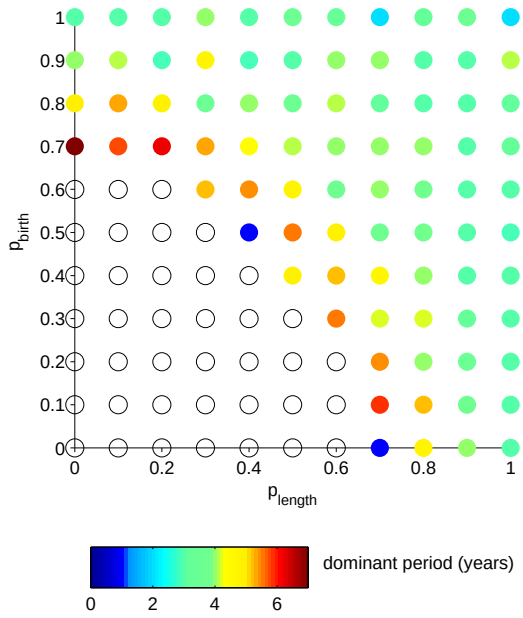

Figure 5.6: Dominant periods of the cycles produced in $p_{length} - p_{birth}$ parameter space, with the vole birth rate dependent on the level of silica S at the "census date" (as well as the breeding season length). In this figure, the maximum birth rate $a_{max} = 1.1$, and the maximum season length $l_{max} = 8$. The uncoloured dots denote when the vole density increases unbounded (due to lack of regulation by silica; see Appendix B). The numerical method used to determine the periods is the same as is used in Figure 5.4, and the same initial conditions are used. This figure should be compared to the bottom middle plot of Figure 5.4, which shows the corresponding results for the original model set-up. In this figure, there is a more symmetrical pattern; parameters p_{length} and p_{birth} have more similar effects.

cycles.

The significance of the underlying mechanism has motivated a further extension to our model. In order to make the model more realistic, we additionally experiment with setting the vole birth rate and breeding season length to depend on the silica S averaged over the previous month, as opposed to the silica level at one time point only. The resulting patterns are similar to those in Figure 5.4 but periods are generally lower. The overall conclusions are unaffected by this modification.

5.6 Discussion

In this study we explore and compare the effects of plant defence strategies in combination with seasonality on the population dynamics of a herbivore. We examine two different mechanisms: firstly, with the herbivore birth rate dependent on the level of plant defence; secondly, with the length of the breeding season dependent on the

level of plant defence. Our results indicate that the means by which seasonality is implemented is crucial. When the plant defence affects the breeding season length, there is a significantly higher likelihood of multi-year cycles compared to when it affects the birth rate.

We have parameterised our model for a specific system, namely field voles (*Microtus agrestis*) in Kielder Forest, Northern UK, and the silica content in the grass (*Deschampsia caespitosa*) they feed on. The implication of our findings is that a regulatory factor, silica in this instance, is important for the occurrence of multi-year cycles if it affects the season length, but less significant if it affects the birth rate.

Our model includes a delay term representing the time taken for the inducible plant defence to be produced after herbivory has occurred, in concurrence with both experimental (Reynolds *et al.*, submitted, a) and theoretical (Underwood, 1999) studies. A delay is known to be a potentially destabilising factor (Haberman, 1977; Underwood, 1999), and as a result we additionally considered the effects of changing the delay length, and also the effect of removing this delay. We demonstrated that our main conclusion, that a variable breeding season length is a more powerful driver of multi-year cycles than a variable birth rate, holds irrespective of the delay in the production of the inducible plant defence.

Seasonal variations are ubiquitous in natural systems, and can exert strong pressures on population dynamics. Our findings highlight the complexity of the interaction between seasonal forcing and the unforced dynamics. This has also been shown in models of disease systems (Schwartz and Smith, 1983) and in predator–prey models (e.g. Kuznetsov *et al.*, 1992; Rinaldi *et al.*, 1993). Here we demonstrate that the way in which seasonality is incorporated makes a significant difference to its effect on the dynamics, and that it is therefore crucial in seasonal models to incorporate patterns of forcing that most closely correspond to biologically realistic assumptions.

Changes in the length and intensity of the breeding season have been claimed by some authors to be an epiphenomenon of rodent cycles, with little demographic importance (Norrdahl and Korpimäki, 2002). In contrast, Smith *et al.* (2006) found that variation in the breeding season length, with the length a function of past population densities, can give rise to realistic population cycles, demonstrating that a variable breeding season length may have important implications for the population dynamics of a system. Our model, with the additional effect of a plant defence mechanism, also predicts such population cycles and suggests that the breeding season length can have a significant effect on population behaviour. In addition, seasonality is shown to be important in shaping the population dynamics of the grey-sided vole (*Clethrionomys rufocanus*) in Hokkaido, Japan (Stenseth *et al.*, 2003). In that study, using both data and models, it is demonstrated that the length of winter plays a key role in driving population cycles. Our findings, concerning a different

vole species in a different location, are in agreement with this.

We have parameterised our model using empirical data on a specific herbivore–plant defence system, and found that multi-year cycles can be generated for realistic parameters. In particular, we have shown that seasonality can give rise to cycles of similar periodicity to those seen in the field (Lambin *et al.*, 2000). This result lends support to the hypothesis that inducible plant defences may contribute to cyclic fluctuations, and is consistent with previous theoretical studies on other systems (Lundberg *et al.*, 1994; Underwood, 1999). The model of Lundberg *et al.* (1994) typically generates damped oscillations, and they speculate that seasonal perturbations may play a significant role in the maintenance of population cycles. Our work confirms the importance of seasonality in achieving population cycles resembling those seen in nature.

It should be noted that we have used data from greenhouse experiments to parameterise some components of this model. An important next step is to use field data to obtain parameter values, once this becomes available. In addition, a possible extension is to take the same model framework and reparameterize for a different herbivore–plant defence system.

Our work highlights the complexity of the role seasonal forcing plays in shaping population dynamics. We have found that seasonality can have dramatic dynamical effects, and that this is strongly dependent on the type of seasonal mechanism. For a given ecological system, the elucidation of the seasonal mechanism involved is critical in order for the seasonal effects to be determined. The prospect that global climate change will rapidly modify current seasonal patterns provides further motivation for research into seasonality and its effects.

5.7 Appendix A

In this appendix we determine the parameter values for which the trivial steady state $(H, S) = (0, S_0)$ is stable, using Floquet theory. At the trivial steady state the herbivore birth rate will be at its maximum a_{max} in the breeding season. Let $a(t)$ represent the seasonal birth rate in this case. Then

$$a(t) = \begin{cases} a_{max} & \text{in the breeding season} \\ 0 & \text{in the non-breeding season.} \end{cases} \tag{5.3}$$

Thus $a(t)$ is periodic with period 12 months.

Firstly, linearising the system (5.1) and (5.2) with (5.3) about the trivial steady

state gives

$$\frac{dH}{dt} = (a(t) - b)H(t) \tag{5.4}$$

$$\frac{dS^*}{dt} = -cS^*(t) \tag{5.5}$$

where $S^*(t) = S(t) - S_0$. The solution of equation (5.4) depends on the season:

$$H(t) = \begin{cases} m_1 e^{(a_{max}-b)t} & \text{in the breeding season} \\ m_2 e^{-bt} & \text{in the non-breeding season} \end{cases}$$

where m_1 and m_2 are constants. The solution of equation (5.5) is

$$S^*(t) = m_3 e^{-ct}$$

in both seasons, where m_3 is a constant.

We now seek a fundamental matrix for this system. To be specific, consider the solution over 12 months starting at the beginning of the non-breeding season. Initial conditions $(H(0), S^*(0)) = (0, 1)$ give $m_3 = 1$ and $S^*(12) = e^{-12c}$. Also, $m_2 = 0$ so $H = 0$ at the end of the non-breeding season, which is the start of the breeding season also. Therefore $m_1 = 0$ and $H(12) = 0$.

Starting at $(1, 0)$ gives $m_3 = 0$ and $S^*(12) = 0$. Also, $m_2 = 1$ so $H(t) = e^{-bt}$ in the non-breeding season. At the end of the non-breeding season, and the start of the breeding season, $t = 12-l$. At the trivial equilibrium, the season length l will be at its maximum, l_{max}. So

$$H(12 - l) = e^{-b(12-l_{max})} = m_1 e^{(a_{max}-b)(12-l_{max})}$$

$$\Rightarrow \quad m_1 = \frac{e^{-b(12-l_{max})}}{e^{(a_{max}-b)(12-l_{max})}} = e^{-a_{max}(12-l_{max})}$$

and

$$H(12) = e^{-a_{max}(12-l_{max})} e^{12(a_{max}-b)} = e^{a_{max}l_{max}-12b}.$$

A fundamental matrix, denoted here by M, is therefore

$$M = \begin{bmatrix} 0 & 1 \\ 1 & 0 \end{bmatrix}^{-1} \begin{bmatrix} 0 & e^{a_{max}l_{max}-12b} \\ e^{-12c} & 0 \end{bmatrix} = \begin{bmatrix} e^{-12c} & 0 \\ 0 & e^{a_{max}l_{max}-12b} \end{bmatrix}$$

with eigenvalues

$$\mu_1 = e^{-12c} \quad \text{and} \quad \mu_2 = e^{a_{max}l_{max}-12b}.$$

Floquet theory implies that the condition for the trivial steady state to be stable

is that both $\mid \mu_1 \mid < 1$ and $\mid \mu_2 \mid < 1$. Since $\mu_1 < 1$ always holds, the condition for stability is

$$\mu_2 < 1, \text{ i.e. } a_{max} l_{max} - 12b < 0, \text{ i.e. } a_{max} l_{max} < 12b.$$

This is the required condition.

5.8 Appendix B

In this appendix we determine the parameter values for which the vole density $H \to \infty$. For large H, the equations become, to leading order,

$$\frac{dH}{dt} = (a(t) - b)H(t) \tag{5.6}$$

$$\frac{dS}{dt} = K + cS_0 - cS(t). \tag{5.7}$$

The silica level will be at its maximum to leading order for large H, so the breeding season length and birth rate will be at their minimum values. Therefore

$$a(t) = \begin{cases} a_{max}(1 - p_{birth}) & \text{in the breeding season} \\ 0 & \text{in the non-breeding season} \end{cases}$$

and the breeding season length is $l_{max}(1 - p_{length})$. The solution of equation (5.6) is then

$$H(t) = \begin{cases} m_4 e^{(a_{max}(1-p_{birth})-b)t} & \text{in the breeding season} \\ m_5 e^{-bt} & \text{in the non-breeding season} \end{cases}$$

where m_4 and m_5 are constants. Therefore, the solutions of equation (5.6) will tend to infinity if and only if

$$\begin{aligned} (a_{max}(1 - p_{birth}) - b)\frac{l_{max}(1 - p_{length})}{12} - b\frac{(12 - l_{max}(1 - p_{length}))}{12} &\geq 0 \\ \Leftrightarrow l_{max}(1 - p_{length})a_{max}(1 - p_{birth}) &\geq 12b. \end{aligned}$$

When this inequality holds the silica effects are too weak to self-regulate; there is not enough control on the herbivore population by silica. In real systems, other factors will regulate the herbivore population, for example the spread of disease may increase and resources may become limited at very high population densities.

Chapter 6

A comparison between seasonal forcing in a herbivore–plant and a predator–prey model

In the preceding chapter, we considered a herbivore–plant defence system, giving voles and silica as a specific example. Our findings indicate that a variable breeding season length is a more powerful driver of multi-year cycles than a variable herbivore birth rate. In this chapter, we aim to determine whether a variable season length is important when other factors can affect population density.

In the first section of this chapter, we consider the vole–silica model of Chapter 5 with a modified method of representing a variable season length: we change the model so that the breeding season length is no longer dependent on silica. We next examine a vole–predator model, and compare the influences of predation and variability of season length on the dynamical behaviour. Our objective is to assess the relative impact of a variable season length in these two different systems.

There has been much debate in the literature over the relative importance of food resources and predation in the regulation of herbivore populations. Much data seems to suggest that trophic interactions are the major determinants of cyclic dynamics (Stenseth, 1999; Turchin, 2003), yet there are conflicting views on whether predation or food resources is the significant factor. Vole population cycles have traditionally been thought to reflect interactions with predators (Korpimäki and Krebs, 1996), and many studies have supported the idea that predation causes vole cycles, and argued against the importance of food resources in cycling (e.g. Henttonen *et al.*, 1987, Klemola *et al.*, 2000a; Klemola *et al.*, 2003). In contrast, other studies have concluded that predation is not the cause of vole cycles (Graham and Lambin, 2002), and instead it is the interaction between the voles and their food that is the key driver (e.g. Agrell *et al.*, 1995; Massey *et al.*, 2008). In view of this debate, it seems

appropriate to consider predation as the second factor / regulatory influence in this chapter.

Our findings indicate that while in the modified vole–silica model a variable season length promotes multi-year cycles more significantly than a variable birth rate, in the vole–predator system, the predation effect is a more powerful driver of multi-year cycles than a variable season length.

6.1 Herbivore–plant defence model

In the first instance, we look at the vole–silica model as described and analysed in Chapter 5, but change what determines the breeding season length. We amend the model set-up in this way to enable a comparison of the impacts of different population interactions in a consistent framework; this modification allows us to study the dynamical effects of silica and also of an alternative factor. The vole–silica model was developed to represent the interaction between vole density and the silica in the grass they consume, and was motivated by empirical evidence that this interaction has the potential to drive vole population oscillations (Massey and Hartley, 2006; Massey *et al.*, 2008). Grass produces an elevated level of silica in response to herbivory by voles (Massey *et al.*, 2007a). Silica has been proposed as the primary defence in many grasses (Massey *et al.*, 2007b).

Vole reproduction can be negatively affected by previous high population density (Agrell *et al.*, 1995). Recall that the vole–silica model of Chapter 5 is parameterised for the particular case of field voles (*Microtus agrestis*) in Kielder Forest, Northern UK. There is evidence from Kielder that the timing of the onset of the vole reproductive season is correlated with the population density at the start of the previous season (Ergon *et al.*, 2011), and, furthermore, that this relationship is important in the generation of vole population cycles (Smith *et al.*, 2006). In light of this, we set the breeding season length to be dependent on vole density at the start of the previous breeding season. Note that in the previous chapter we were testing the hypothesis that silica was the mechanism behind the correlation between past vole density and breeding season length, but here we model directly the (delayed) density-dependence.

This modified vole–silica model is as follows:

$$\frac{dV}{dt} = a(S(t),t)V(t) - bV(t) \tag{6.1}$$

$$\frac{dS}{dt} = \frac{K(V(t-\tau))^2}{V_0^2 + (V(t-\tau))^2} + cS_0 - cS(t) \tag{6.2}$$

where V represents the vole density and S the silica level. The parameters in the

model remain the same as in the model described in Chapter 5 (equations (5.1) and (5.2)), with $V_0 = H_0$. During the breeding season, the vole birth rate is dependent on S (as shown in Figure 6.1(a), and as in the model described in Chapter 5); in the non-breeding season, the birth rate $a = 0$. The breeding season length is dependent on V at the start of the previous breeding season (Figure 6.1(b)). We denote by a_{max} and a_{min} the maximum and minimum birth rates respectively. Similarly, l_{max} and l_{min} are the maximum and minimum breeding season lengths respectively.

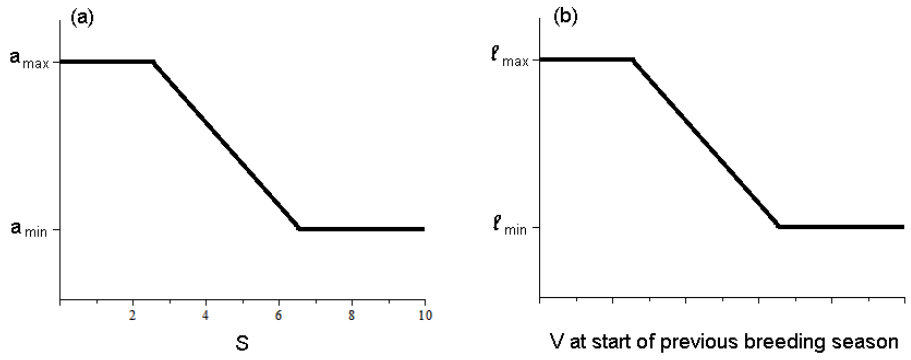

Figure 6.1: (a) Vole birth rate a as a function of silica S and (b) vole breeding season length l as a function of the vole population density V at the start of the previous breeding season.

Thus in this model, silica affects the vole birth rate during the breeding season, and the length of the breeding season is determined by past vole density. We use two parameters, p_{length} and p_{birth}, to characterise the seasonal effects, both taking values in $[0, 1]$, where p_{birth} is the strength of the silica effect on the vole birth rate and p_{length} the extent of the variability in the season length. These parameters are defined such that

$$a_{min} = a_{max}(1 - p_{birth})$$

$$l_{min} = l_{max}(1 - p_{length}).$$

For the other parameters in the model, we use the same estimates as described in Chapter 5. Recall that these estimates are based on a combination of greenhouse and field data.

6.1.1 Results

We solve equations (6.1) and (6.2) numerically across a range of values of p_{birth} and p_{length}. Due to the seasonal forcing, the solutions are cyclic, with either annual or multi-year cyclicity. (Note that multi-year cyclicity can include quasi-periodic or chaotic solutions.) The dominant period of these cycles is determined, and the results for three values of the maximum birth rate a_{max} are illustrated in Figure 6.2. The unfilled dots indicate when there is unbounded increase of vole population density. This occurs for low values of p_{birth} and p_{length}, as in this case there is a lack of sufficient regulation of the population (see Subsection 5.5.1 and Section 5.8 for further details). The axes of these plots are significant: along these, only one effect is influencing the dynamics.

When $a_{max} = 0.5$, there are annual cycles (dark blue dots) for the majority of parameter space. Multi-year cycles are generated for high values of p_{length} and low values of p_{birth}. In the plots for $a_{max} = 1$ and 1.5, the cycles with the longest periods occur for high p_{length} and low p_{birth}. In general, an increase in the variability of the season length leads to a greater likelihood of multi-year cycles, and a lengthening of the period of the cycles; an increase in the variability of the birth rate has the opposite effect. Therefore a variable season length is a more powerful driver of multi-year behaviour. These results, with this modified method of representing a variable season length, are consistent with those of the previous chapter.

In this modified model, the breeding season is not linked to silica content. The advantage of this is that we can assess, in a consistent manner, the impact of a variable breeding season when a different factor affects the vole population dynamics. Above we explored the impact of a plant defence (silica) on vole dynamics, and next we consider the impact of predation.

6.2 Predator–prey system

To test whether our findings hold more widely, we now move on to exploring seasonal mechanisms in a different system. We consider a predator–prey model, and assess the relative importance of the predation effect and the variability of breeding season length in driving multi-year cycles.

Predation is an established cause of population cycling in prey species. There is substantial evidence that the interaction between voles and their mustelid predators drives the vole population oscillations observed in Fennoscandia (e.g. Henttonen *et al.*, 1987; Hanski *et al.*, 1993, 2001; Hanski and Henttonen, 1996, 2002). However, in other geographical areas less of a consensus exists, and also there have been influen-

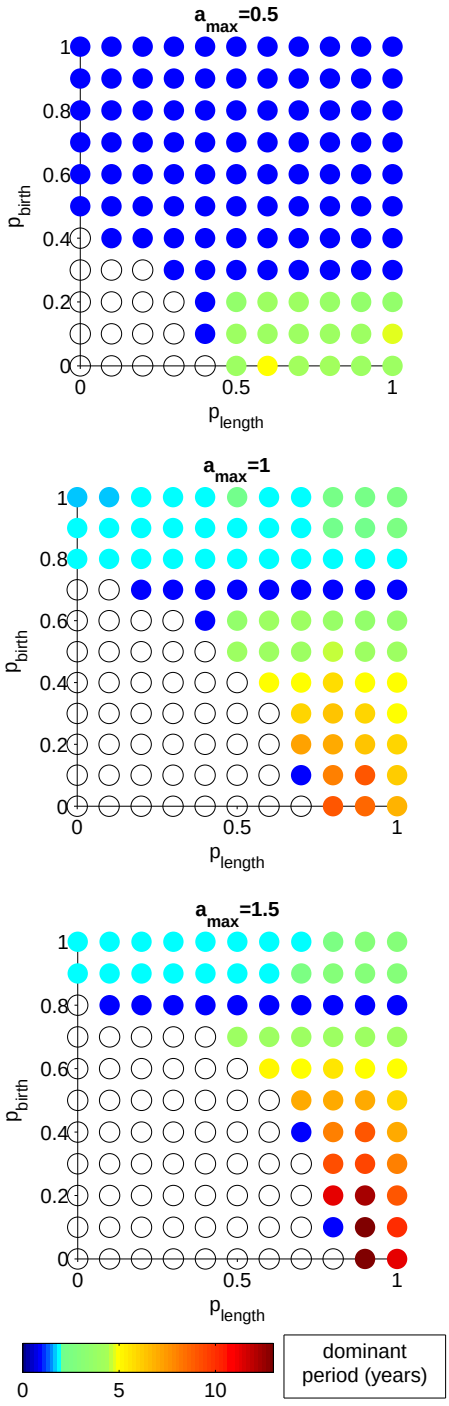

Figure 6.2: Dominant periods of the cycles produced by the vole–silica model (equations (6.1) and (6.2)), for different parameter combinations. The uncoloured dots denote when the vole density increases unbounded (due to lack of regulation). After 490 years, the densities are assessed at yearly intervals over 10 years. The difference between the maximum and minimum densities is compared to 5% (chosen arbitrarily) of the mean density. If the difference is smaller, then the cycles are deemed annual (dark blue dots); if larger, they are non-annual. For the non-annual cycles, fast Fourier transform is used to generate power spectra, from which the dominant period is established. For more details of this method, see the legend to Figure 5.4.

tial reviews that have concluded that predation is not driving the oscillations in some cases (Chitty, 1960; Krebs and Myers, 1974; Taitt and Krebs, 1985). Additionally, results of experiments conducted by Graham and Lambin (2002), involving the experimental reduction of weasel (*Mustela nivalis*) density through trapping, indicate that predation is not sufficient to drive population cycles of field voles in Kielder Forest. Therefore, although predation is not believed to be universally important in causing population cycles, it nonetheless has the potential to significantly impact the dynamics of vole populations.

We model a predator–prey system as follows:

$$\frac{dV}{dt} = A(t)V(t) - p_{pred}\frac{V(t)}{V(t)+V_0}P(t) - dV(t) \tag{6.3}$$

$$\frac{dP}{dt} = \delta p_{pred}\frac{V(t)}{V(t)+V_0}P(t) - cP(t) \tag{6.4}$$

where V is the prey density and P the predator density. $A(t)$ is the seasonal prey birth rate (0 in the non-breeding season and taking a constant value a in the breeding season). The season length is defined in the same way as for the vole–silica model described in Section 6.1: the season length is dependent on V at the start of the previous season, as shown in Figure 6.1(b). Parameter p_{length} characterises the variability of the season length. The natural death rate for the prey is d, and for the predator is c, and δ is the conversion rate of predation to new births. The predation term

$$\frac{p_{pred}}{V(t)+V_0}$$

is the functional response of the predators to changes in the prey density. The parameter p_{pred} is a measure of the extent to which the prey are affected by predation, i.e. the strength of the predation effect.

In the previous section, silica affected the vole birth rate. Here, predation affects the vole death rate. Using this model we intend to examine and compare the dynamic effects of predation and of a variable breeding season length on cyclic voles. Our previous findings show that a variable breeding season length gives a greater likelihood of multi-year cycles than a variable birth rate. Our objective here is to determine whether a variable season length is a more important driver of multi-year cycles than predation.

We choose parameter values based on the field vole (*M. agrestis*)–weasel (*M. nivalis*) interaction. The estimate for the vole death rate is chosen to be the same as in the previous section, and as given in Chapter 5: 0.22 per month. We also choose to use the same value for V_0 as used previously. Annual mortality for weasels is 77.5% (King, 1989), so $e^{-c} = 0.225$, which gives an estimate of the predator death

rate of $c = 1.49$ per year or $c = 0.12$ per month. When prey are abundant, female weasels can have two litters per season; there is an average of six young per litter, and the average of three females in the first litter can breed themselves in the same season (King, 1989). This gives a maximum per capita productivity of 15 per year, so that the maximum per capita predator birth rate (δp_{pred}) is 0.23 per month. We look at a range of p_{pred} values and choose the value of δ to ensure δp_{pred} is equal to 0.23 for a p_{pred} value within the range covered. We fix $\delta = 0.52$ in this study.

6.2.1 Region in parameter space where $V \to \infty$

In a similar manner to the vole–silica model (Chapter 5; Section 6.1), we do not include a carrying capacity / crowding effect in the predator–prey model (equations (6.3) and (6.4)). We assume that any regulation on the prey population is by predation (controlled by p_{pred}) or by a change in the season length (controlled by p_{length}), and this allows an assessment of the relative impact of these factors. Additionally, the vole carrying capacity is notoriously difficult to estimate empirically (O'Mahony *et al.*, 1999). As a result, there are instances when the vole density increases without bound. We seek the region in parameter space for which this occurs, in order to exclude it from our analysis. (This is less straightforward than for the model in Chapter 5, due to the nonlinearity of the vole equation.) For large V, the model equations become, to leading order:

$$\frac{dV}{dt} = (A(t) - d)V(t) - p_{pred}P(t) \tag{6.5}$$

$$\frac{dP}{dt} = \delta p_{pred}P(t) - cP(t) \tag{6.6}$$

where $A(t) = a$ in the breeding season and 0 otherwise. As V is large, the leading order breeding season length is the minimum possible value, $l_{max}(1 - p_{length})$. There are two cases to consider: $\delta p_{pred} < c$ and $\delta p_{pred} > c$.

$\underline{\delta p_{pred} < c}$:
$\delta p_{pred} < c \Rightarrow P \to 0$, and so $V \to \infty$ if and only if $al_{max}(1 - p_{length}) \geq 12d$ (by a similar calculation to that in Section 5.8).

$\underline{\delta p_{pred} > c}$:
$\delta p_{pred} > c \Rightarrow P \to \infty$. So if $a < d$ then V remains finite. However, more work is required if $a > d$.

To determine the outcome when $a > d$ and $\delta p_{pred} > c$, let us consider the solutions of equations (6.5) and (6.6) over 12 months, starting at the beginning of the breeding

season. Let t^* be the end of the breeding season (and the start of the non-breeding season). Then $t^* = l_{max}(1 - p_{length})$.

The solution of equation (6.6) is $P(t) = P(0)e^{(\delta p_{pred} - c)t}$. So

$$\frac{dV}{dt} = (A(t) - d)V(t) - p_{pred}P(0)e^{(\delta p_{pred} - c)t}.$$

Between $t = 0$ and $t = t^*$, $A(t) = a$, and therefore

$$V(t) = \frac{p_{pred}P(0)}{a - d - \delta p_{pred} + c}e^{(\delta p_{pred} - c)t} - p_{pred}P(0)C_1 e^{(a-d)t}$$

where C_1 is a constant of integration. Between t^* and $t = 12$ months, $A(t) = 0$, and thus

$$V(t) = \frac{p_{pred}P(0)}{d - \delta p_{pred} + c}e^{(\delta p_{pred} - c)t} - p_{pred}P(0)C_2 e^{(-d)t}.$$

Using the above solutions and applying continuity at $t = t^*$ gives

$$\frac{V(12)}{P(0)} - \frac{e^{-12d+at^*}V(0)}{P(0)} = p_{pred}\Phi \tag{6.7}$$

where

$$\Phi = \frac{e^{12(\delta p_{pred} - c)}}{-d - \delta p_{pred} + c} - e^{-12d}e^{(\delta p_{pred} - c + d)t^*}\left(\frac{1}{-d - \delta p_{pred} + c} - \frac{1}{a - d - \delta p_{pred} + c}\right)$$
$$- \frac{e^{-12d+at^*}}{a - d - \delta p_{pred} + c}$$

(this is always negative for relevant parameter values). We seek the region in parameter space where ratio $V(12)/V(0) \geq 1$ ($\Rightarrow V(12) \geq V(0) \Rightarrow V \to \infty$).

The two terms on the left hand side of equation (6.7) are large. Therefore to leading order as $V \to \infty$, $V(12) - e^{-12d+at^*}V(0) = 0$, which gives $V(12)/V(0) = e^{-12d+at^*}$. Therefore

$$V(12)/V(0) \geq 1 \Rightarrow e^{-12d+at^*} \geq 1 \Rightarrow -12d + at^* \geq 0$$

$$\Rightarrow -12d + al_{max}(1 - p_{length}) \geq 0. \tag{6.8}$$

Note that this inequality is dependent on a and p_{length}, but not p_{pred}. If $a < d$, then (6.8) never holds (as $l_{max} \leq 12$ and $p_{length} \leq 1$), so this one condition defines the region to be excluded for all cases.

We can also numerically analyse equation (6.7). The ratio $V(12)/V(0)$ can be calculated for a range of parameter values, and the region in parameter space where $V(12)/V(0) \geq 1$ can be determined. This region is independent of the strength

of predation, p_{pred}, in agreement with the above calculation. Due to this independence, we can focus on $p_{length} - a$ parameter space. Figure 6.3 shows numerical results plotted in this parameter plane, with the line $-12d + al_{max}(1 - p_{length}) = 0$ superimposed. Thus the derived result (6.8) is confirmed by numerical testing. The vole density will tend to infinity for large a and small p_{length}.

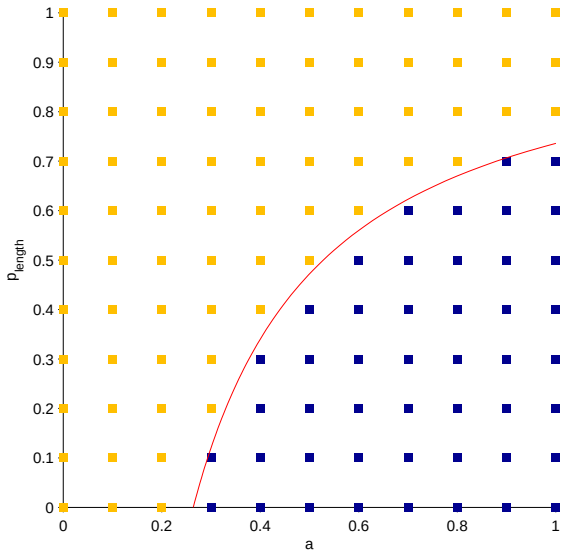

Figure 6.3: Isolating the region in $p_{length} - a$ parameter space where vole density tends to ∞, for representative values of other parameters. The coloured squares indicate the value of the ratio $V(12)/V(0)$, as calculated from equation (6.7): blue denotes that $V(12)/V(0) \geq 1$; orange denotes that $V(12)/V(0) < 1$. When $V(12)/V(0) \geq 1$, then the vole density tends to ∞. The red line is $-12d + al_{max}(1 - p_{length}) = 0$, correctly separating the region to be excluded.

To summarize, the condition for population density remaining finite is $al_{max}(1 - p_{length}) < 12d$, and we exclude other parameter combinations from our considerations. Vole density tending to infinity is an obviously unrealistic outcome, and thus we are excluding an unrealistic parameter regime.

6.2.2 Results: Determinant of multi-year cycles

We now examine whether variability of season length or variability of prey removal by predation is the more likely cause of multi-year cycles. Equations (6.3) and (6.4) are solved across a range of values of p_{length} and p_{pred}, for three different values of the vole birth rate a; the results are illustrated in Figure 6.4. As previously, the unfilled dots correspond to solutions where vole density increases without bound,

due to lack of regulation, and are thus excluded (as explained in Subsection 6.2.1). Note that while our aim is to compare this system to that described in the last section, the values of a used in Figure 6.4 are different from the a_{max} values used in Figure 6.2. For this predator–prey model, the vole density will increase without bound (i.e. there will be unfilled dots) for more than half of the parameter space, for values of a above 0.528. We therefore use lower values of a than the a_{max} values used in Figure 6.2, so that non-excluded solutions are well represented. In other ways, we have attempted to set up this model framework so that it can be fairly compared to that of the vole–silica system, for example by using the same values for parameters V_0 and the natural vole death rate.

As the season length variability increases (i.e. p_{length} increases), there is in general a shortening of cycle periods. For this system, p_{length} is not driving multi-year cycles. Indeed, for $a = 0.3$ and $a = 0.35$, the parameter p_{length} has little effect on the transition from annual cycles (dark blue dots) to multi-year cycles. In contrast, as the predation strength increases (i.e. p_{pred} increases), the cycle periods consistently get longer. Any annual cycles become multi-year cycles with an increase in p_{pred}. Hence our model predicts that a variable breeding season length is not the important driver of multi-year cycles in all systems; in this case, it is the predation strength that most powerfully promotes multi-year cyclic behaviour.

When the predation effect is strong, the cycles predicted by the model have relatively long periods. These cycles feature intervals of very low vole density separated by peaks in population density (Figure 6.5). Both predator and prey densities drop to low values, and then there is a gradual build up of prey density before the next crash in population numbers. These cycles show behaviour very different to those produced by the vole–silica model; for example, compare Figure 6.5 with the vole–silica cycles illustrated in Figure 5.5: the vole–silica cycles do not show such extended intervals of very low vole density, nor such sharp decreases in vole numbers. This result highlights that predation can have a powerful impact on the prey dynamics.

6.3 Discussion

For the vole–silica interaction, our results suggest that a variable season length is a significant driver of multi-year cycles in population density. This model was parameterised for the field vole population in Kielder Forest. From our results we can therefore predict that the vole population cycles in Kielder Forest are sensitive to changes in the season length. Field evidence from Kielder Forest is consistent with this prediction: changes in the vole population cycles over time have been noted, and attributed to climatic changes that have caused shorter winters (Bierman *et*

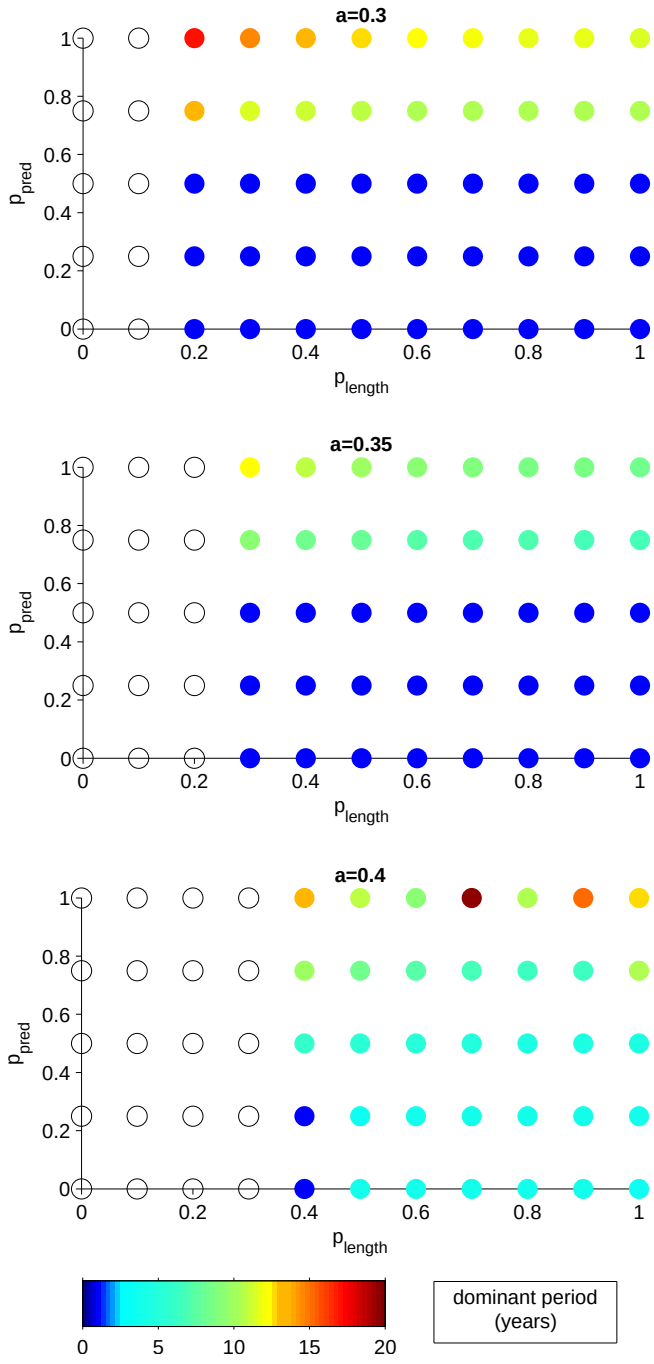

Figure 6.4: Dominant periods of the cycles produced by the vole–weasel model (equations (6.3) and (6.4)), for different parameter combinations. The uncoloured dots denote when the vole density increases unbounded (due to lack of regulation). After 490 years, the densities are assessed at yearly intervals over 10 years. The difference between the maximum and minimum densities is compared to 5% (chosen arbitrarily) of the mean density. If the difference is smaller, then the cycles are deemed annual (dark blue dots); if larger, they are non-annual. For the non-annual cycles, fast Fourier transform is used to generate power spectra, from which the dominant period is established. For more details of this method, see the legend to Figure 5.4. Parameter values are as given in the main text.

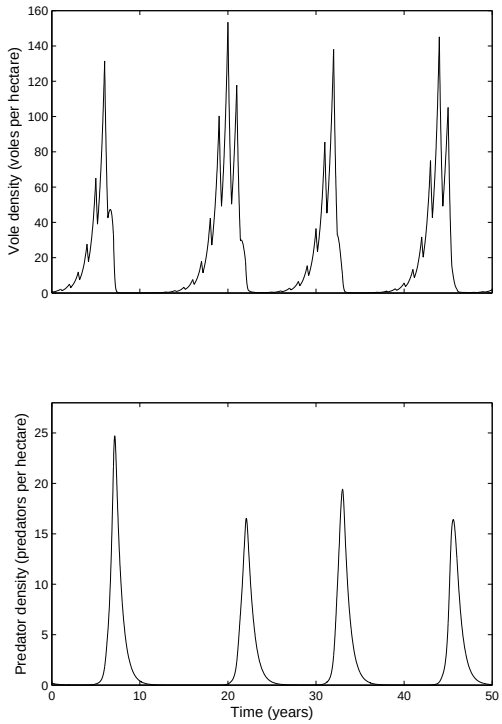

Figure 6.5: Population densities of vole and predator with a strong predation effect ('high' p_{pred}). Parameters are: $a = 0.35$, $p_{length} = 0.3$, $p_{pred} = 1$, and other parameters as given in the main text. Initial conditions are: $V = 30$ and $P = 3$ per hectare for $t = 0$. Solutions are shown after 400 years. Note the intervals of very low vole density.

al., 2006). Changes are reported to have taken place in the amplitude, periodicity, and synchrony of the cycles over the study period (1984–2004). Population density estimates indicate that the variability in vole densities in the spring has decreased, whereas the variability in autumn densities has remained relatively constant. The vole dynamics appear to have become less strongly cyclic over time; in the early part of the study period, there is clear multi-year cycling, but towards the end annual cyclicity is the more dominant pattern (Figure 6.6). Over the same time period, the number of days with ground snow cover over the winter in Kielder decreased significantly. Shorter winters correspond to a reduction in the value of the parameter p_{length} in our model. Our theoretical results indicate that this leads to a decreased likelihood of multi-year cycles, consistent with the observation of the change in periodicity in the field.

The second model described in this chapter has predicted that in a vole–weasel system, the interaction with the predator has a stronger influence on the population dynamics than a variable season length. Many studies have investigated predation as a mechanism for vole cycles, particularly for the regular and pronounced multi-year vole cycles in Fennoscandia. Vole populations in this region often show cycles

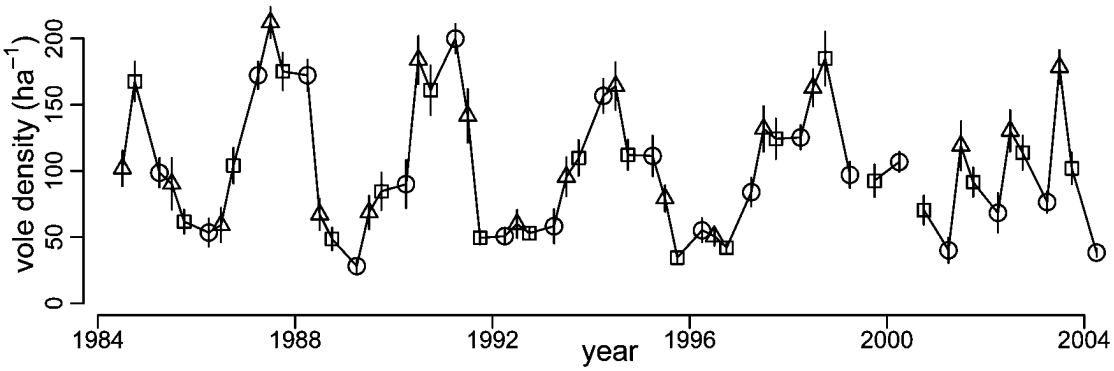

Figure 6.6: Estimated seasonal log densities (mean ± SE) (voles per hectare) of the field vole population in Kielder Forest from 1984 to 2004. Triangles show the summer densities, squares show autumn densities, and circles show spring densities. Reproduced with permission of The University of Chicago from Bierman *et al.* (2006). Copyright 2006 by The University of Chicago.

of three to five years (Korpimäki and Krebs, 1996). There is strong seasonal forcing in boreal and arctic regions. Our results suggest that even for such pronounced seasonality, it will be the interaction with the predator that is the main driver of multi-year cycles. In Fennoscandia, the view that specialist predation causes cycles has been well developed and is richly supported (e.g. Henttonen *et al.*, 1987; Hanski *et al.*, 1993, 2001; Hanski and Henttonen, 1996, 2002). For instance, predator exclusion experiments (Klemola *et al.*, 2000a and references therein) support the idea that predation is a key contributor to cycles. Our findings imply that climate change should not have a strong effect on Fennoscandian vole cycles; the empirical data on this is inconclusive (Ims *et al.*, 2008; Brommer *et al.*, 2010). The least weasel (*M. nivalis*) and the field vole (*M. agrestis*) are considered to be the key specialist predator and the key prey species in the multispecies communities in the boreal forest region in Fennoscandia (Hanski *et al.*, 2001), and are the species studied in this chapter.

The predation exclusion experiments mentioned above show that predator removal disrupts the multi-year cyclic pattern. In our model, the removal of predators can be modelled by setting the strength of predation $p_{pred} = 0$. For certain parameter values, our model predictions support the experimental findings. For example, in Figure 6.4, for $a = 0.35$ there are multi-year cycles, of a similar period to those seen in Fennoscandia, for large p_{pred} values, but only annual cycles for $p_{pred} = 0$. However, this result does not apply for all parameters: for instance, for $a = 0.4$ multi-year cycles are seen for most values of p_{length} when $p_{pred} = 0$.

We can conclude that the relative impact of a variable season length on vole population dynamics is not the same in all cases; in particular, a variable season length is not always the dominant regulator of cycles. For a vole–silica system, we

find that a variable season length is an important driver of multi-year cycles, and has a greater effect than a variable birth rate dependent on silica. In contrast, in a vole–predator system, our results indicate that a variable season length is not a driver of multi-year cycles, and the strength of the predation effect is more significant.

In the vole–silica model, the parameter p_{birth} only has an effect during the breeding season. It controls the strength of the silica effect on the birth rate within the breeding season. As a result, its influence is contingent on the parameter p_{length}, which controls the variability of the breeding season length. Thus p_{length} determines when p_{birth} has its effect. This is a possible explanation as to why p_{length} is the most powerful parameter in terms of driving multi-year cycles in the vole–silica model. In the vole–predator model, the parameter p_{pred}, the strength of predation, has an effect throughout the year, and is therefore not contingent on parameter p_{length} in the same way. As an experiment, we set the predation term of the vole–predator model (in equation (6.3)) to be seasonal, i.e. the term

$$-p_{pred}\frac{V(t)}{V(t)+V_0}P(t)$$

is set to 0 in the non-breeding season. This is not intended to be representative of a real system, but an artificial set-up to test a hypothesis. The results for vole birth rate $a = 0.4$ are shown in Figure 6.7; the longest period here is for high p_{length} and high p_{pred}. This figure should be compared to the bottom panel of Figure 6.4, which is the corresponding figure with non-seasonal predation; all parameters are the same in these figures, and the only difference is the addition of seasonality in the predation term for Figure 6.7. When the extent of the influence of parameter p_{pred} is dependent on the breeding season length, which is controlled by parameter p_{length}, then p_{length} has a more significant effect.

6.3.1 Future work

Our predator–prey model assumes that the predator is a specialist, and so only feeds on voles. To extend this work, one could consider a generalist predator, having alternative food sources, either instead of or as well as the specialist. Small mustelids like the least weasel are examples of specialists, while avian predators are examples of generalists. Both types of predator operate in Kielder Forest and in Fennoscandia, and so considering a generalist predator would be an appropriate addition to the model. In Kielder Forest, avian predators include kestrels, short-eared owls and tawny owls. Predation by these is significant: for example, tawny owls, the most abundant vole-eating raptor in this area, have the potential to remove around 11% of the standing population of voles in low vole years, and 14% in high vole years

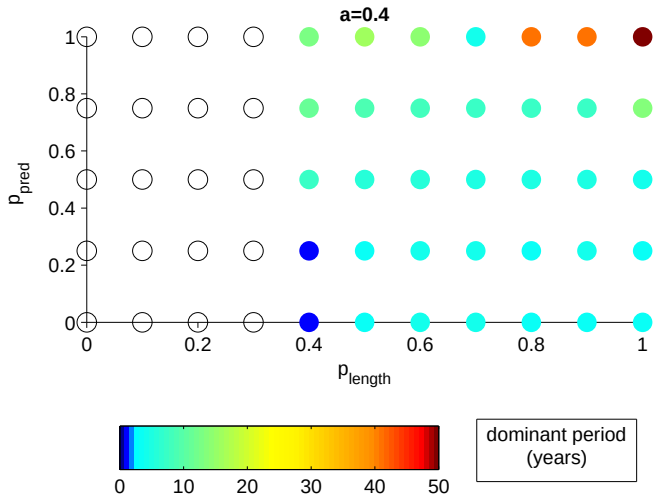

Figure 6.7: Dominant periods of the cycles produced by the vole–weasel model with a seasonal predation term, for different values of p_{length} and p_{pred}. The same procedure is used to determine period length as is used for Figure 6.4, and the same parameter values are used. This figure should be compared with the bottom panel of Figure 6.4, which is the corresponding result with a non-seasonal predation term.

(Petty *et al.*, 2000).

We have looked at two different systems, namely herbivore–plant defence and predator–prey, and have concluded that a variable breeding season length has different effects on population dynamics in the two cases. An interesting extension would be to look at a disease model (host–parasite), and examine the relative influence of seasonality mechanisms in that framework. A wide variety of pathogens have been detected in vole populations (e.g. Fichet-Calvet *et al.*, 2003; Bown *et al.*, 2004), and there is evidence that interactions with disease can contribute to vole population oscillations (Soveri *et al.*, 2000; Cavanagh *et al.*, 2004). Smith *et al.* (2008) model disease effects on vole population dynamics, with a seasonal birth rate, and parameterize for cowpox virus in the cyclic field vole (*M. agrestis*) populations of Kielder Forest. Their model predictions suggest that disease has the potential to cause multi-year cyclicity. Further analysis that examines the interplay between infectious disease and seasonality would therefore be warranted.

Chapter 7

Discussion

In this thesis, mathematical modelling is used to examine potential drivers of population dynamical behaviours. There is a focus on population cycles, a term used to describe periodic fluctuations in abundance. Population cycles are commonly observed in nature, and yet their causes are not always clear. Examples of important cycling systems that are prominent in the literature include microtine rodents (e.g. Hanski and Henttonen, 2002), and forest insects (e.g. Berryman, 1996). A wide range of factors have been attributed to promoting such cyclic dynamics (Berryman, 2002; Turchin, 2003), including trophic interactions, disease, and maternal effects. In this study, we consider several mechanisms that may contribute to population cycles in natural systems; broadly, these are changes to resistance due to infection risk and the interplay between trophic interactions and seasonality.

Comprehensive discussions of the findings of this thesis are presented in previous chapters. Here we provide a general overview of the work and highlight potential areas for future research.

7.1 Density-dependent effects on disease resistance

Chapter 2 explores the implications of density-dependent prophylaxis (DDP) for the population dynamics of a host–pathogen system. DDP describes an increase in the level of pathogen resistance with host population density, in response to the increased risk of infection. We show that DDP can either reduce or increase the tendency of the populations to cycle, depending on the delay in the onset of DDP. Thus this delay is critical. Our result indicates that it is essential to either estimate the delay in biological systems or vary the delay in mathematical models in order to understand the dynamical influence of DDP.

The results presented in Chapter 3 show that a time delay can cause complex patterns in parameter space. The destabilising influence of a delay is well known

(e.g. Haberman, 1977). However, in some cases a delay can be stabilising (e.g. Beddington and May, 1975). In our system, we find that a delay can be both destabilising and stabilising.

The modelling philosophy used in the work on DDP could be modified to consider a different mechanism in which density affects host resistance to infectious disease; by extending our work we could examine the population dynamical consequences of maternal effects. This is when the environment of the mother influences the characteristics of the offspring. Maternal effects have been identified in a wide range of organisms, including several species of forest Lepidoptera (Ginzburg and Taneyhill, 1994 and references therein). There is evidence that maternal effects may contribute to population fluctuations, for example in microtine rodents (Inchausti and Ginzburg, 1998). A model could be constructed to assess the impact of maternal effects acting on offspring disease resistance. In this case the level of disease resistance is determined not by the environment that the individual itself experiences (as with DDP), but by the environment experienced by the mother. If born into a high density environment, the offspring will have an increased level of resistance, which remains constant throughout its life. This is in contrast to the DDP case, where resistance is plastic throughout the life of the host. It would be interesting to compare the population dynamical consequences of these two scenarios.

7.2 Seasonality and trophic interactions

In the latter part of the thesis, we develop and analyse a model representing the interaction between herbivores and a plant defence mechanism. We focus on a specific population of herbivores, namely field voles (*Microtus agrestis*) in Kielder Forest, Northern UK. These voles undergo regular multi-year population cycles. The main food of this vole population is the grass species *Deschampsia caespitosa*. This grass responds to herbivory by increasing its levels of silica. Our modelling aims to test the hypothesis that the interaction between voles and silica contributes to the oscillatory nature of the vole dynamics. The work presented in Chapter 4 highlights how evidence gained from empirical experiments can be combined with theoretical modelling techniques to formulate hypotheses on the determinants of population behaviour. In particular, laboratory experiments on the silica induction response are used to fit the response of silica to herbivores in model systems. This can be combined with data from field measurements to produce best fit parameters, and the resulting theoretical analysis indicates that silica production in response to herbivory could cause cycles similar to those observed in the field. This highlights how interdisciplinary work that generates theory based on empirical evidence can increase our understanding of key population drivers of natural systems. The silica–

vole interaction is the focus of current field experiments and future work would modify the model structure and parameters to reflect new information generated by these studies.

A key environmental factor that is experienced by vole populations is that they are subject to seasonal forcing with a defined breeding and non-breeding season. The manner in which seasonality impacts on vole life-history is uncertain, and so in Chapter 5 we examine the relative importance of different seasonal mechanisms. We conclude that in this system, a variable breeding season is a more significant driver of multi-year cycles than a variable birth rate. Hence we demonstrate that the way in which seasonality is incorporated makes a significant difference to its effect on the dynamics. It is therefore crucial in seasonal models to incorporate patterns of forcing that most closely correspond to biologically realistic assumptions.

In Chapter 6, we develop a vole–predator model, and compare the impact of a variable breeding season and predation. We conclude that in this case predation is the more important driver of multi-year population cycles. Thus our findings demonstrate that a variable season length is not always the dominant regulator of cycles.

The seasonal model of vole populations could be extended in several ways. We consider a specialist predator in this model framework, meaning that the predator feeds only on the voles. An interesting extension to this work would be to consider instead a generalist predator, i.e. one with alternative food sources. (For an example of a model incorporating the action of generalist predators see Turchin and Hanski (1997).) Voles are also known to be hosts for many infectious diseases (e.g. Fichet-Calvet *et al.*, 2003; Bown *et al.*, 2004) and studies have indicated that infectious disease may promote population cycles by delaying reproduction (Smith *et al.*, 2008). This effect could be incorporated into a similar framework to that used for silica and predation to provide a comprehensive view of the interplay between seasonality and other potential drivers of population cycles.

Our work highlights the complexity of the role played by seasonal forcing in shaping population dynamics. Our study has been motivated by specific systems but the findings produce hypotheses that are relevant in general. We find that seasonality can have dramatic dynamical effects, and that this is strongly dependent on both the type of seasonal mechanism and the particular system modelled. With the prospect that global climate change will modify current patterns of seasonality, it is critical to understand the impact of seasonal forcing on population dynamics. Climate change is projected to have dramatic effects on species abundance and distribution (IPCC, 2007). In particular, climatic changes have already had an impact on population cycles and outbreaks, and this is predicted to continue (IPCC, 2007). One example is the massive outbreak of spruce bark beetles (a serious insect pest) in

Alaska, which caused significant mortality of trees. Also, fluctuations in fish abundance are increasingly regarded as a biological response to climatic effects on the ocean. As discussed in Chapter 6, changes over time in the vole population cycles in Kielder are attributed to climatic changes (Bierman *et al.*, 2006). Using seasonal models such as those described in this thesis, it may be possible to predict the future effects of climatic changes.

In conclusion, our study of the populations described in this thesis has provided important insights into the mechanisms driving population cycles in nature. It is vital that these underlying mechanisms are understood if we are to manage and control future population levels.

References

Abbott, K.C., Morris, W.F. and Gross, K. 2008. Simultaneous effects of food limitation and inducible resistance on herbivore population dynamics. *Theoretical Population Biology* 73: 63-78.

Agrell, J., Erlinge, S., Nelson, J., Nilsson, C. and Persson, I. 1995. Delayed density dependence in small-rodent populations. *Proceedings of the Royal Society of London B* 262: 65-70.

Akçakaya, H.R. 1992. Population cycles of mammals: evidence for a ratio-dependent predation hypothesis. *Ecological Monographs* 62: 119-142.

Altizer, S., Dobson, A., Hosseini, P., Hudson, P., Pascual, M. and Rohani, P. 2006. Seasonality and the dynamics of infectious diseases. *Ecology Letters* 9: 467-484.

Anderson, R.M. and May, R.M. 1979. Population biology of infectious diseases: Part I. *Nature* 280: 361-367.

Anderson, R.M. and May, R.M. 1981. The population dynamics of microparasites and their invertebrate hosts. *Philosophical Transactions of the Royal Society of London B* 291: 451-524.

Barnes, A.I. and Siva-Jothy, M.T. 2000. Density-dependent prophylaxis in the mealworm beetle *Tenebrio molitor* L. (Coleoptera: Tenebrionidae): cuticular melanization is an indicator of investment in immunity. *Proceedings of the Royal Society of London B* 267: 177-182.

Batzli, G.O. 1985. The role of nutrition in population cycles of microtine rodents. *Acta Zoologica Fennica* 173: 13-17.

Batzli, G.O. 1992. Dynamics of small mammal populations: a review. In: D.R. McCullough and R.H. Barrett (eds), *Wildlife 2001: Populations*, pp.831-850. New York: Elsevier.

Beddington, J.R. andMay, R.M. 1975. Time delays are not necessarily destabilizing. *Mathematical Biosciences* 27: 109-117.

Benz, G. 1974. Negative feedback by competition for food and space, and by cyclic induced changes in the nutritional base as regulatory principles in the population dynamics of the larch budmoth, *Zeiraphera diniana* (Guenée) (Lep., Tortricidae). *Zeitschrift für Angewandte Entomologie* 76: 196-228.

Berryman, A.A. 1996. What causes population cycles of forest Lepidoptera? *Trends in Ecology and Evolution* 11: 28-32.

Berryman, A.A. 2002. Population cycles: Causes and analysis. In: A.A. Berryman (ed.), *Population cycles: The case for trophic interactions*, pp.3-28. Oxford: Oxford University Press.

Bierman, S.M., Fairbairn, J.P., Petty, S.J., Elston, D.A., Tidhar, D. and Lambin, X. 2006. Changes over time in the spatiotemporal dynamics of cyclic populations of field voles (*Microtus agrestis* L.). *The American Naturalist* 167: 583-590.

Bonsall, M.B., Godfray, H.C.J., Briggs, C.J. and Hassel, M.P. 1999. Does host self-regulation increase the likelihood of insect–pathogen population cycles? *The American Naturalist* 153: 228-235.

Boonstra, R. 1994. Population cycles in microtines: the senescence hypothesis. *Evolutionary Ecology* 8: 196-219.

Boonstra, R. and Boag, P.T. 1987. A test of the Chitty hypothesis: inheritance of life-history traits in meadow voles *Microtus pennsylvanicus*. *Evolution* 41: 929-947.

Boonstra, R. and Krebs, C.J. 2006. Population limitation of the northern red-backed vole in the boreal forests of northern Canada. *Journal of Animal Ecology* 75: 1269-1284.

Boonstra, R., Krebs, C.J. and Stenseth, N.C. 1998. Population cycles in small mammals: the problem of explaining the low phase. *Ecology* 79: 1479-1488.

Boots, M. and Begon, M. 1993. Trade-offs with resistance to a granulosis virus in the Indian meal moth, examined by a laboratory evolution experiment. *Functional Ecology* 7: 528-534.

Bowers, R.G., Begon, M. and Hodgkinson, D.E. 1993. Host–pathogen population cycles in forest insects? Lessons from simple models reconsidered. *Oikos* 67: 529-538.

Bown, K.J., Bennett, M. and Begon, M. 2004. Flea-borne *Bartonella grahamii* and *Bartonella taylorii* in bank voles. *Emerging Infectious Diseases* 10: 684-687.

Brizuela, M.A., Detling, J.K. and Cid, M.S. 1986. Silicon concentration of grasses growing in sites with different grazing histories. *Ecology* 67: 1098-1101.

Brommer, J.E., Pietiäinen, H., Ahola, K., Karell, P., Karstinen, T. and Kolunen, H. 2010. The return of the vole cycle in southern Finland refutes the generality of the loss of cycles through 'climatic forcing'. *Global Change Biology* 16:577-586.

Bryant, J.P. 1981. Phytochemical deterrence of snowshoe hare browsing by adventitious shoots of four Alaskan trees. *Science* 213: 889-890.

Bryant, J.P., Chapin, F.S. and Klein, D.R. 1983. Carbon/nutrient balance of boreal plants in relation to vertebrate herbivory. *Oikos* 40: 357-368.

Bryant, J.P., Wieland, G.D., Clausen, T. and Kuropat, V. 1985. Interactions of snowshoe hare and feltleaf willow in Alaska. *Ecology* 66: 1564-1573.

Burthe, S. 2005. The dynamics of cowpox and vole tuberculosis in cyclic wild field vole populations. PhD thesis. University of Liverpool.

Burthe, S., Telfer, S., Begon, M., Bennett, M., Smith, M.A. and Lambin, X. 2008. Cowpox virus infection in natural field vole *Microtus agrestis* populations: significant negative impacts on survival. *Journal of Animal Ecology* 77: 110-119.

Cavanagh, R.D., Lambin, X., Ergon, T., Bennett, M., Graham, I.M., van Soolingen, D. and Begon, M. 2004. Disease dynamics in cyclic populations of field voles (*Microtus agrestis*): cowpox virus and vole tuberculosis (*Mycobacterium microti*). *Proceedings of the Royal Society of London B* 271: 859-867.

Charnov, E.L. and Finerty, J.P. 1980. Vole population cycles: a case for kin-selection? *Oecologia* 45: 1-2.

Chitty, D. 1960. Population processes in the vole and their relevance to general theory. *Canadian Journal of Zoology* 38: 99-113.

Chitty, D. 1967. The natural selection of self-regulatory behaviour in animal populations. *Proceedings of the Ecological Society of Australia* 2: 51-78.

Christian, J.J. 1950. The adreno-pituitary system and population cycles in mammals. *Journal of Mammalogy* 31: 247-259.

Cooke, K.L. and van den Driessche, P. 1986. On zeroes of some transcendental equations. *Funkcialaj Ekvacioj* 29: 77-90.

Cotter, S.C., Hails, R.S., Cory, J.S. and Wilson, K. 2004. Density-dependent prophylaxis and condition-dependent immune function in Lepidopteran larvae: a multivariate approach. *Journal of Animal Ecology* 73: 283-293.

Cotterill, J.V., Watkins, R.W., Brennon, C.B. and Cowan, D.P. 2007. Boosting silica levels in wheat leaves reduces grazing by rabbits. *Pest Management Science* 63: 247-253.

Crowcroft, P. 1991. *Elton's ecologists: a history of the Bureau of Animal Population.* Chicago: The University of Chicago Press.

Dalin, P. and Bjorkman, C. 2003. Adult beetle grazing induces willow trichome defence against subsequent larval feeding. *Oecologia* 134: 112-118.

Desy, E.A. and Batzli, G.O. 1989. Effects of food availability and predation on prairie vole demography: a field experiment. *Ecology* 70: 411-421.

Dietz, K. 1982. Overall population patterns in the transmission cycle of infectious disease agents. In: R.M. Anderson and R.M. May (eds), *Population biology of infectious diseases*, pp.87-102. New York: Springer.

Doedel, E.J. 1981. AUTO: a program for the automatic bifurcation analysis of autonomous systems. *Congressus Numerantium* 30: 265-284.

Edelstein-Keshet, L. and Rausher, M.D. 1989. The effects of inducible plant defenses on herbivore populations. 1. Mobile herbivores in continuous time. *The American Naturalist* 133: 787-810.

Elton, C.S. 1924. Periodic fluctuations in the numbers of animals: their causes and effects. *The British Journal of Experimental Biology* 2: 119-163.

Elton, C. 1927. *Animal Ecology.* London: Sidgwick & Jackson.

Elton, C. and Nicholson, M. 1942. The ten-year cycle in numbers of the lynx in Canada. *Journal of Animal Ecology* 11: 215-244.

Epstein, E. 1999. Silicon. *Annual Review of Plant Physiology and Plant Molecular Biology* 50: 641-664.

Ergon, T., Ergon, R., Begon, M., Telfer, S. and Lambin, X. 2011. Delayed density-dependent onset of spring reproduction in a fluctuating population of field voles. *Oikos* 120: 934-940.

Ergon, T., Lambin, X. and Stenseth, N.C. 2001. Life-history traits of voles in a fluctuating population respond to the immediate environment. *Nature* 411: 1043-1045.

Fichet-Calvet, E., Giraudoux, P., Quere, J.P., Ashford, R.W. and Delattre, P. 2003. Is the prevalence of *Taenia taeniaeformis* in *Microtus arvalis* dependent on population density? *Journal of Parasitology* 89: 1147-1152.

Fowler, S.V. and Lawton, J.H. 1985. Rapidly induced defenses and talking trees: the devil's advocate position. *The American Naturalist* 126: 181-195.

Fox, J.F. and Bryant, J.P. 1984. Instability of the snowshoe hare and woody plant interaction. *Oecologia* 63: 128-135.

Gakkhar, S., Sahani, S.K. and Negi, K. 2009. Effects of seasonal growth on delayed prey–predator model. *Chaos, Solitons and Fractals* 39: 230-239.

Gali-Muhtasib, H.U., Smith, C.C. and Higgins, J.J. 1992. The effect of silica in grasses on the feeding-behavior of the prairie vole, *Microtus ochrogaster*. *Ecology* 73: 1724-1729.

Ginzburg, L.R. and Taneyhill, D.E. 1994. Population cycles of forest Lepidoptera: a maternal effect hypothesis. *Journal of Animal Ecology* 63: 79-92.

Graham, A.L., Allen, J.E. and Read, A.F. 2005. Evolutionary causes and consequences of immunopathology. *Annual Review of Ecology, Evolution, and Systematics* 36: 373-397.

Graham, I.M. and Lambin, X. 2002. The impact of weasel predation on cyclic field-vole survival: the specialist predator hypothesis contradicted. *Journal of Animal Ecology* 71: 946-956.

Greenman, J., Kamo, M. and Boots, M. 2004. External forcing of ecological and epidemiological systems: a resonance approach. *Physica D* 190: 136-151.

Greenman, J.V. and Norman, R.A. 2007. Environmental forcing, invasion and control of ecological and epidemiological systems. *Journal of Theoretical Biology* 247: 492-506.

Guckenheimer, J. and Holmes, P. 1986. *Nonlinear oscillations, dynamical systems, and bifurcations of vector fields*. New York: Springer Verlag.

Gurney, W.S.C. and Nisbet, R.M. 1998. *Ecological Dynamics*. New York: Oxford University Press.

Haberman, R. 1977. *Mathematical models: mechanical vibrations, population dynamics, and traffic flow*. Englewood Cliffs, N.J.: Prentice-Hall.

Hale, J.K. and Verduyn Lunel, S.M. 1993. *Introduction to functional differential equations*. New York: Springer.

Halitschke, R., Schittko, U., Pohnert, G., Boland, W. and Baldwin, I.T. 2001. Molecular interactions between the specialist herbivore *Manduca sexta* (Lepidoptera, Sphingidae) and its natural host *Nicotiana attenuata*. III. Fatty acid-amino acid conjugates in herbivore oral secretions are necessary and sufficient for herbivore-specific plant responses. *Plant Physiology* 125: 711-717.

Hanski, I. and Henttonen, H. 1996. Predation on competing rodent species: a simple explanation of complex patterns. *Journal of Animal Ecology* 65: 220-232.

Hanski, I. and Henttonen, H. 2002. Population cycles of small rodents in Fennoscandia. In: A.A. Berryman (ed.), *Population cycles: The case for trophic interactions*, pp.44-68. Oxford: Oxford University Press.

Hanski, I., Henttonen, H., Korpimäki, E., Oksanen, L. and Turchin, P. 2001. Small-rodent dynamics and predation. *Ecology* 82: 1505-1520.

Hanski, I. and Korpimäki, E. 1995. Microtine rodent dynamics in northern Europe: Parameterized models for the predator–prey interaction. *Ecology* 76: 840-850.

Hanski, I., Turchin, P., Korpimäki, E. and Henttonen, H. 1993. Population oscillations of boreal rodents: regulation by mustelid predators leads to chaos. *Nature* 364: 232-235.

Hansson, L. 1971. Small rodent food, feeding and population dynamics. *Oikos* 22: 183-198.

Hansson, L. and Henttonen, H. 1985. Gradients in density variations of small rodents: the importance of latitude and snow cover. *Oecologia* 67: 394-402.

Hartley, S.E. and Firn, R.D. 1989. Phenolic biosynthesis, leaf damage, and insect herbivory in birch (*Betula-pendula*). *Journal of Chemical Ecology* 15: 275-283.

Haukioja, E. 1980. On the role of plant defenses in the fluctuation of herbivore populations. *Oikos* 35: 202-213.

Haukioja, E. 1991a. Induction of defenses in trees. *Annual Review of Entomology* 36: 25-42.

Haukioja, E. 1991b. Cyclic fluctuations in density: Interactions between a defoliator and its host tree. *Acta Oecologica* 12: 77-88.

Henttonen, H., Oksanen, T., Jortikka, A. and Haukisalmi, V. 1987. How much do weasels shape microtine cycles in the northern Fennoscandian taiga? *Oikos* 50: 353-365.

Hochberg, M.E. 1991a. Viruses as costs to gregarious feeding behaviour in the Lepidoptera. *Oikos* 61: 291-296.

Hochberg, M.E. 1991b. Non-linear transmission rates and the dynamics of infectious disease. *Journal of Theoretical Biology* 153: 301-321.

Högstedt, G., Seldal, T. and Breistøl, A. 2005. Period length in cyclic animal populations. *Ecology* 86: 373-378.

Huitu, O., Koivula, M., Korpimäki, E., Klemola, T. and Norrdahl, K. 2003. Winter food supply limits growth of northern vole populations in the absence of predation. *Ecology* 84: 2108-2118.

Huntzinger, M., Karban, R., Young, T.P. and Palmer, T.M. 2004. Relaxation of induced indirect defenses of acacias following exclusion of mammalian herbivores. *Ecology* 85: 609-614.

Hutchinson, G.E. 1948. Circular causal systems in ecology. *Annals of the New York Academy of Sciences* 50: 221-246.

Ims, R.A., Henden, J.-A., and Killengreen, S.T. 2008. Collapsing population cycles. *Trends in Ecology and Evolution* 23: 79-86.

Inchausti, P. and Ginzburg, L.R. 1998. Small mammal cycles in northern Europe: patterns and evidence for a maternal effect hypothesis. *Journal of Animal Ecology* 67: 180-194.

IPCC, 2007: Climate Change 2007 - Impacts, Adaptation, and Vulnerability. Contribution of Working Group II to the Fourth Assessment Report of the Intergovernmental Panel on Climate Change. Parry, M.L., Canziani, O.F., Palutikof, J.P., van der Linden, P.J. and Hanson, C.E. (eds). Cambridge: Cambridge University Press.

Ireland, J.M., Mestel, B.D. and Norman, R.A. 2007. The effect of seasonal host birth rates on disease persistence. *Mathematical Biosciences* 206: 31-45.

Ireland, J.M., Norman, R.A. and Greenman, J.V. 2004. The effect of seasonal host birth rates on population dynamics: the importance of resonance. *Journal of Theoretical Biology* 231: 229-238.

Jedrzejewska, B. and Jedrzejewski, W. 1998. *Predation in vertebrate communities: the Bialowieza primeval forest as a case study.* Berlin: Springer.

Jones, L.H.P. and Handreck, K.A. 1967. Silica in soils, plants and animals. *Advances in Agronomy* 19: 107-149.

Kaitaniemi, P., Ruohomaki, K., Ossipov, V., Haukioja, E. and Pihlaja, K. 1998. Delayed induced changes in the biochemical composition of host plant leaves during an insect outbreak. *Oecologia* 116: 182-190.

Kapari, L., Haukioja, E., Rantala, M.J. and Ruuhola, T. 2006. Defoliating insect immune defense interacts with induced plant defense during a population outbreak. *Ecology* 87: 291-296.

Karban, R. and Baldwin, I.T. 1997. *Induced response to herbivory.* Chicago: University of Chicago Press.

Karban, R. and Carey, J.R. 1984. Induced resistance of cotton seedlings to mites. *Science* 225: 53-54.

Keeling, M.J., Rohani, P. and Grenfell, B.T. 2001. Seasonally forced disease dynamics explored as switching between attractors. *Physica D* 148: 317-335.

Kent, A., Jensen, S.P. and Doncaster, C.P. 2005. Model of microtine cycles caused by lethal toxins in non-preferred food plants. *Journal of Theoretical Biology* 234: 593-604.

Kindomihou, V., Sinsin, B. and Meerts, P. 2006. Effect of defoliation on silica accumulation in five tropical fodder grass species in Benin. *Belgian Journal of Botany* 139: 87-102.

King, C. 1989. *The natural history of weasels and stoats.* London: Croom Helm.

Klemola, T., Klemola, N., Andersson, T. and Ruohomäki, K. 2007. Does immune function influence population fluctuations and level of parasitism in the cyclic geometrid moth? *Population Ecology* 49: 165-178.

Klemola, T., Koivula, M., Korpimäki, E. and Norrdahl, K. 2000a. Experimental tests of predation and food hypotheses for population cycles of voles. *Proceedings of the Royal Society of London B* 267: 351-356.

Klemola, T., Norrdahl, K. and Korpimäki, E. 2000b. Do delayed effects of overgrazing explain population cycles in voles? *Oikos* 90: 509-516.

Klemola, T., Pettersen, T. and Stenseth, N.C. 2003. Trophic interactions in population cycles of voles and lemmings: a model-based synthesis. *Advances in Ecological Research* 33: 75-160.

Korpimäki, E. and Krebs, C.J. 1996. Predation and population cycles of small mammals. *BioScience* 46: 754-764.

Kraaijeveld, A.R. and Godfray, H.C.J. 1997. Trade-off between parasitoid resistance and larval competitive ability in *Drosophila melanogaster*. *Nature* 389: 278-280.

Krebs, C.J. 1996. Population cycles revisited. *Journal of Mammalogy* 77: 8-24.

Krebs, C.J., Boonstra, R., Boutin, S. and Sinclair, A.R.E. 2001. What drives the 10-year cycle of snowshoe hares? *BioScience* 51: 25-35.

Krebs, C.J., Cowcill, K., Boonstra, R. and Kenney, A.J. 2010. Do changes in berry crops drive population fluctuations in small rodents in the southwestern Yukon? *Journal of Mammalogy* 91: 500-509.

Krebs, C.J., Gaines, M.S., Keller, B.L., Myers, J.H. and Tamarin, R.H. 1973. Population cycles in small rodents. *Science* 179: 35-41.

Krebs, C.J., Gilbert, B.S., Boutin, S., Sinclair, A.R.E. and Smith, J.N.M. 1986. Population biology of snowshoe hares. I. Demography of food-supplemented populations in the southern Yukon, 1976-1984. *Journal of Animal Ecology* 55: 963-982.

Krebs, C.J. and Myers, J.H. 1974. Population cycles in small mammals. *Advances in Ecological Research* 8: 267-399.

Kuang, Y. 1993. *Delay differential equations with applications in population dynamics*. Boston: Academic Press.

Kunimi, Y. and Yamada, E. 1990. Relationship between larval phase and susceptibility of the armyworm, *Pseudaletia separata* Walker (Lepidoptera: Noctuidae) to a nuclear polyhedrosis virus and a granulosis virus. *Applied Entomology and Zoology* 25: 289-297.

Kuznetsov, Yu.A., Muratori, S. and Rinaldi, S. 1992. Bifurcations and chaos in a periodic predator–prey model. *International Journal of Bifurcation and Chaos* 2: 117-128.

Lack, D. 1954. *The natural regulation of animal numbers.* Oxford: Clarendon Press.

Lambin, X., Bretagnolle, V. and Yoccoz, N.G. 2006. Vole population cycles in northern and southern Europe: Is there a need for different explanations for single pattern? *Journal of Animal Ecology* 75: 340-349.

Lambin, X., Petty, S.J. and MacKinnon, J.L. 2000. Cyclic dynamics in field vole populations and generalist predation. *Journal of Animal Ecology* 69: 106-118.

Lindgren, A., Klint, J. and Moen, J. 2007. Defense mechanisms against grazing: a study of trypsin inhibitor responses to simulated grazing in the sedge *Carex bigelowii*. *Oikos* 116: 1540-1546.

Long, G.H., Chan, B.H.K., Allen, J.E., Read, A.F. and Graham, A.L. 2008. Experimental manipulation of immune-mediated disease and its fitness costs for rodent malaria parasites. *BMC Evolutionary Biology* 8: 128.

Lotka, A.J. 1925. *Elements of physical biology.* Baltimore: Williams & Wilkins Co.

Lundberg, S., Järemo, J. and Nilsson, P. 1994. Herbivory, inducible defence and population oscillations: a preliminary theoretical analysis. *Oikos* 71: 537-540.

Mackin-Rogalska, R. and Nabaglo, L. 1990. Geographical variation in cyclic periodicity and synchrony in the common vole, *Microtus arvalis*. *Oikos* 59: 343-348.

Massey, F.P., Ennos, A.R. and Hartley, S.E. 2006. Silica in grasses as a defence against insect herbivores: contrasting effects on folivores and a phloem feeder. *Journal of Animal Ecology* 75: 595-603.

Massey, F.P., Ennos, A.R. and Hartley, S.E. 2007a. Herbivore specific induction of silica-based plant defences. *Oecologia* 152: 677-683.

Massey, F.P., Ennos, A.R. and Hartley, S.E. 2007b. Grasses and the resource availability hypothesis: the importance of silica-based defences. *Journal of Ecology* 95: 414-424.

Massey, F.P. and Hartley, S.E. 2006. Experimental demonstration of the antiherbivore effects of silica in grasses: impacts on foliage digestibility and vole growth rates. *Proceedings of the Royal Society of London B* 273: 2299-2304.

Massey, F.P., Massey, K., Ennos, A.R. and Hartley, S.E. 2009. Impacts of silica-based defences in grasses on the feeding preferences of sheep. *Basic and Applied Ecology* 10: 622-630.

Massey, F.P., Smith, M.J., Lambin, X. and Hartley, S.E. 2008. Are silica defences in grasses driving vole population cycles? *Biology Letters* 4: 419-422.

May, R.M. 1972. Limit cycles in predator–prey communities. *Science* 177: 900-902.

McKean, K.A., Yourth, C.P., Lazzaro, B.P. and Clark, A.G. 2008. The evolutionary costs of immunological maintenance and deployment. *BMC Evolutionary Biology* 8: 76.

McNaughton, S.J. 1979. Grazing as an optimization process: grass–ungulate relationships in the Serengeti. *The American Naturalist* 113: 691-703.

McNaughton, S.J. and Tarrants, J.L. 1983. Grass leaf silicification: natural selection for an inducible defense against herbivores. *Proceedings of the National Academy of Sciences of the United States of America* 80: 790-791.

McNaughton, S.J., Tarrants, J.L., McNaughton, M.M. and Davis, R.H. 1985. Silica as a defense against herbivory and a growth promotor in African grasses. *Ecology* 66: 528-535.

Molano-Flores, B. 2001. Herbivory and calcium concentrations affect calcium oxalate crystal formation in leaves of Sida (Malvaceae). *Annals of Botany* 88: 387-391.

Moret, Y. and Schmid-Hempel, P. 2000. Survival for immunity: the price of immune system activation for bumblebee workers. *Science* 290: 1166-1168.

Myers, J.H. and Williams, K.S. 1984. Does tent caterpillar attack reduce the food quality of red alder foliage? *Oecologia* 62: 74-79.

Myllymäki, A. 1977. Intraspecific competition and home range dynamics in the field vole *Microtus agrestis*. *Oikos* 29: 553-569.

Nicholson, A.J. 1954. An outline of the dynamics of animal populations. *Australian Journal of Zoology* 2: 9-65.

Nicholson, A.J. 1957. The self-adjustment of populations to change. *Cold Spring Harbor Symposium on Quantitative Biology* 22: 153-173.

Nisbet, R.M. and Gurney, W.S.C. 1982. *Modelling fluctuating populations*. New York: John Wiley & Sons.

Norman, R., Begon, M. and Bowers, R.G. 1994. The population dynamics of microparasites and vertebrate hosts: the importance of immunity and recovery. *Theoretical Population Biology* 46: 96-119.

Norrdahl, K. and Korpimäki, E. 2002. Changes in population structure and reproduction during a 3-yr population cycle of voles. *Oikos* 96: 331-345.

Oksanen, T., Oksanen, L., Jedrzejewski, W., Jedrzejewska, B., Korpimäki, E. and Norrdahl, K. 2000. Predation and the dynamics of the bank vole, *Clethrionomys glareolus*. *Polish Journal of Ecology* 48: 197-217.

Oksanen, L., Oksanen, T., Lukkari, A. and Siren, S. 1987. The role of phenol-based inducible defense in the interaction between tundra populations of the vole *Clethrionomys rufocanus* and the dwarf shrub *Vaccinium myrtillus*. *Oikos* 50: 371-380.

O'Mahony, D., Lambin, X., MacKinnon, J.L. and Coles, C.F. 1999. Fox predation on cyclic field vole populations in Britain. *Ecography* 22: 575-581.

O'Reagain, P.J. and Mentis, M.T. 1989. Leaf silicification in grasses - a review. *Journal of the Grassland Society of Southern Africa* 6: 37-43.

Ostfeld, R.S. 1985. Limiting resources and territoriality in microtine rodents. *The American Naturalist* 126: 1-15.

Ostfeld, R.S. and Canham, C.D. 1993. Effects of meadow vole population-density on tree seedling survival in old fields. *Ecology* 74: 1792-1801.

Ostfeld, R.S. and Canham, C.D. 1995. Density-dependent processes in meadow voles - an experimental approach. *Ecology* 76: 521-532.

Ostfeld, R.S., Canham, C.D. and Pugh, S.R. 1993. Intrinsic density-dependent regulation of vole populations. *Nature* 366: 259-261.

Petty, S.J., Lambin, X., Sherratt, T.N., Thomas, C.J., Mackinnon, J.L., Coles, C.F., Davison, M. and Little, B. 2000. Spatial synchrony in field vole *Microtus agrestis* abundance in a coniferous forest in northern England: the role of vole-eating raptors. *Journal of Applied Ecology* 37: 136-147.

Rammul, U., Oksanen, T., Oksanen, L., Lehtela, J., Virtanen, R., Olofsson, J., Strengbom, J., Rammul, I. and Ericson, L. 2007. Vole–vegetation interactions in an experimental, enemy free taiga floor system. *Oikos* 116: 1501-1513.

Reeson, A.F., Wilson, K., Gunn, A., Hails, R.S. and Goulson, D. 1998. Baculovirus resistance in the noctuid *Spodoptera exempta* is phenotypically plastic and responds to population density. *Proceedings of the Royal Society of London B* 265: 1787-1791.

Reilly, J.R. and Hajek, A.E. 2008. Density-dependent resistance of the gypsy moth *Lymantria dispar* to its nucleopolyhedrovirus, and the consequences for population dynamics. *Oecologia* 154: 691-701.

Reynolds, J.J.H., White, A., Sherratt, J.A. and Boots, M. 2011. The population dynamical consequences of density-dependent prophylaxis. *Journal of Theoretical Biology* 288: 1-8.

Reynolds, J.J.H., Massey, F.P., Lambin, X., Reidinger, S., Sherratt, J.A., Smith, M.J., White, A. and Hartley, S.E. (submitted, a) Delayed induced silica defences in grasses and their potential for destabilising herbivore population dynamics.

Reynolds, J.J.H., Sherratt, J.A., White, A. and Lambin, X. (submitted, b) A comparison of the dynamical impact of seasonal mechanisms in a herbivore–plant defence system.

Reynolds, O.L., Keeping, M.G. and Meyer, J.H. 2009. Silicon-augmented resistance of plants to herbivorous insects: a review. *Annals of Applied Biology* 155: 171-186.

Rhoades, D.F. 1983. Herbivore population dynamics and plant chemistry. In: R.F. Denno and M.S. McClure (eds), *Variable plants and herbivores in natural and managed systems*, pp.155-220. New York: Academic Press.

Rinaldi, S., Muratori, S. and Kuznetsov, Y. 1993. Multiple attractors, catastrophes and chaos in seasonally perturbed predator–prey communities. *Bulletin of Mathematical Biology* 55: 15-35.

Roberts, M.G. and Kao, R.R. 1998. The dynamics of an infectious disease in a population with birth pulses. *Mathematical Biosciences* 149: 23-36.

Ruiz-González, M.X., Moret, Y. and Brown, M.J.F. 2009. Rapid induction of immune density-dependent prophylaxis in adult social insects. *Biology Letters* 5: 781-783.

Ruohomaki, K., Tanhuanpaa, M., Ayres, M.P., Kaitaniemi, P., Tammaru, T. and Haukioja, E. 2000. Causes of cyclicity of *Epirrita autumnata* (Lepidoptera, Geometridae): grandiose theory and tedious practice. *Population Ecology* 42: 211-223.

Ryder, J.J., Miller, M.R., White, A., Knell, R.J. and Boots, M. 2007. Host–parasite population dynamics under combined frequency- and density-dependent transmission. *Oikos* 116: 2017-2026.

Ryder, J.J., Webberley, K.M., Boots, M. and Knell, R.J. 2005. Measuring the transmission dynamics of a sexually transmitted disease. *Proceedings of the National Academy of Sciences of the United States of America* 102: 15140-15143.

Sadd, B.M. and Siva-Jothy, M.T. 2006. Self-harm caused by an insect's innate immunity. *Proceedings of the Royal Society of London B* 273: 2571-2574.

Schmid-Hempel, P. 2003. Variation in immune defence as a question of evolutionary ecology. *Proceedings of the Royal Society of London B* 270: 357-366.

Schultz, J.C. and Baldwin, I.T. 1982. Oak leaf quality declines in response to defoliation by gypsy moth larvae. *Science* 217: 149-151.

Schwartz, I.B. and Smith, H.L. 1983. Infinite subharmonic bifurcation in an SEIR epidemic model. *Journal of Mathematical Biology* 18: 233-253.

Sherratt, J.A. and Smith, M.J. 2008. Periodic travelling waves in cyclic populations: field studies and reaction-diffusion models. *Journal of the Royal Society Interface* 5: 483-505.

Sinclair, A.R.E., Krebs, C.J., Smith, J.N.M. and Boutin, S. 1988. Population biology of snowshoe hares. III. Nutrition, plant secondary compounds and food limitation. *Journal of Animal Ecology* 57: 787-806.

Smith, H. 2010. *An introduction to delay differential equations with applications to the life sciences*. New York: Springer.

Smith, M.J., White, A., Lambin, X., Sherratt, J.A. and Begon, M. 2006. Delayed density-dependent season length alone can lead to rodent population cycles. *The American Naturalist* 167: 695-704.

Smith, M.J., White, A., Sherratt, J.A., Telfer, S., Begon, M. and Lambin, X. 2008. Disease effects on reproduction can cause population cycles in seasonal environments. *Journal of Animal Ecology* 77: 378-389.

Soveri, T., Henttonen, H., Haukisalmi, V., Rudbäck, E., Sukura, A., Tanskanen, R., Schildt, R., Husu, J. and Laakkonen, J. 2000. Disease patterns in field and bank vole populations during a cyclic decline in Central Finland. *Comparative Immunology, Microbiology and Infectious Diseases* 23: 73-89.

Stenseth, N.C. 1985. Mathematical models of microtine cycles: models and the real world. *Acta Zoologica Fennica* 173: 7-12.

Stenseth, N.C. 1999. Population cycles in voles and lemmings: density dependence and phase dependence in a stochastic world. *Oikos* 87: 427-461.

Stenseth, N.C., Hansson, L. and Myllymäki, A. 1977. Food selection of the field vole *Microtus agrestis*. *Oikos* 29: 511-524.

Stenseth, N.C. and Ims, R.A. 1993. The history of lemming research: from the Nordic Sagas to *The biology of lemmings*. In: N.C. Stenseth and R.A. Ims (eds), *The biology of lemmings*, pp.3-34. London: Academic Press.

Stenseth, N.C., Viljugrein, H., Saitoh, T., Hansen, T.F., Kittilsen, M.O., Bølviken, E. and Glöckner, F. 2003. Seasonality, density dependence, and population cycles in Hokkaido voles. *Proceedings of the National Academy of Sciences of the United States of America* 100: 11478-11483.

Taitt, M.J. and Krebs, C.J. 1985.Population dynamics and cycles.In: R.H. Tamarin (ed.), *Biology of New World Microtus*, Special Publication of the American Society of Mammalogists 8: 567-620.

Tamai, K. and Ma, J.F. 2003. Characterization of silicon uptake by rice roots. *New Phytologist* 158: 431-436.

Tkadlec, E. and Stenseth, N.C. 2001. A new geographical gradient in vole population dynamics. *Proceedings of the Royal Society of London B* 268: 1547-1552.

Turchin, P. 2003. *Complex population dynamics: A theoretical / empirical synthesis*. Princeton: Princeton University Press.

Turchin, P. and Batzli, G.O. 2001. Availability of food and the population dynamics of arvicoline rodents. *Ecology* 82: 1521-1534.

Turchin, P. and Hanski, I. 1997. An empirically based model for latitudinal gradient in vole population dynamics. *The American Naturalist* 149: 842-874.

Turchin, P., Oksanen, L., Ekerholm, P., Oksanen, T. and Henttonen, H. 2000. Are lemmings prey or predators? *Nature* 405: 562-565.

Turchin, P. and Ostfeld, R.S. 1997. Effects of density and season on the population rate of change in the meadow vole. *Oikos* 78: 355-361.

Turchin, P. and Taylor, A.D. 1992. Complex dynamics in ecological time-series. *Ecology* 73: 289-305.

Underwood, N.C. 1998. The timing of induced resistance and induced susceptibility in the soybean–Mexican bean beetle system. *Oecologia* 114: 376-381.

Underwood, N. 1999. The influence of plant and herbivore characteristics on the interaction between induced resistance and herbivore population dynamics. *The American Naturalist* 153: 282-294.

Underwood, N. and Rausher, M. 2002. Comparing the consequences of induced and constitutive plant resistance for herbivore population dynamics. *The American Naturalist* 160: 20-30.

Vicari, M. and Bazely, D.R. 1993. Do grasses fight back? The case for antiherbivore defences. *Trends in Ecology and Evolution* 8: 137-141.

Volterra, V. 1926. Fluctuations in the abundance of a species considered mathematically. *Nature* 118: 558-560.

Wellington, W.G. 1960. Qualitative changes in natural populations during changes in abundance. *Canadian Journal of Zoology* 38: 290-314.

White, A., Bowers, R.G. and Begon, M. 1996. Population cycles in self-regulated insect pathogen systems: resolving conflicting predictions. *The American Naturalist* 148: 220-225.

White, K.A.J. and Wilson, K. 1999. Modelling density-dependent resistance in insect–pathogen interactions. *Theoretical Population Biology* 56: 163-181.

Wilson, K. and Reeson, A.F. 1998. Density-dependent prophylaxis: evidence from Lepidoptera–baculovirus interactions? *Ecological Entomology* 23: 100-101.

Wilson, K., Thomas, M.B., Blanford, S., Doggett, M., Simpson, S.J. and Moore, S.L. 2002. Coping with crowds: Density-dependent disease resistance in desert locusts. *Proceedings of the National Academy of Sciences of the United States of America* 99: 5471-5475.

Xiao, Y., Bowers, R.G. and Tang, S. 2009. The effect of delayed host self-regulation on host–pathogen population cycles in forest insects. *Journal of Theoretical Biology* 258: 240-249.

Zynel, C.A. and Wunder, B.A. 2002. Limits to food intake by the prairie vole: effects of time for digestion. *Functional Ecology* 16: 58-66.